THE CRITICAL POINTS OF POYNTING VECTOR FIELDS

Thesis by

Syed Azhar Abbas Rizvi

In Partial Fulfillment of the Requirements

for the Degree of

Doctor of Philosophy

California Institute of Technology

Pasadena, California

1988

(Submitted April 28, 1988)

بِسْمِ اللّٰهِ الرَّحْمٰنِ الرَّحِيْمِ ○

اِقْرَاْ بِاسْمِ رَبِّكَ الَّذِى خَلَقَ ○ خَلَقَ الْاِنْسَانَ مِنْ عَلَقٍ ○

اِقْرَاْ وَرَبُّكَ الْاَكْرَمُ ○ الَّذِى عَلَّمَ بِالْقَلَمِ ○

عَلَّمَ الْاِنْسَانَ مَالَمْ يَعْلَمْ ○

In the name of Allah the Beneficient, the Merciful.

Read in the name of your Lord who created,

Created man from a clot of congealed blood,

Read; and your Lord is most Bountiful,

He who taught the use of the pen,

Taught man that which he knew not.

Quran, Sura XCVI, 1-5

To my parents

Syed Izhar Abbas Rizvi
&
Kaneez-e-Haider,

and all my teachers.

They gave me their very best.

ACKNOWLEDGEMENTS

All praise and thanks are due to Allah Who is the Lord and Sustainer of the universe.

I sincerely thank my advisor Dr. Charles H. Papas for initiating this work. This work could not have been completed without his constant guidance, encouragement and useful criticisms. His kindness, patience, attention to details and a unique way of looking at complex physical phenomena in terms of simple models, was a source of inspiration.

I wish to thank Dr. Jakob J. van Zyl for reading through the first draft of this thesis. His suggestions on presentation and style were very useful. I also wish to acknowledge warm conversations with Drs. Nader Engheta, Jakob van Zyl and Sassan Bassiri, in our research group, on topics related and unrelated to the electromagnetic field theory.

I am indebted to Caltech for the financial support during the tenure of my graduate studies. I am grateful to the faculty for sharing their knowledge with me. I am thankful to Ms. Linda Dozsa and Ms. Janice Tucker of the Electrical Engineering department for efficiently taking care of all my adminstrative paper work. Thanks are also due to Ms. Paula Samazan of the EE/APh departmental

library for going out of her way to procure necessary reference material.

A sound mind resides in a healthy body. While a lot of intellectual pursuits kept my mind occupied, coach C. Dodd helped me to stay physically fit. I thank him for teaching me the art of swimming although he insisted on calling it a science.

I am grateful to my parents and my brothers and sisters who gave me a leave of absence from my responsiblities. I thank Hossein Shahidi for making my stay in Los Angeles a pleasant one. Finally I take this opportunity to thank my long time friend Zahir Ebrahim who is largely responsible for convincing me to pursue a program of graduate studies.

ABSTRACT

In a thought provoking paper Maxwell† studied the flow of water on the Earth's surface and how this flow is affected by the local geography. His results linking number of hills and lake bottoms to valleys are simple and the conclusions elegant. Critical points such as summits and lake bottoms play a key role in the overall organization and structuring of the flow lines. This is the spirit in which electromagnetic power flow represented by the Poynting vector field (S) is studied in this thesis. The specialized case of a planar S field which arises due to a single electromagnetic field component E_z or H_z is dealt with here in considerable detail.

In order to analyse the behaviour of the flow lines of a plane Poynting vector field in the neighbourhood of a critical point, the S field is expanded in a Taylor series. Critical points can be classified according to their order, degeneracy or structural stability. The order of a critical point refers to the degree of the leading non zero term in the Taylor series. A critical point is non degenerate if this leading term is sufficient to give a qualitative description of the flow lines in the neighbourhood. A critical point is structurally stable if the flow lines in the neighbourhood do not change drastically when there is a small perturbation of the

† *The Scientific Papers of James Clerk Maxwell*, ed. W. D. Niven, vol. 2, 233–240, Dover Publications, New York (1952).

electromagnetic field. It is found that lowest order critical points, i.e., elementary center point and elementary saddle point, are the only structurally stable critical points. These critical points are always non degenerate. All degenerate and non elementary critical points are found to be structurally unstable. A formula for the index of rotation of the S field at a critical point is derived. The behaviour of the electric or the magnetic field component which lies in the x-y plane is also studied. It is shown that structurally unstable configurations of flow lines change into structurally stable configurations under small perturbations in such a way that the index of rotation is conserved. The statements made above in connection with the behaviour of flow lines and structural stability are illustrated with the help of examples involving linearly polarized system of interfering plane and/or cylindrical waves.

The flow lines of the S field in the vicinity of a perfectly conducting surface are studied. It is found that in structurally stable situations these lines are either parallel to the surface or they form critical points of half saddle type on this surface. Two types of problems involving flow lines and conducting surfaces are identified. The interior problem deals with the situations where all the flow lines are inside a region bounded by a perfect conductor. In the exterior problems all the flow lines are outside a region bounded by a perfectly conducting surface. Conclusions regarding the existence of critical points and the behaviour of flow lines are drawn in the two above mentioned problems. These conclusions are verified by computation of flow lines in a few well known problems of scattering and diffraction.

Finally the critical points of three dimensional Poynting vector fields are considered. A complete classification of these critical points requires further study at this time. In this thesis only structurally stable critical points are classified for

these **S** fields. An example demonstrating the existence of such critical points is given.

TABLE OF CONTENTS

Chapter I

Preliminaries

§1. The Poynting Vector

About a century ago in 1884 Poynting and Heaviside derived an expression which has been the subject of much interest. This expression is called Poynting's theorem. It can be derived from the Maxwell's equations by elementary manipulations (see, e.g., Papas [1]) and is given as,

$$\oint_S (\mathbf{E} \times \mathbf{H}) \cdot \mathbf{e}_n \, da + \int_V \mathbf{E} \cdot \mathbf{J} \, dv = - \int_V (\mathbf{E} \cdot \frac{\partial \mathbf{D}}{\partial t} + \mathbf{H} \cdot \frac{\partial \mathbf{B}}{\partial t}) \, dv. \qquad (1)$$

The vectors **E**, **H**, **D**, **B**, and **J** are called electric and magnetic field intensities, electric displacement, magnetic induction and the current densities respectively. The right hand side represents the rate of decrease of stored electromagnetic energy which is balanced by the terms on the left hand side of the expression. The second term on the left expresses the amount of power lost which implies that the first term on the left gives the amount of power flowing out through the closed surface bounding a given volume. A phantom controversy arises when the integrands in (1) are interpreted as respective densities.

The Poynting's vector is defined as

$$\mathbf{S}(\mathbf{r}, t) = \mathbf{E}(\mathbf{r}, t) \times \mathbf{H}(\mathbf{r}, t) \qquad (2)$$

and from (1) its flux over a closed surface gives total flow of power from the volume under consideration. The interpretation of **S** as power flow density is not unique and has been criticised in the literature. For a discussion on this subject the reader is referred to Stratton [2]. One frequently cited objection is that the definition given by (2) implies non-zero power flow in crossed static electric and magnetic fields. For example the lines of **S** field close on themselves and provide a picture of circulating energy flow for the case of an electromagnetic field generated by a static electric charge placed on a bar magnet. This has disturbed many authors and they have persevered to find an alternative definition for power flux density, e.g., [3],[4]. Lorrain [5] pointed out static electromagnetic fields possess angular momentum whenever lines of **S** field form closed loops, therefore arguing that the picture of circulating energy flow provided by the conventional definition of the Poynting vector is entirely plausible. The alternative expressions for the power flux density given in [3] and [4] are defined in terms of magnetic vector potential and scalar electric potential and hence these definitions are gauge dependent. It has been shown by Birkeland [6] that if the power flux vector at a certain position and time depends only on the electric and magnetic fields at that position and time then the conventional definition given in (2) is unique up to a constant. Acceptance of Poynting vector as power flow vector has led to the investigation of its properties. Recently Latmiral [7] has pointed out the significance of $\nabla \times \mathbf{S}$ as differential radiation pressure.

For the purpose of this thesis the Poynting vector will be considered as the best measure of power flux density. This section will be concluded with words from Stratton [2] which express this viewpoint rather well.

> "The hypotheses of an energy density in the electromagnetic field and a flow of intensity $\mathbf{S} = \mathbf{E} \times \mathbf{H}$ has ... proved extraordinarily fruitful. A theory is not an absolute truth but a self consistent analytical formulation of

the relations governing a group of natural phenomena. By this standard there is every reason to retain the Poynting-Heaviside viewpoint until a clash with new experimental evidence shall call for its revision."

§2. Flow Lines and Critical Points

Throughout this thesis only time harmonic electromagnetic fields will be considered. The time dependence $\exp(-i\omega t)$ will be assumed for the field quantities **E**, **H** and **J**. This factor will be suppressed. The time dependence will be given explicitly wherever the need arises. The term Poynting vector will be used to imply the time average Poynting vector which is defined as

$$\mathbf{S}(\mathbf{r}) = \frac{1}{2}\Re\{\mathbf{E}(\mathbf{r}) \times \mathbf{H}^*(\mathbf{r})\}, \tag{3}$$

where **E** is phasor electric field, $\mathbf{H}^*$ is complex conjugate of the phasor magnetic field and $\Re$ denotes the real part of the expression. In this thesis attention will be focused on regions of space which do not contain sources or sinks of electromagnetic power. In most of the practical problems the generation or loss of power occurs only in bounded regions of space. The bounded regions containing sources or sinks can be eliminated from consideration without great loss of generality. The Poynting's theorem for time average Poynting vector field in regions devoid of sources or sinks is given as

$$\oint_S \mathbf{S} \cdot \mathbf{e}_n \, da = 0. \tag{4}$$

This is sometimes stated in differential form as

$$\nabla \cdot \mathbf{S} = 0. \tag{5}$$

The study of time average flow of electromagnetic energy is now reduced to the study of lines of **S**, which may also be called flow lines. Due to the restrictions imposed above, **S** is a solenoidal vector field and its flow lines are continuous in the regions of interest.

In principle the lines of flow can be obtained by solving the following differential equation

$$\frac{dx}{S_x} = \frac{dy}{S_y} = \frac{dz}{S_z}, \tag{6}$$

where S_x, S_y and S_z are cartesian components of **S**. Solution of (6) is by no means a trivial matter. In a lot of cases the qualitative behaviour of flow lines alone provides sufficient amount of information. In order to facilitate any further discussion on the subject a number of terms will have to be defined first. Consider a point P and its neighbourhood where $\mathbf{S} \neq 0$. The direction cosines of the flow line through P are well defined, hence a unique line segment can be drawn through P. Such a point is called an *ordinary point*. On the other hand if there exists a point P such that the Poynting vector at P is zero and does not vanish in the neighbourhood of P then such a point is called an *isolated critical point* of the Poynting vector field. It is the presence of critical points which drastically modifies the behaviour of flow lines. It is evident that the direction cosines of a line through P cannot be uniquely defined. Therefore a line of flow through a critical point, if indeed there is any, may not be unique. Since the critical points play a major role in determining the pattern of flow lines, an attempt will be made in this thesis to understand the behaviour of the Poynting vector field in the neighbourhood of its critical points.

§3. Plane Poynting Vector Fields

In general the Poynting vector field is three dimensional and its flow lines are space curves. It is difficult to visualize, represent and study these space curves in much detail except in a few simple cases. For this reason the problem will be simplified by assuming that the electric and the magnetic fields are two dimensional. By two dimensional it is meant that the field vectors are independent of z-coordinate in a cartesian coordinate system. It can be easily shown that two

dimensional electromagnetic fields are completely specified in terms of z-directed components of **E** and **H**. Specifically, the total electromagnetic field can be written down as

$$\mathbf{E} = E_z \mathbf{e}_z + \frac{i}{\omega\epsilon} \nabla H_z \times \mathbf{e}_z \,, \tag{7a}$$

$$\mathbf{H} = H_z \mathbf{e}_z - \frac{i}{\omega\mu} \nabla E_z \times \mathbf{e}_z \,, \tag{7b}$$

where E_z and H_z are functions of x and y only. The Poynting vector for this field can be expressed using (3) as

$$\begin{aligned} \mathbf{S} &= \frac{1}{2\omega\mu} \Re\{iE_z \nabla E_z^*\} + \frac{1}{2\omega\epsilon} \Re\{iH_z \nabla H_z^*\} + \frac{1}{\omega^2\mu\epsilon} \Re\{\nabla E_z^* \times \nabla H_z\} \\ &= \mathbf{S}_e + \mathbf{S}_h + \mathbf{S}_{eh} \,. \end{aligned} \tag{8}$$

It follows from (8) that the partial vector fields $\mathbf{S}_e$ and $\mathbf{S}_h$ are entirely transverse to $\mathbf{e}_z$ while $\mathbf{S}_{eh}$ is parallel to $\mathbf{e}_z$. Another simplifying assumption will be made at this point to make sure that the Poynting vector field is plane vector field. It will be assumed that the partial Poynting vector field $\mathbf{S}_{eh}$ of an electromagnetic field under consideration is identically zero. The flow lines of such plane fields are directed plane curves which can be easily visualized and sketched on paper. It is also observed from (8) that the components $\mathbf{S}_e$ and $\mathbf{S}_h$ are completely specified by E_z and H_z respectively. Therefore the electromagnetic field can be partitioned in an E-polarized field and an H-polarized field. The E-polarized field is given as

$$\mathbf{E}_1 = E_z \mathbf{e}_z \,, \tag{9a}$$

$$\mathbf{H}_1 = \frac{-i}{\omega\mu} \nabla E_z \times \mathbf{e}_z \,, \tag{9b}$$

while the H-polarized field is given as

$$\mathbf{H}_2 = H_z \mathbf{e}_z \,, \tag{10a}$$

$$\mathbf{E}_2 = \frac{i}{\omega\epsilon} \nabla H_z \times \mathbf{e}_z \,. \tag{10b}$$

The Poynting vectors of E-polarized and H-polarized fields are $\mathbf{S}_e$ and $\mathbf{S}_h$ respectively. The total power flux density is just the sum of the power flux densities of both the polarizations for the case of plane Poynting vector fields.

In what follows the critical points of the Poynting vector fields $\mathbf{S}_e$ generated by E-polarized fields given by (9) will be studied. The case for H-polarized fields given by (10), which generate the Poynting vector field $\mathbf{S}_h$ is analogous. This is not a seriously limiting restriction. There is a whole class of problems in the electromagnetic field theory in which the fields are either E-polarized or H-polarized. For example scattering by cylindrical objects or by long edges is solved separately for each polarization. When an electromagnetic field is a sum of fields due to both the polarizations then the critical points of the total Poynting vector field do not have a simple correspondence with the critical points of partial fields $\mathbf{S}_e$ and $\mathbf{S}_h$. It is clear from (8) that the total Poynting vector field will also have a critical point where both $\mathbf{S}_e$ and $\mathbf{S}_h$ have a critical point. There may be additional critical points at isolated points where $\mathbf{S}_e$ and $\mathbf{S}_h$ cancel each other.

A Plane Poynting vector field is also obtained if the flow lines of $\mathbf{S}_e + \mathbf{S}_h$ are parallel straight lines and the partial field $\mathbf{S}_{eh}$ does not vanish identically. In this case a cartesian coordinate system can be chosen such that the total Poynting vector field has the following representation,

$$\mathbf{S} = S_y(x)\mathbf{e}_y + S_z(x,y)\mathbf{e}_z\,. \tag{11}$$

It is immediately observed that the points where $\mathbf{S}$ field vanishes are not isolated in the $y-z$ plane. Hence such plane Poynting vector fields do not possess isolated critical points and therefore these fields will not be considered any further.

§4. Index of Rotation

An important property of the critical points of plane vector fields is their

index of rotation. The index of rotation γ is defined as follows. Let there be a closed curve C which encloses only one critical point and there are no critical points on C itself. When the curve C is traversed once in the positive direction, i.e., counterclockwise, the angle between the vector at the moving point on C and a fixed direction changes. If the total change in this angle is $2n\pi$ then the index of rotation of the critical point is defined to be n. It can be easily shown that n can only take integral values. For example the two vector fields shown in figures 1(a) and 1(b) have indices of rotation, $\gamma = 1$ and $\gamma = -2$ respectively. The dots denote the location of the critical points in this figure and subsequent figures.

It should be noted that the index γ is independent of the choice of curve C. The index of a critical point can be measured using the geometrical method employed for its definition or it can be calculated analytically with the help of Poincaré's formula,

$$\gamma = \frac{1}{2\pi} \oint_C \frac{S_x\, dS_y - S_y\, dS_x}{S_x^2 + S_y^2}, \tag{12}$$

where S_x and S_y are cartesian components of vector field S(r). In most of the cases the integration indicated in (12) is very complicated. In such cases it is advantageous to use the geometric method. Index of rotation is a very important concept. A number of properties of the plane vector fields can be derived with the help of this concept. Two important theorems on this subject will now be stated without proof. These theorems will be utilized later on in this thesis. For a proof of these theorems and a comprehensive discussion on this topic the reader is referred to the excellent work of Krasnoselśkiy et al. [8].

Theorem 1. *If a closed curve C has a finite number of critical points in its interior each with its own index of rotation γ_i then the total index of rotation γ on C is*

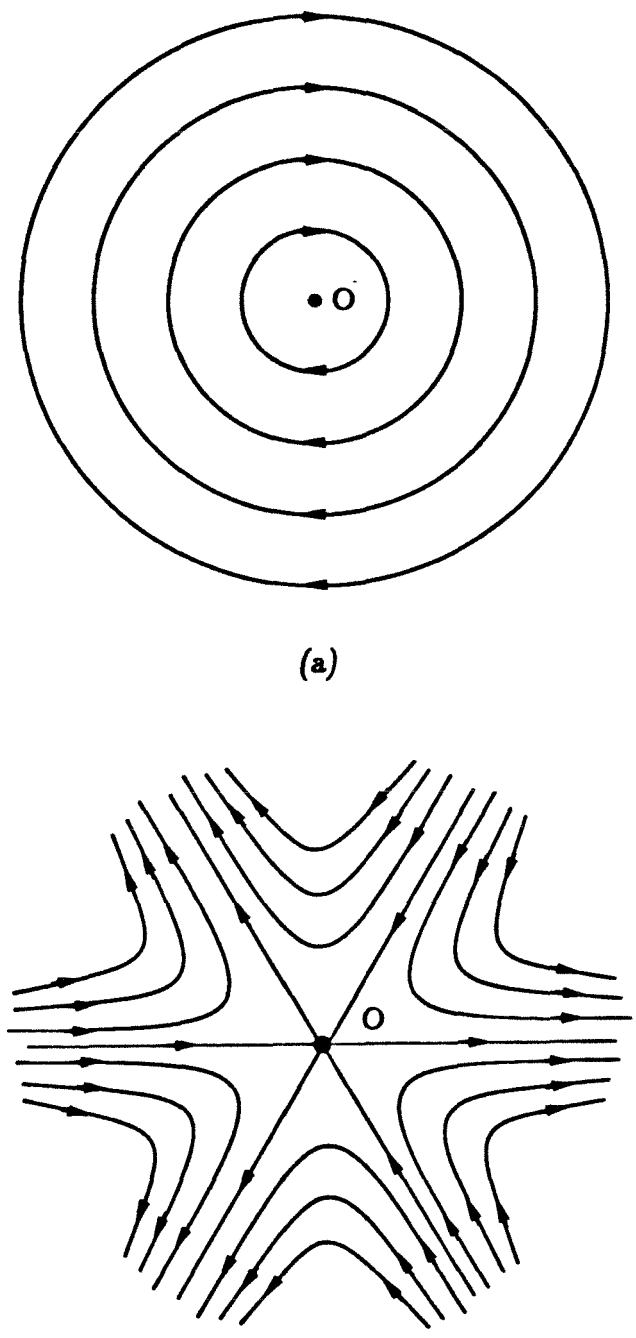

Figure 1. *Critical point is located at O. (a) The index of rotation is 1. (b) The index of rotation is -2.*

the sum of the individual indices of rotation of the critical points, i.e.,

$$\gamma = \sum_i \gamma_i \,. \tag{13}$$

This theorem provides the means to calculate the index of rotation on any given curve without critical points.

Theorem 2. *Two vector fields have an identical index of rotation on a closed curve C if and only if they are homotopic to each other.*

A vector field $\mathbf{S}_p$ is homotopic to another vector field $\mathbf{S}_q$ on a closed curve if the field $\mathbf{S}_p$ can be continuously transformed into the field $\mathbf{S}_q$ without going through a null vector, i.e., a critical point. If a vector field $\mathbf{S}$ can be partitioned as

$$\mathbf{S} = \mathbf{S}_p + \mathbf{S}_q \tag{14a}$$

such that

$$|\mathbf{S}_p| > |\mathbf{S}_q|. \tag{14b}$$

then the component vector field $\mathbf{S}_p$ is called the principal part $\mathbf{S}$ field. Krasnoselśkiy et al. [8] go on to prove that a vector field is homotopic to its principal part. This theorem provides an easy method to calculate the index of rotation if a simple principal part can be extracted from the total field. This method will be utilized in section 8 to calculate the index of rotation of a critical point.

§5. Wave Momentum and Poynting Vector

Consider an E-polarized electromagnetic field. This field is completely described in terms of a complex scalar function of two variables namely the coordinates x and y. This function can be chosen as z directed component of the electric

field. Let this function be expressed in terms of its real and imaginary parts or in terms of its amplitude and phase, i.e.,

$$\begin{aligned} E_z(x,y) &= R(x,y) + iI(x,y) \\ &= A(x,y)\exp\{i\phi(x,y)\}\,. \end{aligned} \tag{15}$$

The functions R, I, A, and ϕ are real valued functions. In physically realizable problems the electric field is well behaved. Therefore it is reasonable to assume that the functions R, I and A are continuous and differentiable. It should be noted that at the points where the amplitude A goes to zero the phase ϕ may become ambiguous. At such points the representation of the electric field in terms of its real and imaginary parts is unique and hence more convenient. The Poynting vector of this field is calculated using (3) and (9) as

$$\begin{aligned} \mathbf{S} &= \frac{1}{2\omega\mu}(R\nabla I - I\nabla R) \\ &= \frac{1}{2\omega\mu}A^2\nabla\phi\,. \end{aligned} \tag{16}$$

There is an interesting interpretation of the Poynting vector in terms of wave momentum for this field. The electric field may be written as

$$E_z(x,y,t) = A(x,y)\cos\{\phi(x,y) - \omega t\}\,, \tag{17}$$

which describes a wave motion in $x-y$ plane. In analogy with plane waves a wave velocity $\mathbf{v}$ may be defined as

$$\mathbf{v} = \frac{\omega}{|\nabla\phi|^2}\nabla\phi\,. \tag{18}$$

The energy density of the wave is proportional to square of its amplitude and therefore the wave momentum $\mathbf{p}$ may be calculated as

$$\mathbf{p} = \frac{2(\text{Energy density})}{|\mathbf{v}|^2}\mathbf{v} \propto \frac{2}{\omega}A^2\nabla\phi\,. \tag{19}$$

Accordingly momentum of the wave is proportional to its Poynting vector.

Chapter II

Classification

§6. Taylor Series Expansion at Critical Points

In regions of space devoid of charges or currents the electric field satisfies homogeneous Helmholtz's equation. Therefore the real and imaginary parts of E_z also satisfy homogeneous Helmholtz's equation, i.e.,

$$\nabla^2 R + k^2 R = 0 \tag{20}$$

and

$$\nabla^2 I + k^2 I = 0\,, \tag{21}$$

where $k = \omega\sqrt{\mu\epsilon}$. The behaviour of the Poynting vector at any particular point can now be studied. For this purpose let the origin of the coordinate system be placed at the point of interest. Circular cylindrical coordinate system with radial coordinate ρ and angular coordinate θ has been employed here. This choice facilitates the ensuing analysis. The solutions to the above differential equations (20) and (21) can be expanded in a series of eigenfunctions which are valid on a disk $\rho < \rho_0$. It is well known that such eigenfunction expansions for Helmholtz's equation in two dimensions are given as

$$R(\rho,\theta) = \sum_{j=0}^{\infty} A_j J_j(k\rho)\cos(j\theta + \alpha_j) \tag{22}$$

and

$$I(\rho,\theta) = \sum_{l=0}^{\infty} B_l J_l(k\rho)\cos(l\theta+\beta_l)\,, \tag{23}$$

where J_j and J_l are Bessel functions of order j and l respectively. A_j, B_l, α_j and β_l are constants of the eigenfunction expansion. These constants can be evaluated for a given problem. Here they are completely arbitrary.

The Poynting vector can now be calculated using (16) and it is given as

$$\begin{aligned}\mathbf{S} = \frac{1}{2\eta}\sum_{j=0}^{\infty}\sum_{l=0}^{\infty} A_j B_l \Big\{ &\cos(j\theta+\alpha_j)\cos(l\theta+\beta_l) \\ &\big\{J_j(k\rho)J_l'(k\rho) - J_l(k\rho)J_j'(k\rho)\big\}\mathbf{e}_\rho + \frac{1}{k\rho}J_j(k\rho)J_l(k\rho) \\ &\big\{j\sin(j\theta+\alpha_j)\cos(l\theta+\beta_l) - l\cos(j\theta+\alpha_j)\sin(l\theta+\beta_l)\big\}\mathbf{e}_\theta\Big\}. \end{aligned}\tag{24}$$

The primes denote differentiation with respect to the argument. The constant η is the impedence of the medium defined as $\eta = \sqrt{\mu/\epsilon}$. Since the Poynting vector field will be investigated in a small neighbourhood around the origin, the Bessel functions $J_n(k\rho)$ may be written as

$$J_n(k\rho) = \frac{1}{2^n n!}(k\rho)^n + O\,(k\rho)^{n+1}\,, \tag{25}$$

where $O\,(k\rho)^{n+1}$ implies that rest of the terms are of the order equal to or greater than $n+1$. Therefore in a small neighbourhood around the origin the components of the Poynting vector can be written down as

$$\begin{aligned} S_\rho = \frac{1}{2\eta}\sum_{j=0}^{\infty}\sum_{l=0}^{\infty} &A_j B_l \cos(j\theta+\alpha_j)\cos(l\theta+\beta_l) \\ &\left\{\frac{l-j}{2^{j+l}j!\,l!}(k\rho)^{j+l-1} + O\,(k\rho)^{j+l+1}\right\}, \end{aligned}\tag{26a}$$

$$\begin{aligned} S_\theta = \frac{1}{2\eta}\sum_{j=0}^{\infty}\sum_{l=0}^{\infty} &A_j B_l \{j\sin(j\theta+\alpha_j)\cos(l\theta+\beta_l) - l\cos(j\theta+\alpha_j)\sin(l\theta+\beta_l)\} \\ &\left\{\frac{1}{2^{j+l}j!\,l!}(k\rho)^{j+l-1} + O\,(k\rho)^{j+l+1}\right\}. \end{aligned}\tag{26b}$$

This may be recognized as the Taylor series expansion of the Poynting vector field around the origin. It is useful to extract the leading term of the above Taylor series. If the expansion coefficients A_j are zero for all $j < m$ and the coefficients B_l vanish for all $l < n$ then the leading non zero terms in (26) may be concisely written as

$$S_\rho = \frac{-C_{mn}}{m+n} (k\rho)^{m+n-1} v'(\theta) + O(k\rho)^{m+n} , \tag{27a}$$

$$S_\theta = C_{mn} (k\rho)^{m+n-1} v(\theta) + O(k\rho)^{m+n} , \tag{27b}$$

where

$$C_{mn} = \frac{A_m B_n}{\eta 2^{m+n+1} n!\, m!} , \tag{28}$$

$$v(\theta) = m \sin(m\theta + \alpha_m) \cos(n\theta + \beta_n) - n \cos(m\theta + \alpha_m) \sin(n\theta + \beta_n) . \tag{29}$$

Throughout this thesis the variables m and n will be used to denote the leading terms in the eigenfunction expansion of R and I respectively. It is observed from equation (27) that the origin is a critical point if and only if $m + n \geq 2$.

A critical point will be called *non degenerate* if the function $v(\theta)$ has no roots or only simple roots. This condition implies that the coefficients α_m and β_n should be such that the set of simultaneous equations

$$\cos(m\theta + \alpha_m) = 0 , \tag{30a}$$

$$\cos(n\theta + \beta_n) = 0 . \tag{30b}$$

has no real solutions. Otherwise the critical point will be referred to as a *degenerate* critical point. If the critical point is non degenerate then the truncated Poynting vector field

$$\mathbf{S}_1 = C_{mn} (k\rho)^{m+n-1} \left\{ -\frac{v'(\theta)}{m+n} \mathbf{e}_\rho + v(\theta) \mathbf{e}_\theta \right\} \tag{31}$$

also has an isolated critical point at the origin. If the critical point is degenerate then $\mathbf{S}_1 = 0$ for $\theta = \theta_i$, where θ_i are solutions to the set of simultaneous

equations (30). If there is at least one value of θ which satisfies (30) then there are exactly $2\gcd(m,n)$ other such values of θ. The behaviour of the flow lines in a small angular sector around θ_i cannot be described correctly by the truncated Poynting vector field $\mathbf{S}_1$ alone. For this purpose higher order terms in (26) should be taken into account.

It may be noted that if $m = n$ and $\alpha_m = \beta_n$ then the leading terms of R and I are proportional and the resulting $\mathbf{S}_1$ is identically zero. It may appear that this critical point is a degenerate critical point but this is not the case. In section 10 it will be shown how to handle this situation by a simple transformation of eigenfunction expansions (22) and (23). At this point it is assumed that if $m = n$ then $\alpha_m \neq \beta_n$. This is not a restrictive assumption. Critical points of any type will not be left out of the classification scheme because of this assumption.

§7. Non Degenerate Critical Points

In this section the behaviour of flow lines in the neighbourhood of a non degenerate critical point will be studied. For this purpose flow lines of the truncated Poynting vector field $\mathbf{S}_1$ will be studied first. The differential equation for the flow lines given by (6) can be modified for the case of two dimensional Poynting vector fields. This modified equation in cylindrical polar coordinates is given as

$$\frac{d\rho}{d\theta} = \rho\frac{S_\rho}{S_\theta}. \tag{32}$$

Substituting the components of $\mathbf{S}_1$ in (32) gives the required differential equation for the flow lines of truncated Poynting vector field, i.e.,

$$\frac{d\rho}{d\theta} = -\frac{1}{m+n}\rho\frac{v'(\theta)}{v(\theta)}. \tag{33}$$

Integration of (33) yields,

$$\rho = K\Big(\big|v(\theta)\big|\Big)^{-1/(m+n)}, \tag{34}$$

where K is the constant of integration. Equation (34) gives a family of curves which coincides with the flow lines of field $\mathbf{S}_1$. The directions of flow can be attached to these curves by inspection of (31).

The behaviour of flow lines is closely connected with the behaviour of function $f(\theta)$ defined as,

$$f(\theta) = |v(\theta)|. \tag{35}$$

Consider the case when $m = n$ then the function $f(\theta)$ is a constant and

$$\rho = K\Big(m|\sin(\alpha_m - \beta_m)|\Big)^{-1/2m} \tag{36}$$

gives a family of concentric circles centered on the origin. Therefore in this case the flow lines form closed loops around the critical point. Such a critical point is designated as a *center point.*

In the case when $m \neq n$, the function $f(\theta)$ has some real roots in $[0, 2\pi)$. Suppose θ_0 is one of the roots. Then the flow line through a point (ρ_0, θ_0) is a ray $\theta = \theta_0$ as depicted in figure 2(a). If $f(\theta_0)$ is a local maximum then the flow lines cut across the ray $\theta = \theta_0$ orthogonally as shown in figure 2(b). If $f(\theta_0)$ is a local minimum different from zero then the flow lines cut across the ray $\theta = \theta_0$ orthogonally and figure 2(c) is representative of this behaviour. The direction of flow lines in figure 2 has been put arbitrarily and figures with reversed directions are equally valid. The directions θ_0 for which $f(\theta_0) = 0$ are called *critical directions* and the flow lines in or out of the critical point are called *critical rays.*

It can be easily shown that the function $f(\theta)$ has $2\max(m, n)$ maxima and they are located at the roots of $\cos(m\theta + \alpha_m) = 0$ if $\max(m, n) = m$ or at the roots of $\cos(n\theta + \beta_n) = 0$ if $\max(m, n) = n$. It can also be shown that $f(\theta)$ possesses $2\min(m, n)$ local minima different from zero. These minima are located at the roots of $\cos(m\theta + \alpha_m) = 0$ if $\min(m, n) = m$ or at the roots of $\cos(n\theta + \beta_n) = 0$

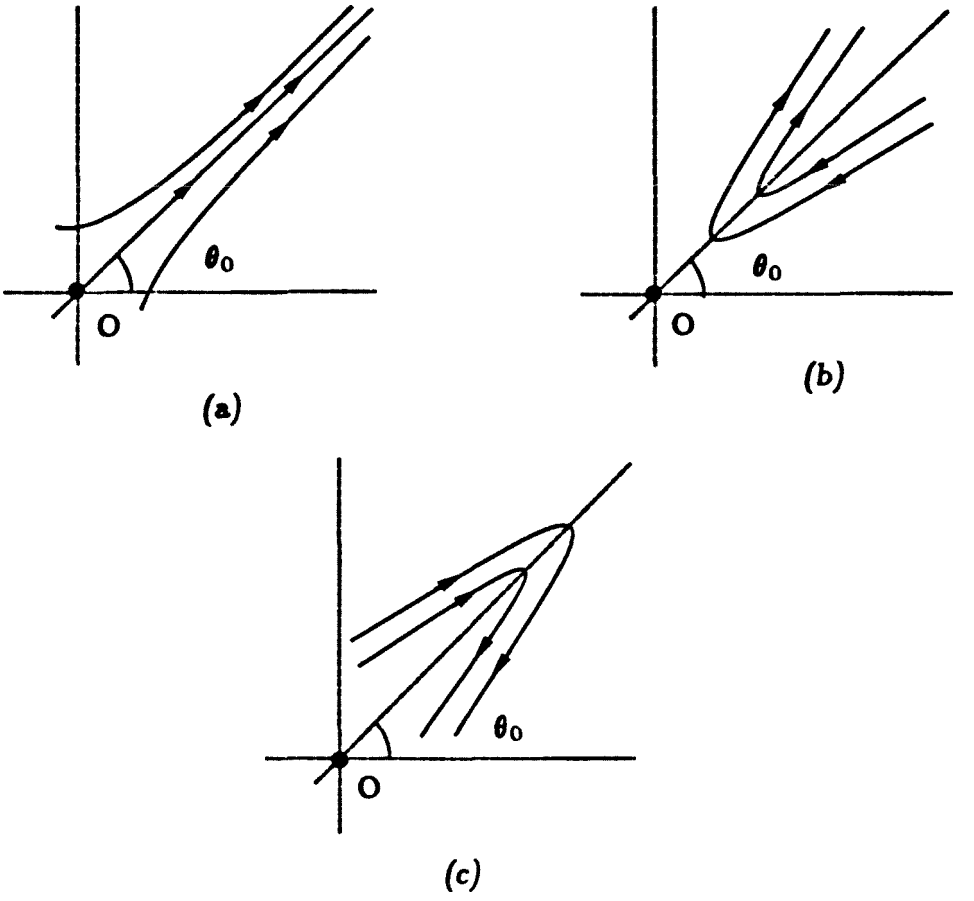

Figure 2. *Possible behaviours of flow lines in a small sector containing the direction θ_0 such that (a) $f(\theta_0)$ is zero, (b) $f(\theta_0)$ is a local maximum and (c) $f(\theta_0)$ is a local minimum.*

if $\min(m,n) = n$. Since $f(\theta)$ is a continuous function it may be deduced from the above discussion that it has exactly $2|m-n|$ simple roots. These roots lie between two extrema of $f(\theta)$ both of which are a local maximum. In short, a non degenerate critical point and the flow lines in its neighbourhood are completely described by four constants m, n, α_m and β_n.

In the case when $\min(m,n) = 0$ the flow lines around the critical point except for their orientation in the $x-y$ plane are characterized by one number alone, i.e., $\max(m,n)$. Such a point is called a *p-sectored saddle point*, where $p = 2\max(m,n)$. In particular if $p = 4$ it is simply called a *saddle point* and if $p = 6$ then it is referred

to in literature as a *monkey saddle*. So much for the nomenclature. In general a critical point can be roughly characterized by the quantity $|m-n|$ alone because its flow lines are homeomorphic to the flow lines of a p-sectored saddle point, where $p = 2|m-n|$. That is to say there are $2|m-n|$ rays coming into or going out of the critical point in critical directions. A circle centered on the critical point is divided by these rays into $2|m-n|$ sectors. In each of these sectors the flow lines form a family of curves which are homeomorphic to one branch of a hyperbola. For the sake of illustration the flow lines in the neighbourhood of two types of critical points are given in figures 3 and 4. In figure 3(a) the function $f(\theta)$ is shown for the case when $m = 2$, $n = 0$ and $\alpha_2 = 0$. The corresponding flow lines are sketched in figure 3(b). In figure 4(a) the function $f(\theta)$ is shown for a critical point whose parameters are $m = 3$, $n = 1$, $\alpha_3 = \pi/2$ and $\beta_1 = 0$. In figure 4(b) the flow lines near this critical point are shown.

Now consider a non degenerate critical point whose Poynting vector field is given by (26). It can be shown using Forster's [9] results that the flow lines of the Poynting vector field in this case will behave essentially as the flow lines of truncated Poynting vector field except in the neighbourhood of a center point. According to Forster a center point of the truncated field may be either a center point or a focal point of the original vector field. A critical point is designated as a *focal point* when all the flow lines in its neighbourhood either emerge from or tend to it as shown in figure 5. Forster's results are general and apply to any plane vector field. But the Poynting vector field is solenoidal and hence field lines cannot emerge from or tend to a single point. Therefore the possiblity of a focal point in the Poynting vector fields has to be ruled out. Hence it is concluded that the behaviour of flow lines in the neighbourhood of a non degenerate critical point is similar to the behaviour of the flow lines of the corresponding truncated field at

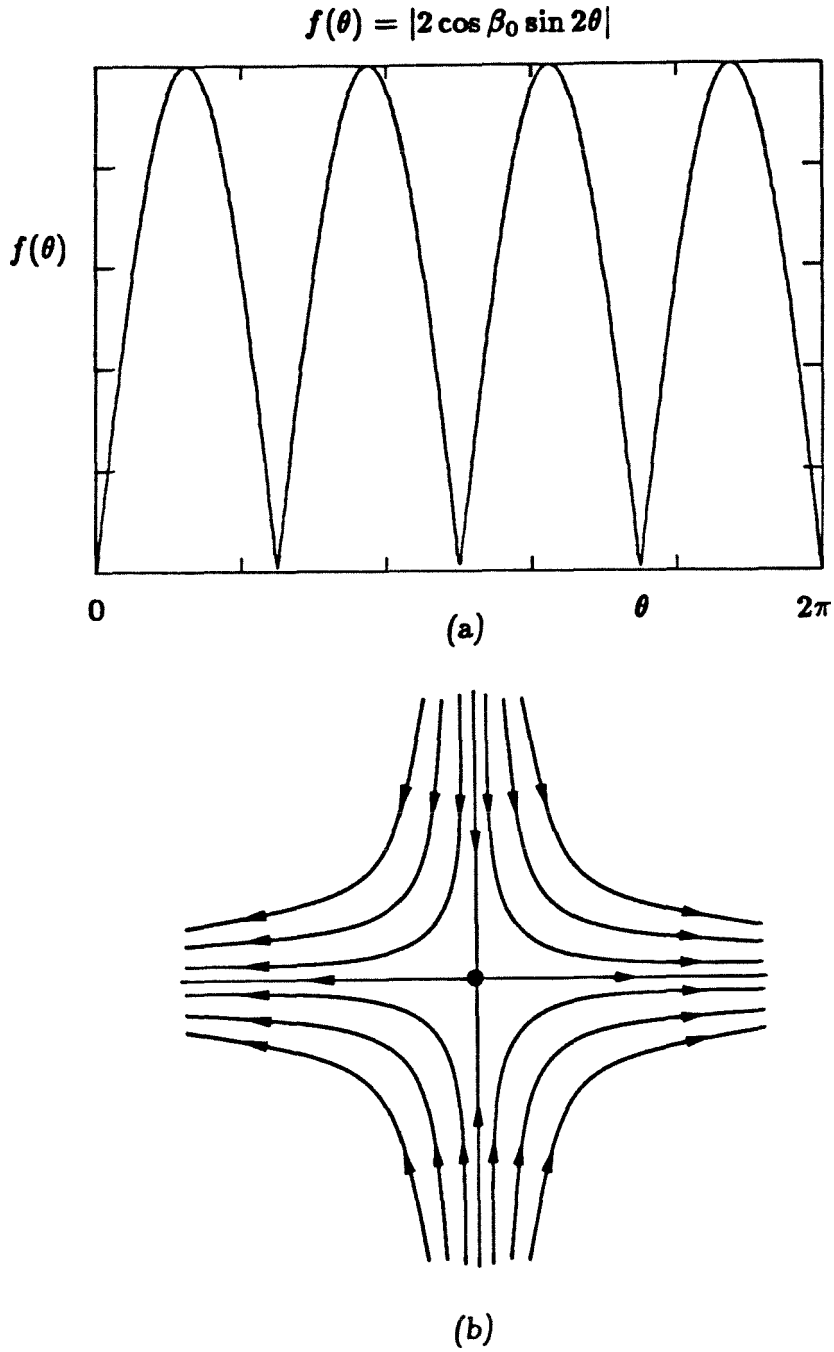

Figure 3. *(a) Plot of the angular function $f(\theta)$ for a critical point whose parameters are $m = 2$, $n = 0$ and $\alpha_2 = 0$. (b) Sketch of the flow lines in the neighbourhood of this critical point.*

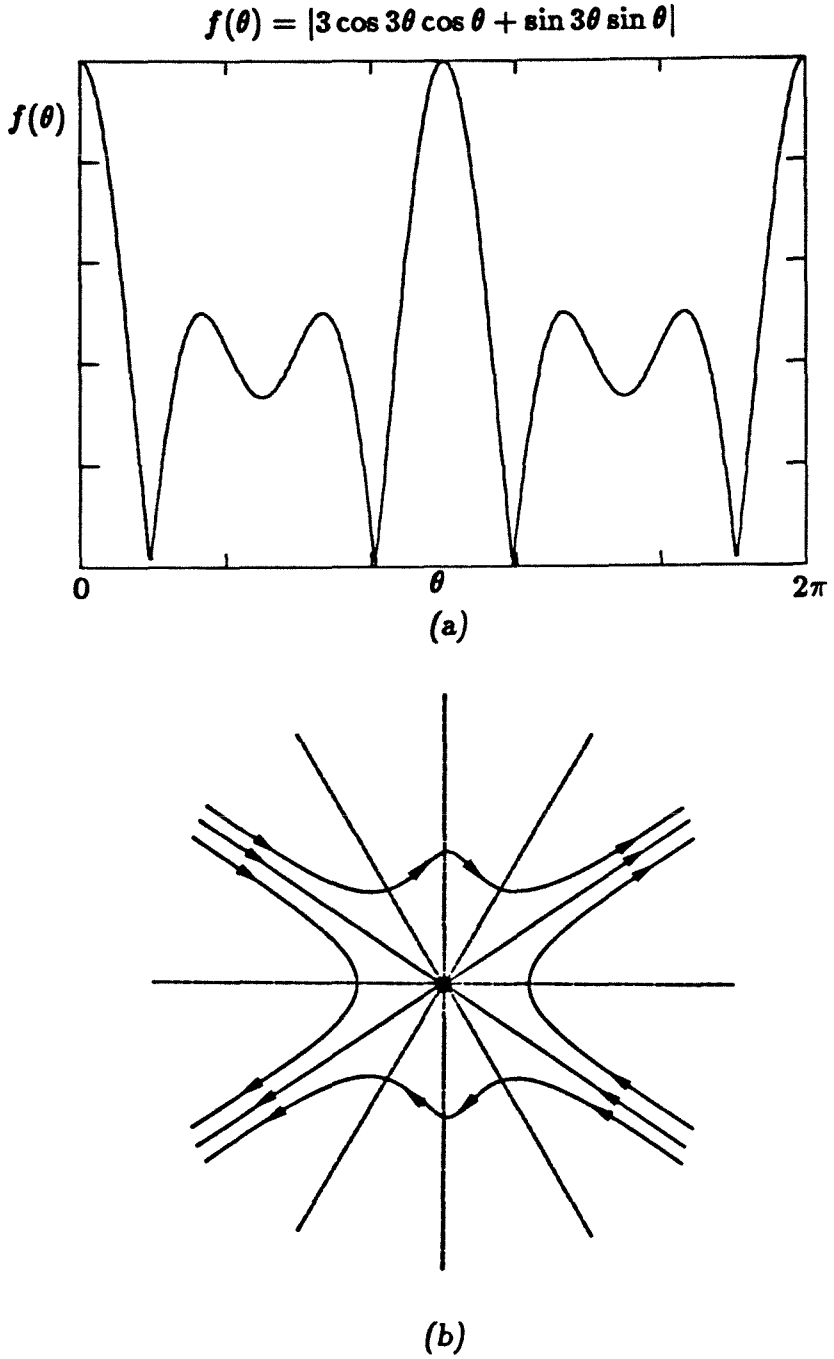

Figure 4. *(a) Plot of the angular function $f(\theta)$ for a critical point whose parameters are $m = 3$, $n = 1$, $\alpha_3 = \pi/2$ and $\beta_1 = 0$. (b) Sketch of the flow lines in the neighbourhood of this critical point.*

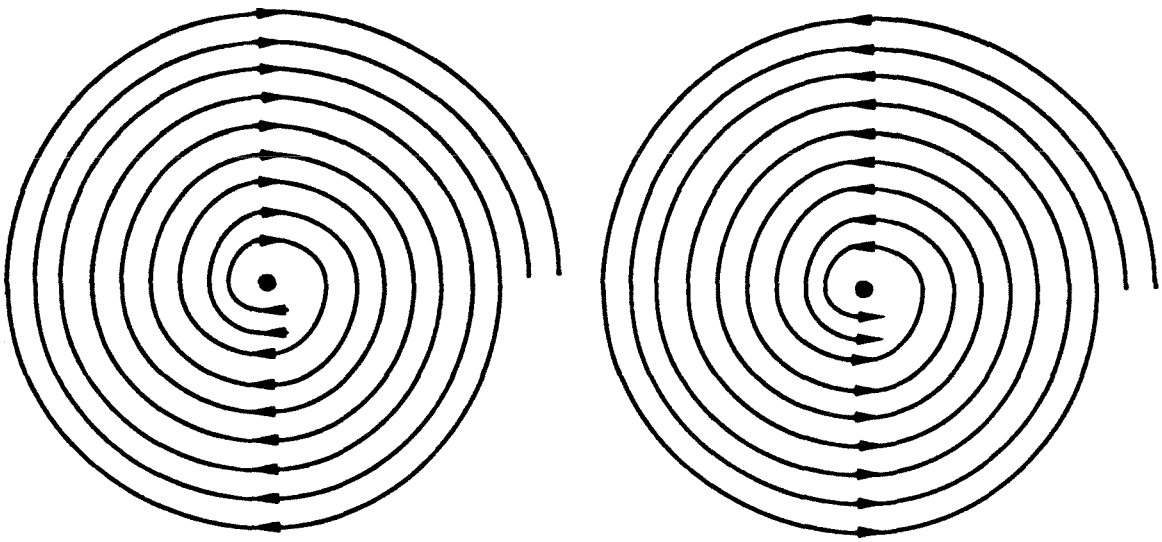

Figure 5. *Lines of flow near a focal point. (a) Focal point behaving as a source. (b) Focal point behaving as a sink.*

that point.

§8. Index of Rotation at Non Degenerate Critical Points

The index of rotation of a non degenerate critical point will now be determined. It has been shown that the index of rotation of a critical point is identical to the index of rotation of the corresponding critical point of the truncated Poynting vector field [10]. The index of rotation γ can be calculated with the help of Poincaré's formula which can be rewritten in terms of cylindrical polar components of the Poynting vector field as

$$\gamma = 1 + \frac{1}{2\pi}\int_0^{2\pi} \frac{S_\rho(\, dS_\theta/d\theta\,) - S_\theta(\, dS_\rho/d\theta\,)}{S_\rho^2 + S_\theta^2}\, d\theta\,. \tag{37}$$

Unit circle is the path chosen to calculate γ, i.e., $k\rho = 1$ in (31). Direct application of (37) leads to a very complicated integral hence the concept of homotopy will

be employed to compute γ. It can be readily verified that the truncated Poynting vector field may be written as

$$\mathbf{S}_1 = \mathbf{S}_p + \mathbf{S}_q\,, \tag{38}$$

where

$$\mathbf{S}_p = C_{mn}(k\rho)^{m+n-1}\Big\{(n-m)\cos\{(n-m)\theta+\beta_n-\alpha_m\}\mathbf{e}_\rho - (n+m)\sin\{(n-m)\theta+\beta_n-\alpha_m\}\mathbf{e}_\theta\Big\}, \tag{38a}$$

$$\mathbf{S}_q = C_{mn}(k\rho)^{m+n-1}\Big\{(m-n)\sin(m\theta+\alpha_m)\sin(n\theta+\beta_n)\mathbf{e}_\rho + \{m\sin(n\theta+\beta_n)\cos(m\theta+\alpha_m) - n\cos(n\theta+\beta_n)\sin(m\theta+\alpha_m)\}\mathbf{e}_\theta\Big\}. \tag{38b}$$

It can easily be shown that

$$|\mathbf{S}_p| > |\mathbf{S}_q|.$$

Hence $\mathbf{S}_p$ represents the principal part of $\mathbf{S}_1$. Therefore the index of rotation will now be calculated with the help of theorem 2. Using the cylindrical polar components of $\mathbf{S}_p$ in (37) the index γ is given as

$$\gamma = 1 - \frac{1}{2\pi}\int_0^{2\pi} \frac{(m+n)(m-n)^2}{m^2+n^2-2mn\cos\{2(m-n)\theta+2\alpha_m-2\beta_n\}}\,d\theta\,. \tag{39}$$

Techniques of complex variables are used to evaluate the above integral which after reduction yields the simple result for the index of rotation

$$\gamma = 1 - |m-n|\,. \tag{40}$$

The index of rotation of the critical point was established using purely analytical techniques. In light of the behaviour of flow lines around the critical point deduced in section 7, the index of rotation can also be calculated from purely

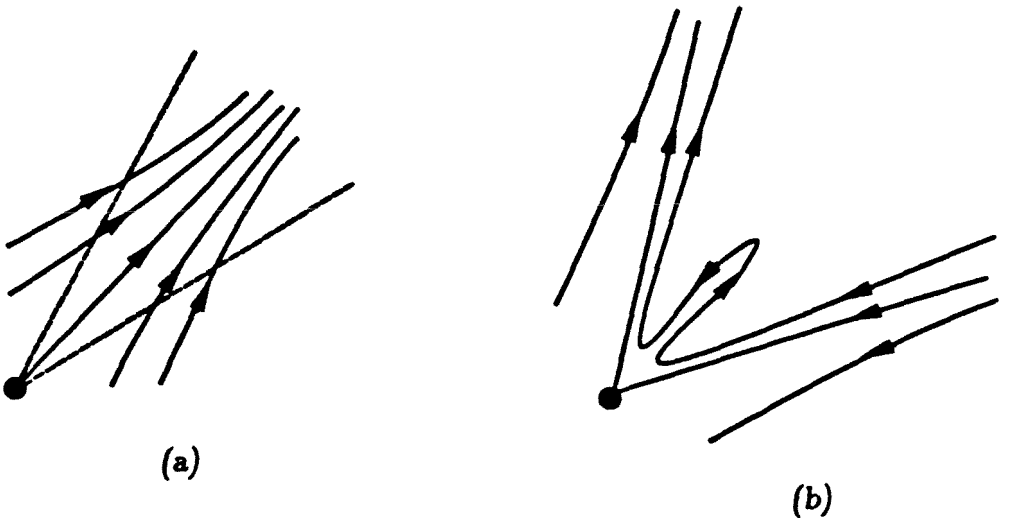

Figure 6. *(a) Flow lines around a critical direction of type II. (b) Flow lines within a hyperbolic domain.*

geometrical arguments. Following Nemytskii and Stepanov [10] a critical direction will be called a critical direction of *type II* if the flow lines, in a small sector containing no other critical direction, behave as depicted in figure 6(a). A sector is labelled as a *hyperbolic domain* if it is bounded by a pair of successive critical directions. A possible behaviour of flow lines in a hyperbolic domain is sketched in figure 6(b) as an example.

If a circular region around the critical point can be completely divided into n_h hyperbolic domains then according to a theorem by Poincaré (see for example [11]) the index of rotation of the critical point is given by

$$\gamma = 1 - \frac{n_h}{2}. \tag{41}$$

Referring back to section 7 it is immediately apparent that the region around the critical point can be completely divided into $2|m - n|$ hyperbolic domains. Therefore the index computed by this method is identical to (40). The method of counting the number of hyperbolic domains to compute the index of rotation will be useful in the discussion of degenerate critical points.

§9. Degenerate Critical Points

This section will be devoted to the study of degenerate critical points. The constants α_m and β_n have to satisfy exactly the set of simultaneous equations (30) for some values of θ. In most of the cases this is not a probable scenario yet the case of degenerate critical points will be taken up for the sake of completeness.

Let θ_0 be a root of the set of simultaneous equations (30) then the truncated Poynting vector field may be expanded in a Taylor series around θ_0. Keeping only the leading terms in this expansion, $\mathbf{S}_1$ may be written as

$$\mathbf{S}_1 = \pm mn(n-m)C_{mn}(k\rho)^{m+n-1}\left\{(\theta-\theta_0)^2\mathbf{e}_\rho - \frac{m+n}{3}(\theta-\theta_0)^3\mathbf{e}_\theta\right\}. \quad (42)$$

The $\pm$ sign in front of (42) is of no practical significance and will depend on which of the roots of system (30) is under consideration. According to Nemytskii and Stepanov [10] the direction θ_0 remains a critical direction if

$$\lim_{\rho\to 0}\lim_{\theta\to\theta_0}\frac{S_\theta}{S_\rho} = 0, \quad (43)$$

where S_ρ and S_θ are the components of the total Poynting vector field. Using the Taylor series expansion (42) in the expression (27) for the components of S, it is easy to show that the condition enunciated in (43) is satisfied. Therefore all the directions θ_0 which are the roots of system of equations (30) remain critical directions for the untruncated Poynting vector field.

To study the behaviour of the flow lines in a small sector $|\theta-\theta_0| < \delta$ and $\rho < \rho_0$, higher order terms in the expansion (27) will have to be taken into account. The next higher order term is of the order $m+n$ in (27). Since the divergence of the Poynting vector is zero term by term in expansion (26), the $(m+n)$th term of S can be written as

$$\mathbf{S} = (k\rho)^{m+n}\left\{\frac{-1}{m+n}g'(\theta)\mathbf{e}_\rho + g(\theta)\mathbf{e}_\theta\right\} \quad (44)$$

in the sector $|\theta - \theta_0| < \delta$ and $\rho < \rho_0$, where δ and ρ_0 are small constants. The form of the function $g(\theta)$ is not important for this discussion except that it is continuous and differentiable which is guaranteed from (26). There are two cases to be considered.

The first case arises when $g(\theta_0) \neq 0$. In this case the function $g(\theta)$ may be approximated as a constant in the sector under consideration. Let g_0 be such a constant. Then the Poynting vector in this sector may be approximately written as

$$\mathbf{S} = \tilde{C}(k\rho)^{m+n-1}\left\{(\theta-\theta_0)^2\mathbf{e}_\rho - \frac{m+n}{3}(\theta-\theta_0)^3\mathbf{e}_\theta\right\} + g_0(k\rho)^{m+n}\mathbf{e}_\theta\,, \qquad (45)$$

where $\tilde{C}$ is a new constant obtained by lumping the constants in (42). In the sector under consideration the flow lines have the behaviour indicated in figure 7(a) according to expression (45). It is assumed that the Poynting vector field given by (45) is sufficient to characterize the flow lines of the untruncated Poynting vector field. It is also seen from figure 7(a) that the critical direction is of type II.

The second case arises when $g(\theta_0) = 0$ but $g'(\theta_0) \neq 0$. In this case $g(\theta)$ may be approximated as a linear function in the sector under consideration, i.e.,

$$g(\theta) = g_1\{\theta - \theta_0\} \qquad \text{in} \qquad |\theta - \theta_0| < \delta,\ \rho < \rho_0, \qquad (46)$$

where g_1 is a constant. Then the Poynting vector, up to the leading term is given as

$$\begin{aligned}\mathbf{S} = \tilde{C}(k\rho)^{m+n-1}&\left\{(\theta-\theta_0)^2\mathbf{e}_\rho - \frac{m+n}{3}(\theta-\theta_0)^3\mathbf{e}_\theta\right\}\\ &+ g_1(k\rho)^{m+n}\left\{\frac{-1}{m+n}\mathbf{e}_\rho + (\theta-\theta_0)\mathbf{e}_\theta\right\}. \qquad (47)\end{aligned}$$

Expression (47) is utilized to investigate the behaviour of the flow lines in a given sector. If $g_1\tilde{C} > 0$ then the qualitative behaviour of the flow lines of S is given in

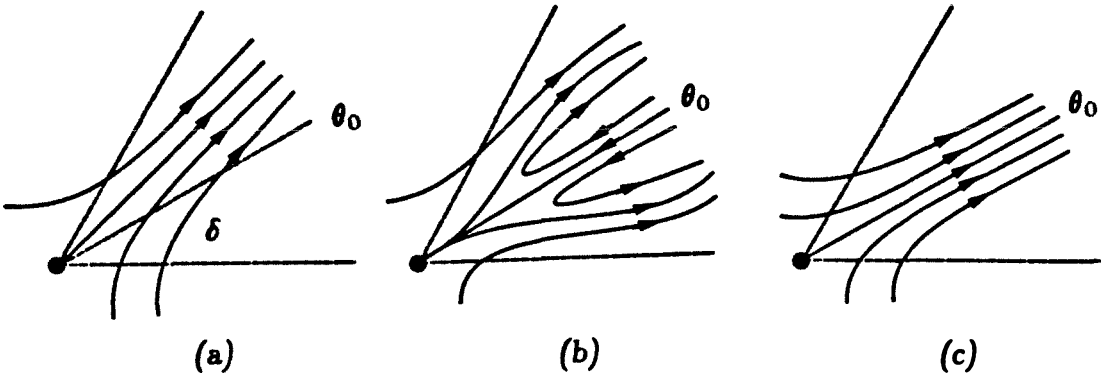

Figure 7. *Behaviour of the flow lines of* **S** *field in the neighbourhood of a critical direction of the truncated Poynting vector field. There are three cases, (a) the constant* $g_0 \neq 0$, *(b) when* $g_1\tilde{C} > 0$, *(c) and when* $g_1\tilde{C} < 0$.

figure 7(b). It is observed that two new hyperbolic domains have been created in this case. If $g_1\tilde{C} < 0$ then the behaviour of flow lines is indicated in figure 7(c). In this case it may be noticed that the critical direction is of type II and no new hyperbolic domain has been created. Once again it is assumed that the behaviour of the Poynting vector field is completely characterized by the approximate field given in (47).

In sectors around the critical point which do not include a critical direction, the behaviour of flow lines is described by the truncated Poynting vector field. This behaviour will depend on the function $f(\theta)$ which has been discussed in section 7. If it happens that both the constants, g_0 and g_1 are zero, i.e., $g(\theta_0) = g'(\theta_0) = 0$ then the next term of higher order in expression (26) should be taken into account. This term will have a representation similar to expression (44) except that the power of $(k\rho)$ will change from $m+n$ to an appropriate greater number. The above method of analysis can once again be applied. This procedure may be repeatedly applied till a function $g(\theta)$ is found such that $g(\theta_0) \neq 0$ or $g'(\theta_0) \neq 0$.

The index of rotation of a degenerate critical point cannot be calculated from a knowledge of m and n of the truncated Poynting vector field only. The behaviour of the flow lines in each of the $2\,\mathrm{gcd}(m,n)$ sectors has to be known to compute the index, γ. With the help of following straightforward geometrical argument the index of rotation can be computed. If there are j_1, j_2 and j_3 sectors with the behaviour of their flow lines as depicted in figures 7(a), 7(b) and 7(c) respectively then

$$j_1 + j_2 + j_3 = 2\,\mathrm{gcd}(m,n)\,. \tag{48}$$

Since the number of hyperbolic sectors increases by $2j_2$, i.e.,only in the case when $g_1\tilde{C} > 0$, the index of rotation is given as

$$\gamma = 1 - |m-n| - j_2\,. \tag{49}$$

This result follows directly from equation (41).

§10. Critical Points Due to Arbitrary Electric Field

In section 6 it was observed that when $m = n$ and $\alpha_m = \beta_n$, the critical point is not a degenerate critical point. In this section this statement will be explained. In the previous discussions all possible behaviours of the flow lines of the Poynting vector field have been classified. This classification has been in terms of real and imaginary parts of the electric field, namely, the functions R and I. The eigenfunction expansions of these functions, given in equations (22) and (23), will be termed as canonical forms. The following question will now be posed. Given an arbitrary electric field, how can one characterize the behaviour of flow lines in the neighbourhood of a critical point using only m and n? This question is crucial because two electric fields differing by an arbitrary phase constant give rise to the same Poynting vector field although they have different real and imaginary

parts. To illustrate this point, consider an arbitrary electric field $\tilde{E}_z$ such that

$$\tilde{E}_z = E_z \exp(i\phi_0)\,, \tag{50}$$

where E_z is canonical electric field and ϕ_0 is a constant. The real and imaginary parts of this electric field in terms of canonical real and imaginary parts are given as

$$\tilde{R} = R\cos\phi_0 - I\sin\phi_0\,, \tag{51a}$$

$$\tilde{I} = R\sin\phi_0 + I\cos\phi_0\,. \tag{51b}$$

If the origin is a critical point then the canonical eigenfunction expansions can be written as

$$R = \sum_{j=m}^{\infty} A_j J_j(k\rho)\cos(j\theta + \alpha_j)\,, \tag{52a}$$

$$I = \sum_{l=n}^{\infty} B_l J_l(k\rho)\cos(l\theta + \beta_l)\,. \tag{52b}$$

If the analysis of the critical point is made, on the basis of leading term, in the expressions for $\tilde{R}$ and $\tilde{I}$, one encounters an apparent discrepancy. It is evident from equations (51) and (52) that the leading terms of $\tilde{R}$ and $\tilde{I}$ are of the same order, which is the minimum of m and n. Thus one may conclude that the critical point is a center point. Such a conclusion would be in error because m and n are not equal in general. An analysis of canonical electric field will yield a different result. To resolve this discrepancy, without the loss of generality suppose that $m \leq n$. Substitution of equation (52) in (51) results in

$$\begin{aligned}\tilde{R} = &\sum_{j=m}^{n-1} A_j J_j(k\rho)\cos\phi_0\cos(j\theta + \alpha_j) \\ &+ \sum_{j=n}^{\infty} J_j(k\rho)\Big\{A_j\cos\phi_0\cos(j\theta + \alpha_j) - B_j\sin\phi_0\cos(j\theta + \beta_j)\Big\}\,,\end{aligned} \tag{53a}$$

$$\tilde{I} = \sum_{j=m}^{n-1} A_j J_j(k\rho) \sin\phi_0 \cos(j\theta + \alpha_j)$$
$$+ \sum_{j=n}^{\infty} J_j(k\rho) \Big\{ A_j \sin\phi_0 \cos(j\theta + \alpha_j) + B_j \cos\phi_0 \cos(j\theta + \beta_j) \Big\} . \quad (53b)$$

If $m = n$ then the first summation in expressions (53a) and (53b) disappears. The leading terms in the expansions of $\tilde{R}$ and $\tilde{I}$ are of the same order. These terms are not proportional to each other. In this case the lines of flow of the Poynting vector field form concentric circles and the origin is a center point.

On the other hand if $m \neq n$ then $\tilde{R}$ and $\tilde{I}$ are of equal order. Their leading terms are proportional. The phase constant ϕ_0 can be calculated from the leading terms as

$$\phi_0 = \tan^{-1} \left\{ \frac{\text{Leading term of } \tilde{I}}{\text{Leading term of } \tilde{R}} \right\} . \quad (54)$$

Using this value of ϕ_0 it is possible to calculate the canonical form of the electric field as

$$R = \tilde{R} \cos\phi_0 + \tilde{I} \sin\phi_0 , \quad (55a)$$

$$I = -\tilde{R} \sin\phi_0 + \tilde{I} \cos\phi_0 . \quad (55b)$$

With the help of m and n of the canonical electric field derived above it will be possible to classify the behaviour of the flow lines. There is no need to calculate the Poynting vector field. The assumption that $m \leq n$ forces the leading term of R to be of order m. This is not restrictive as far as classification of the critical points is concerned. This assumption works because the qualitative behaviour of the flow lines depends only on the quantities $m + n$ and $|m - n|$, which are symmetrical in m and n.

§11. Magnetic Field at Critical Points

In the case of E-polarized electromagnetic fields given by equation (9), the magnetic field is completely in the x-y plane. In general this magnetic field is elliptically polarized and can be written down as

$$\mathbf{H} = \mathbf{H}_R + i\mathbf{H}_I = \frac{1}{\omega\mu}\left(\nabla I \times \mathbf{e}_z - i\nabla R \times \mathbf{e}_z\right). \tag{56}$$

It is of interest to investigate the magnetic field in the neighbourhood of a critical point of the Poynting vector field. The Poynting vector field is approximated by the truncated Poynting vector field $\mathbf{S}_1$ which in turn is calculated using the leading terms of R and I. The magnetic field can be approximately calculated with the help of the same leading terms. The fields near the origin are of particular interest, therefore, the Bessel functions can be approximated as in equation (25). Thus the leading terms of real and imaginary parts of the magnetic field are given as

$$\mathbf{H}_R = \frac{-nB_n}{\eta 2^n n!}(k\rho)^{n-1}\left\{\sin(n\theta+\beta_n)\mathbf{e}_\rho + \cos(n\theta+\beta_n)\mathbf{e}_\theta\right\}, \tag{57a}$$

$$\mathbf{H}_I = \frac{mA_m}{\eta 2^m m!}(k\rho)^{m-1}\left\{\sin(m\theta+\alpha_m)\mathbf{e}_\rho + \cos(m\theta+\alpha_m)\mathbf{e}_\theta\right\}. \tag{57b}$$

The major and minor diameters of the polarization ellipse are designated as d_1 and d_2 respectively. They are calculated to be

$$d_1 = \sqrt{\frac{1}{2}\left\{\mathbf{H}\cdot\mathbf{H}^* + \sqrt{(\mathbf{H}\cdot\mathbf{H}^*)^2 - 4\left(|\mathbf{H}_R \times \mathbf{H}_I|\right)^2}\right\}}, \tag{58a}$$

$$d_2 = \sqrt{\frac{1}{2}\left\{\mathbf{H}\cdot\mathbf{H}^* - \sqrt{(\mathbf{H}\cdot\mathbf{H}^*)^2 - 4\left(|\mathbf{H}_R \times \mathbf{H}_I|\right)^2}\right\}}. \tag{58b}$$

The magnetic field is linearly polarized when $d_2 = 0$. The direction of rotation of the $\mathbf{H}$ vector can be deduced as follows

$$\mathbf{H}_R \times \mathbf{H}_I \cdot \mathbf{e}_z \begin{cases} > 0 & \text{counterclockwise,} \\ = 0 & \text{linear,} \\ < 0 & \text{clockwise.} \end{cases} \tag{59}$$

It can be easily shown that

$$\nabla \times \mathbf{S} = \omega\mu\, \mathbf{H}_R \times \mathbf{H}_I. \tag{60}$$

Therefore information about the polarization of the magnetic field can also be gleaned from the curl of the Poynting vector. In the present case equation (59) implies that

$$mn \sin\Big((m-n)\theta + \alpha_m - \beta_n\Big) \begin{cases} > 0 & \text{counterclockwise,} \\ = 0 & \text{linear,} \\ < 0 & \text{clockwise.} \end{cases} \tag{61}$$

If $m = n$, then the magnetic field is elliptically polarized in the same sense everywhere in the neighbourhood of the critical point, which is a center point. If the condition, $m \neq n \neq 0$ holds, then the region around the critical point is divided into $2|m-n|$ equiangular sectors. The polarization is linear on the boundaries of these sectors. The sense of rotation is alternately clockwise and anticlockwise in the contiguous sectors. It may be recalled that the critical point, for which $m \neq n$, is isomorphic to a saddle point with $2|m-n|$ hyperbolic sectors.

As a result of above discussion it becomes clear that the morphology of flow lines at a critical point may be determined from a knowledge of the sense of rotation of the magnetic field on a small circle around the critical point. For example, suppose, there is a critical point. The sense of rotation of the magnetic field is measured on a circle of small radius, centered on the critical point. It is found that the sense is clockwise on q number of arcs interleaved with q number of arcs on which sense of rotation is anticlockwise. It may then be concluded that critical point under investigation has a flow line structure which is isomorphic to the flow line structure in the neighbourhood of a $2q$-sectored saddle point. As a bonus one may also calculate the index of rotation of the critical point from such a measurement using the expression

$$\gamma = 1 - q\,. \tag{62}$$

If either $m = 0$ or $n = 0$ then the magnetic field is linearly polarized in the vicinity of the critical point.

§12. Elementary Critical Points

The order of a critical point is defined to be the degree of the leading term in the Taylor series expansion of the Poynting vector field given by expression (26). This Taylor series is expanded about the critical points. Therefore in terms of the notation employed in this thesis, the order of a critical point is $(m + n - 1)$. The lowest possible order of any critical point is one. The critical points of order one are called *elementary* critical points. For elementary critical points $m + n = 2$. There are two distinct cases. In the first case m and n are equal while in the second case they are not equal. Elementary critical points are the subject of discussion in this section and both the cases will be dealt separately.

The first case arises when $m = n = 1$. This is the case when the lines of the Poynting vector field are known to circulate the critical point, which is also called a center point. The lowest order critical point of this type will be labelled as an elementary center point. It follows from section 6 that the magnitude of the electric field is zero at this critical point. The phase of the electric field is undefined at this type of critical point. Lines of constant phase emanate radially outward from the critical point and they are sketched in figure 8. The magnetic field at the critical point is not zero. It can be obtained from equation (57) by letting m and n to be equal to one, i.e.,

$$\mathbf{H} = \frac{1}{2\eta}\left\{\left(-B_1 \sin\beta_1 + iA_1 \sin\alpha_1\right)\mathbf{e}_x + \left(-B_1 \cos\beta_1 + iA_1 \cos\alpha_1\right)\mathbf{e}_y\right\}. \qquad (63)$$

The magnetic field is elliptically polarized and the expression for the polarization ellipse is given as

$$\left(A_1^2 \cos^2\alpha_1 + B_1^2 \cos^2\beta_1\right)H_x^2 + \left(A_1^2 \sin^2\alpha_1 + B_1^2 \sin^2\beta_1\right)H_y^2$$

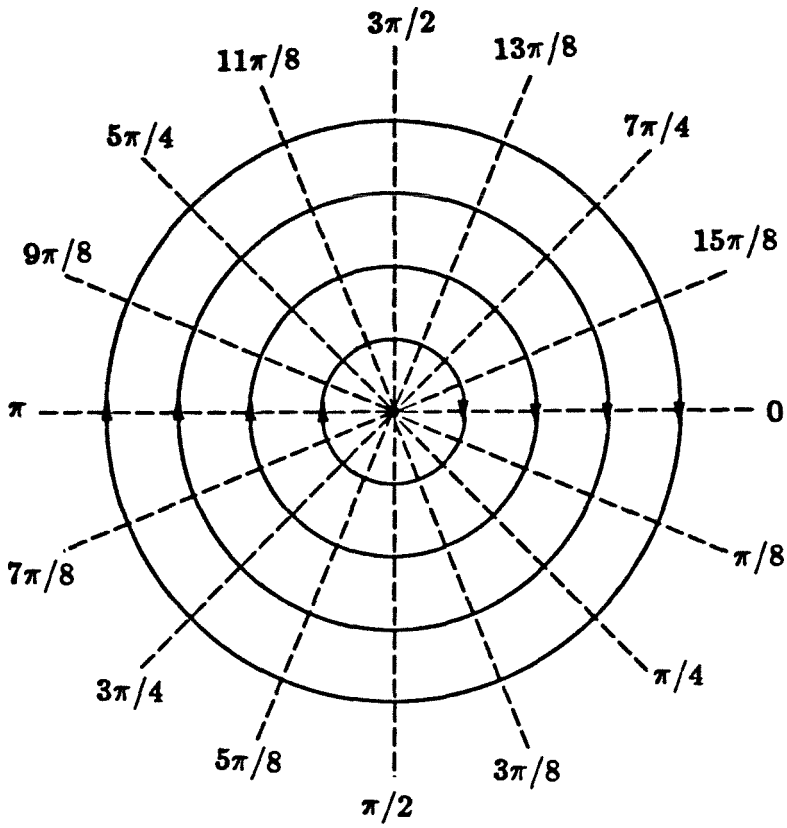

Figure 8. *The lines of flow and the lines of constant phase in the neighbourhood of an elementary center point. The phase is undefined at the center.*

$$-\left(A_1^2 \sin 2\alpha_1 + B_1^2 \sin 2\beta_1\right) H_x H_y = 4\eta^2 A_1^2 B_1^2 \sin^2(\alpha_1 - \beta_1)\,. \quad (64)$$

The electric field energy density, W_e, is zero at the critical point and it increases in the neighbourhood. The contours of constant energy density are ellipses and are given by

$$W_e = \frac{\epsilon}{4}\Big\{\left(A_1^2 \cos^2\alpha_1 + B_1^2 \cos^2\beta_1\right)(kx)^2 + \left(A_1^2 \sin^2\alpha_1 + B_1^2 \sin^2\beta_1\right)(ky)^2 - \left(A_1^2 \sin 2\alpha_1 + B_1^2 \sin 2\beta_1\right)(kx)(ky)\Big\}\,. \quad (65)$$

Comparison of equations (64) and (65) brings out an interesting fact that the polarization ellipse is similar to the contours of constant electric field energy density.

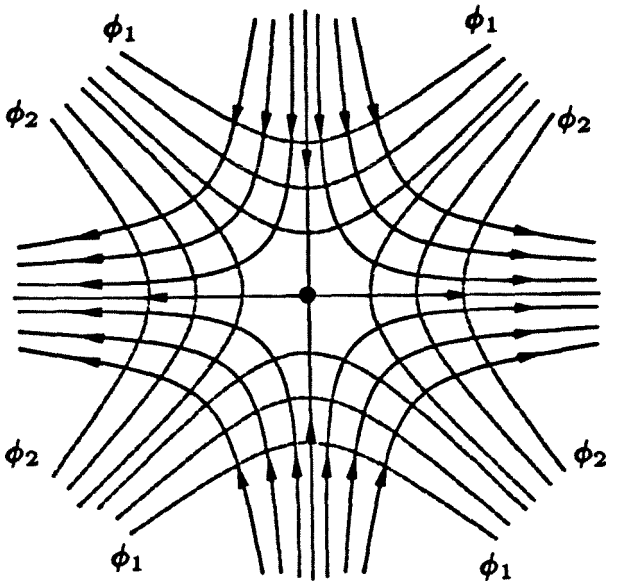

Figure 9. *The lines of flow and the lines of constant phase in the neighbourhood of an elementary saddle point.*

Therefore if the polarization ellipse is measured at one point near an elementary center point, the rate of increase of W_e in different directions can be predicted.

The second case of elemetary critical point arises when $m = 2$ and $n = 0$ or vice versa. Without loss of generality it will be assumed that $m > n$. in this case the lines of flow form a family of rectangular hyperbolae. The lines of constant phase which are orthogonal to the lines of flow also form a family of rectangular hyperbolae. Such a critical point is called an elementary saddle point. The flow lines near an elementary saddle point are depicted in figure 9. The polarization of the magnetic field is linear in the neighbourhood of this critical point. Neither the electric field nor the magnetic field is zero at the elementary saddle point. These fields are in time quadrature at this type of critical point and this is the reason why the Poynting vector is zero.

It may be verified that the elementary critical points are always non degenerate. This verification can be carried out by substituting appropriate values for m and n in equation (29) and checking the conditions stipulated in equation (30). There are reasons to believe that the elementary critical points are encountered more often in real problems than the critical points of higher order. The reasons for this belief will be discussed later. At this juncture it is appropriate to discuss ways and means to detect the elementary critical points and determine their nature. For this purpose consider a long wire made of a good condutor. Let the diameter of this wire be much smaller than the wavelength. Place the wire parallel to the z-axis. It will experience a force proportional the strength of the Poynting vector field and in the same direction. At the critical point the Poynting vector field is zero and hence at this point no net time average force will be exerted on the wire. Therefore in principle one can locate the critical points by moving a wire in the electromagnetic field and measuring force on it. If the electromagnetic field is E-polarized then the current induced in the wire will be proportional to E_z. Therefore at a center point no current will be induced in the wire. At the saddle point the electric field is not zero hence current will be induced in the wire but no average force will be exerted on it. Thus the induced current will distinguish a saddle point from a center point. Another method to distinguish between these two types of critical points is to construct a device similar to a vane. It is constructed with the help of two long straight wires of diameters which are small in comparison with the wavelength. The wires are connected together by a piece of light insulating material such as plastic. A sketch of this contraption appears in figure 10(a). This device is capable of measuring a torque about its axis due to the radiation pressure. If the axis is placed in such a way that it coincides with a center point then a net torque will be exerted on the device and it will rotate. On the other hand if the axis is placed on the saddle point the device will tend to align

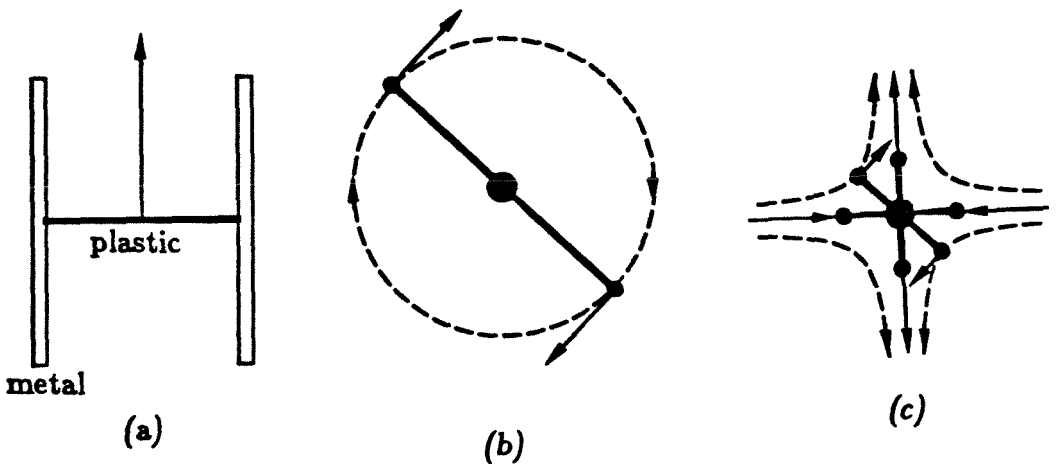

Figure 10. *(a) A device which may be used to distinguish a center point from a saddle point. (b) The behaviour of the device at a center point and (c) a saddle point.*

itself with one of the arms of the saddle point because in this configuration the net force and the net torque on it are zero. The behaviour of this device is illustrated in figure 10. It may be noted that the device described above is sensitive to the curl of the Poynting vector field which is finite and non zero for the center point and zero for the saddle point. At this point it may be noted that Latmiral's [7] suggestion on using a tuned dipole as a true sensor of the curl of **S** is not workable in the case of plane Poynting vector fields. The reason is that once the dipole is aligned with E_z and charges are induced on its ends there is no transverse part of the electric field to act on these charges. Thus there will be no rotation of the dipole.

§13. Wave Interference: Example of Critical Points

In the previous discussions it was assumed that isolated critical points of the Poynting vector field exist. No examples were given. The existence of these points will now be demonstrated in a fairly simple situation. It is well known that the

Poynting vector of a standing wave is zero everywhere. Therefore it is logical to look for critical points in the problems in which the electromagnetic field is a slight variation of a standing wave field. Consider the interference of three linearly polarized plane waves travelling in the directions which make angles 0°, 180° and θ_o with the x-axis. The amplitudes of their respective electric fields are $\frac{1}{2}$, $\frac{1}{2}$ and α. Thus the total electric field is given as

$$\mathbf{E} = \left\{ \frac{1}{2}\exp(ikx) + \frac{1}{2}\exp(-ikx) + \alpha\exp(ikx\cos\theta_o + iky\sin\theta_o) \right\} \mathbf{e}_z . \qquad (66)$$

The first two waves alone would form a standing wave. The case $\theta_o = 90°$ was considered by Braunbek [12] to demonstrate the existence of critical points. This example is rich enough to elucidate many other aspects of critical points rather than merely demonstrate their existence. These aspects will be brought out later by varying the quantities α and θ_o. If $\theta_o = 90°$, then the Poynting vector is given as

$$\mathbf{S} = \frac{\alpha}{2\eta}\left\{ \sin(kx)\sin(ky)\mathbf{e}_x + \big(\alpha + \cos(kx)\cos(ky)\big)\mathbf{e}_y \right\} . \qquad (67)$$

This Poynting vector field does not possess any critical points if $|\alpha| > 1$. If $\alpha = 0$ then the Poynting vector is zero everywhere and all the points are critical points but they are not isolated. If the range of α is restricted such that $0 < |\alpha| \leq 1$ then there are four sets of points where the S field has isolated critical points. Let these sets be denoted by P_1, P_2, P_3 and P_4. These sets are enumerated as

$$P_1 : \left\{ (kx, ky) \;\middle|\; kx = 2q_1\pi \pm \cos^{-1}\alpha\,,\; ky = (2q_2+1)\pi \right\}, \qquad (68a)$$

$$P_2 : \left\{ (kx, ky) \;\middle|\; kx = (2q_1+1)\pi \pm \cos^{-1}\alpha\,,\; ky = 2q_2\pi \right\}, \qquad (68b)$$

$$P_3 : \left\{ (kx, ky) \;\middle|\; kx = (2q_1+1)\pi\,,\; ky = 2q_2\pi \pm \cos^{-1}\alpha \right\}, \qquad (68c)$$

$$P_4 : \left\{ (kx, ky) \;\middle|\; kx = 2q_1\pi\,,\; ky = (2q_2+1)\pi \pm \cos^{-1}\alpha \right\}, \qquad (68d)$$

where q_1 and q_2 are any integers and the range of $\cos^{-1}\alpha$ is restricted to $[0, \pi]$. If $0 < |\alpha| < 1$ then all the critical points are found to be elementary critical points.

Such an analysis also yields the information that points corresponding to the sets P_1 and P_2 are elementary center points and the points corresponding to the sets P_3 and P_4 are elementary saddle points. If $\alpha = 1$ the set P_1 is identical to the set P_4 and the set P_2 is identical to the set P_3. If $\alpha = -1$ then the set P_1 coincides with the set P_3 and the set P_2 coincides with set P_4. In both of the above cases the critical points are not elementary. These are critical points of order 2 with the indices $m = 2$ and $n = 1$.

An explicit expression for the lines of flow of the Poynting vector field can be can be obtained by the integration of differential equation (6). This expression is given by

$$\sin(kx)\cos(ky) + \alpha(kx) = \text{constant}. \tag{69}$$

Sketches of the flow lines for the two cases $0 < |\alpha| < 1$ and $|\alpha| = 1$, are given in figures (11a) and (11b) respectively. A cursory glance at these figures is enough to show that they are qualitatively different. The cases $\alpha = 0$ and $|\alpha| = 1$ are borderline cases in which the behaviour of flow lines changes drastically. Such changes and how they come about will be the next the topic of discussion.

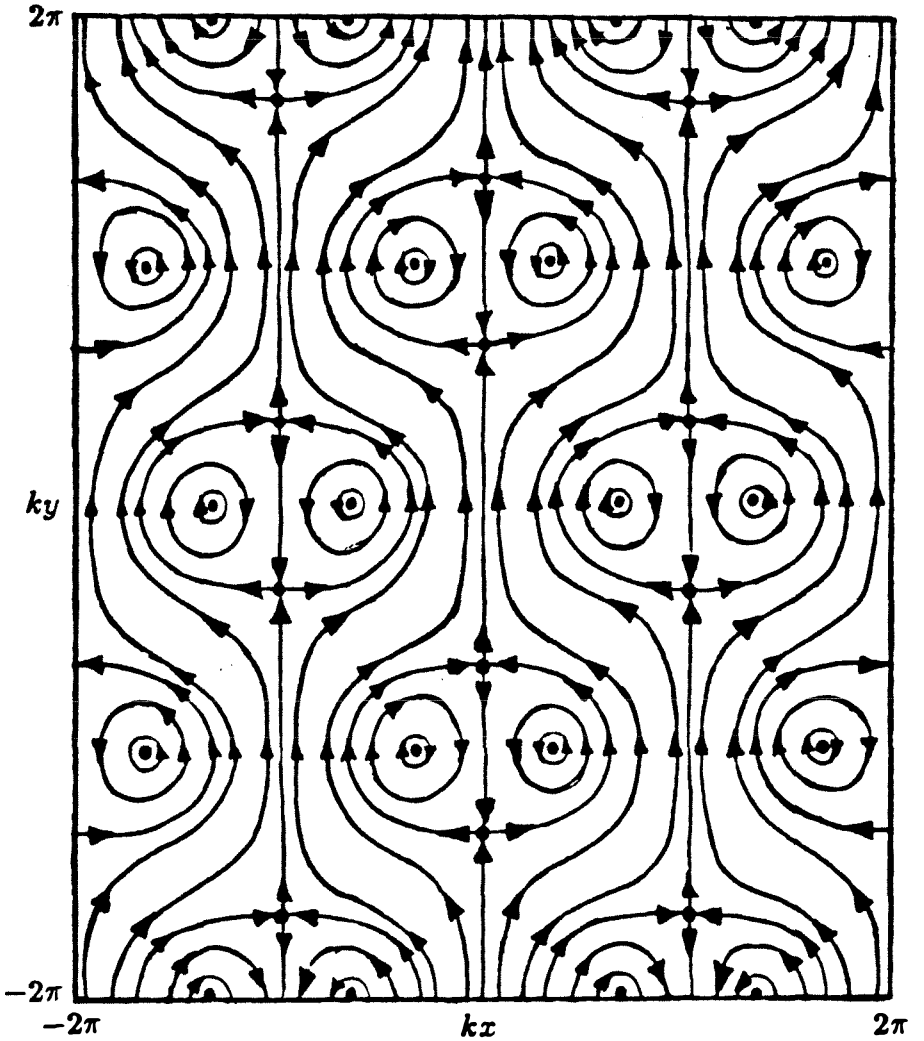

(a)

Figure 11. *(a) Flow lines of the Poynting vector field for the case of three wave interference when* $0 < |\alpha| < 1$.

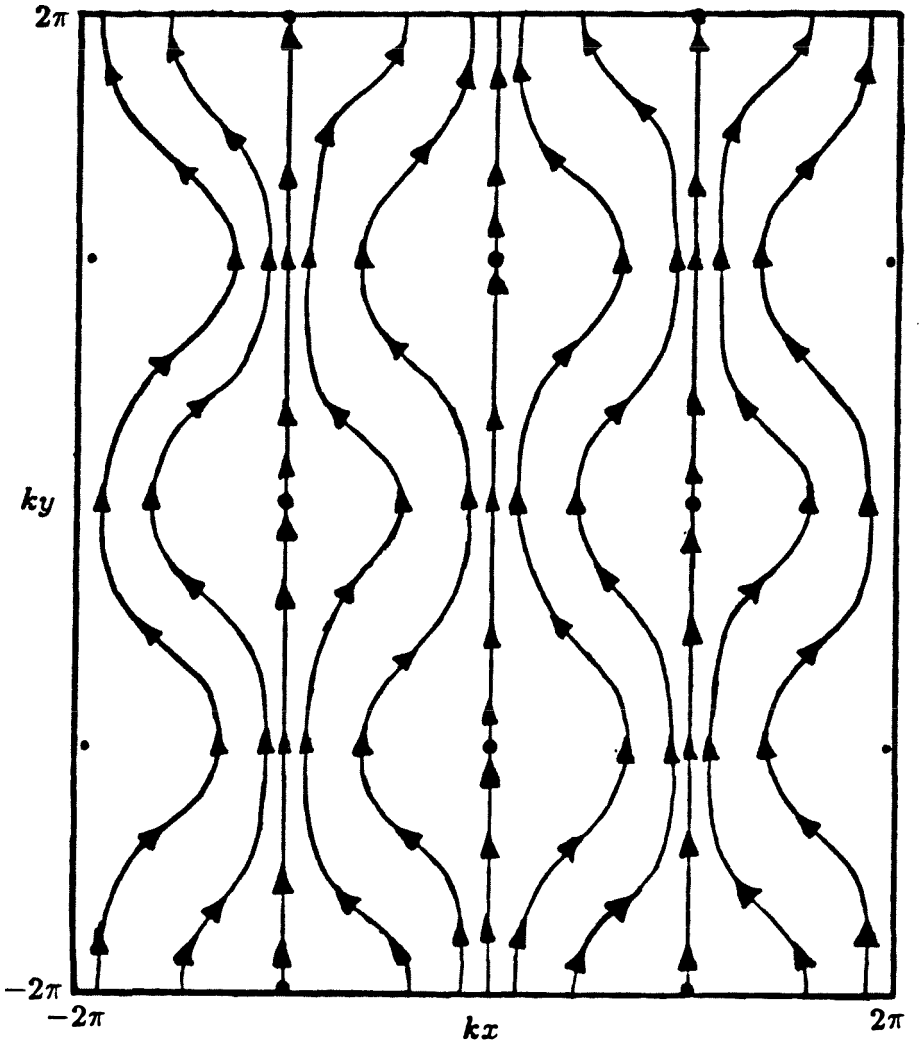

(b)

Figure 11. *(b) Flow lines of the Poynting vector field for the case of three wave interference when* $|\alpha| = 1$.

Chapter III

Structural Stability

§14. Structural Stability of Critical Points

Every electromagnetic field problem gives rise to an associated Poynting vector field. This vector field possesses a qualitative flavour, such as, the form of the flow lines, the type of its critical points, and the relative positioning and interconnections of the critical points. This qualitative flavour is called the structure of the vector field. It was observed in the last section that when the parameter α varied over a certain range, the general picture of the flow lines, i.e., the structure, remained unaltered. But as this parameter crossed a definite value, the picture changed drastically. In other words the structure was catastrophically altered. An appropriate question which may be posed at this point is, what type of Poynting vector fields are structurally stable or unstable?

To understand the problem of structural stability consider a system of flow lines of some electromagnetic field which undergoes a slight perturbation. This perturbation may arise due to two main reasons. Most of the physical problems have to be idealized during the process of mathematical modelling. During this process the effects due to minor factors are disregarded. Thus the solution obtained differs slightly from the actual behaviour. The disregarded minor factors

contitute a physical perturbation of the system. The other source of perturbation is the numerical inaccuracies induced during computation of the results. The allowed perturbations of an electromagnetic field are arbitrary except for an important restriction, i.e., the resulting perturbed Poynting vector field should remain solenoidal. This restriction has some important ramifications. It may be recalled that this restriction was used in connection with the Forster's theorem in section 7 where the perturbations were due to higher order terms only. In the present case addition of lower order terms of small magnitude to the Poynting vector field is also included among allowed perturbations. It was observed in section 7 that the higher order perturbations of the truncated Poynting vector field do not affect the behaviour of flow lines near non degenerate critical points. Since the perturbations considered in this section are more general, the results may be expected to be different.

Mathematical definition of structural stability is quite involved and hence it will not be given here. Interested reader is referred to Lefschetz [13] for the definition and an interesting discussion. Roughly speaking a system of flow lines is called structurally stable in a region if the flow lines remain qualitatively unchanged under small perturbations. If the perturbations satisfy certain conditions of smallness, see, e.g., Sansone and Conti [14], then a number of theorems on the properties of structurally stable systems may be proved. Without going into the details of those theorems some of the relevant properties of such systems will be discussed below. The details may be found in [13] and [14]. The results will be applied to the Poynting vector field.

A structurally stable system has at most a finite number of critical points in a bounded region. The Poynting vector field of a standing wave is zero everywhere. Therefore any region of the $x - y$ plane has an infinite number of critical points.

Hence a standing wave is a structurally unstable system. That is why a travelling wave of arbitrarily small magnitude, interfering with a standing wave gives a finite, non zero Poynting vector field. The structure of the resulting Poynting vector field has been given in figure 11(a). There are only a finite number of critical points in any bounded region of that flow line plot.

A structurally stable system in a region has only elementary critical points in that region and none of them is a center point. This principle has to be modified when the system is the flow lines of a solenoidal vector field. In general an elementary center point is transformed into a focal point under an arbitrary perturbation. The behaviour of a focal point was illustrated in figure 5. As has been discussed above the perturbations which cause such a transformation are not included in the allowed set of perturbations to the S field. Therefore a center point of a solenoidal vector field such as Poynting vector field cannot be transformed into a focal point and hence it is a stable critical point. In the Poynting vector field, elementary center point and elementary saddle point are the only type of elementary critical points which can exist. In the light of the above discussion the modified principle may be stated as: the Poynting vector field is structurally stable in any region which contains only elementary critical points. If there exists a region which contains higher order critical points then the Poynting vector field in that region is structurally unstable. This fact was observed in the previous section when for $|\alpha| = 1$ all the critical points were of order two. It was observed that if $|\alpha|$ is slightly greater than 1 then all the critical points disappear. If $|\alpha|$ is slightly less than 1, four critical points appear in the neighbourhood of the higher order critical point. This phenomenon may be considered as breaking up of the higher order critical point and will be discussed in detail in the next section. At this point the remark about the abundance of elementary critical points made

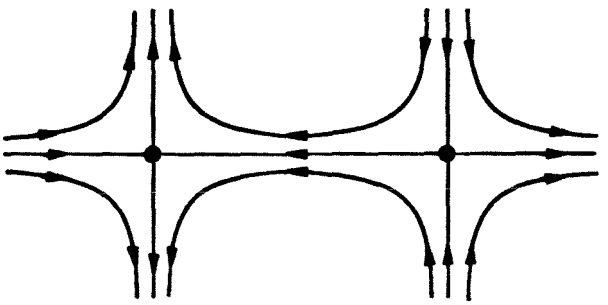

(a)

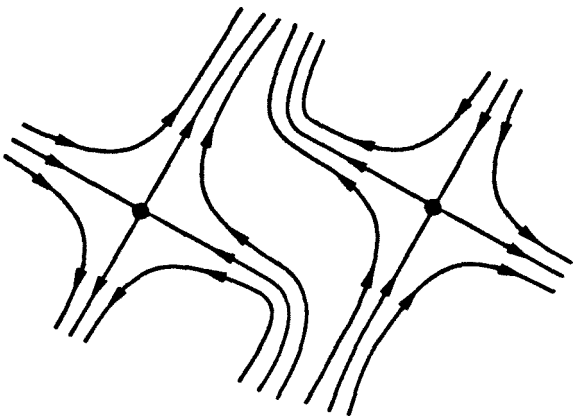

(b)

Figure 12. *Structural instability of a connection between two saddle points. (a) Before the perturbation the two arms of saddle points are connected together. (b) After the pertubation both the saddle points remain but their connection is broken.*

in section 12 can be explained. The reason for that remark is simply this, that the elementary critical points are stable under allowed perturbations while higher order critical points will in general break up into elementary critical points under these perturbations.

Interconnection of elementary saddle points by means of a flow line is structurally unstable. For solenoidal vector fields two distinct cases should be considered. First consider the case of two different saddle points connected together by

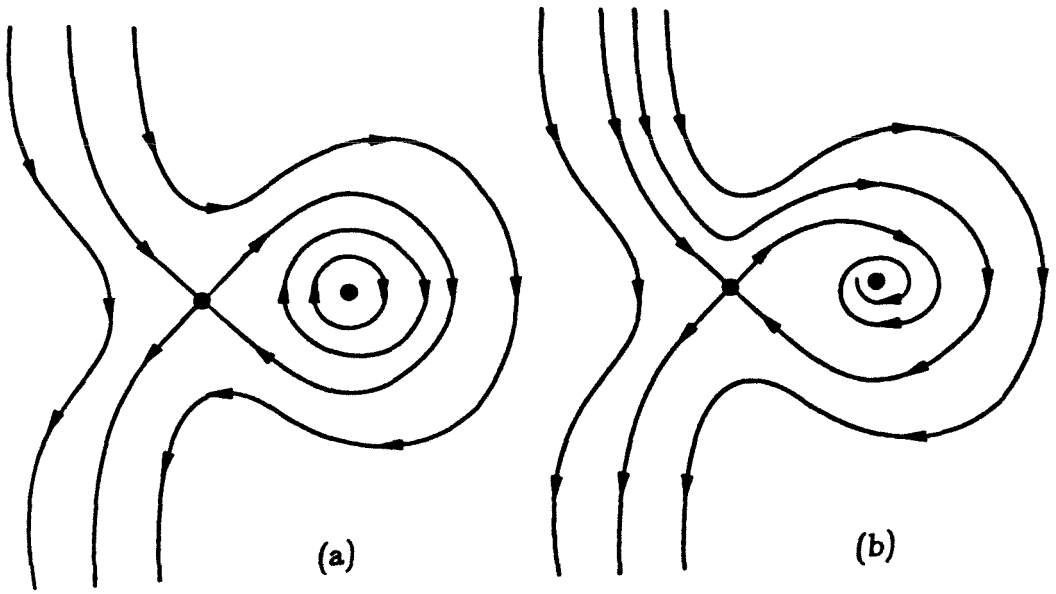

Figure 13. *Structural instability of saddle point self connection for an arbitrary vector field. If the field is solenoidal its initial structure (a) is not altered by the perturbation. If the field is not solenoidal the final structure of its field lines is given by (b).*

a flow line as depicted in figure 12(a). If a perturbation causes a small rotation of the Poynting vector field the arms of the two saddle points are rotated. The interconnection of the saddle points cannot be preserved under rotation. This connection is broken to accommodate the rotation of the vector field. The resulting outcome is depicted in figure 12(b).

Next consider the case of a single saddle point whose two arms are joined together as shown in figure 13(a). Unlike the previous case this connection can be preserved under rotation. The region enclosed by the flow line joining the two arms of the saddle point contains at least one center point. If this region contains more than one critical point the algebraic sum of indices of rotation of those critical points would be unity. This can be easily verified by examining the

index of rotation on a closed curve which just encloses this region. Under a small but otherwise arbitrary perturbation a center point will be converted to a focal point and the vector field will not be solenoidal any more. If there is only one center point in the region the resulting structure of the vector field is depicted in figure 13(b). It may be observed that the flow line joining the two arms of the saddle point in figure 13(a) is absent in figure 13(b). If the perturbation is such that the vector field remains solenoidal then the flow line structure represented by figure 13(b) is not possible. From a study of above two cases it can be concluded that for arbitrary vector fields all saddle interconnections are structurally unstable. But for soleniodal vector fields, like the Poynting vector field, self connection of the saddle points is structurally stable.

§15. Creation, Annihilation and Reorganization of Critical Points

It was stated in the previous section that the higher order critical points tend to break up under small perturbations. To understand this phenomenon a little better, consider the components of a truncated Poynting vector field of order $p = m + n - 1 \geq 2$

$$S_x = F_p(x, y)\,, \tag{70a}$$

$$S_y = G_p(x, y)\,. \tag{70b}$$

F_p and G_p are homogeneous polynomials of degree p in x and y. The description of the Poynting vector field given above can be obtained by converting equation (31) from circular polar coordinates to rectangular coordinates. After a small perturbation these components may be written upto the terms of order p as follows

$$\tilde{S}_x = \sum_{j=0}^{p} \tilde{F}_j(x, y)\,, \tag{71a}$$

$$\tilde{S}_y = \sum_{j=0}^{p} \tilde{G}_j(x, y)\,, \tag{71b}$$

where $\tilde{F}_j$ and $\tilde{G}_j$ are homogeneous polynomials of degree j. In general the origin is not a critical point of the perturbed system (71). The components $\tilde{S}_x$ and $\tilde{S}_y$ may be equated to zero and solved simultaneously to obtain the new location of the critical points. There may be upto p^2 solutions of two simultaneous equations of degree p. Choose only the solutions which lie in a small circle around the origin where the approximations made in equations (70) and (71) are valid. Suppose there are q such solutions where $0 \leq q \leq p^2$. If $q = 0$ then it is said that the critical point has been removed but if q is different from zero then it is said that the critical point has been broken up into q critical points. The perturbation is arbitrary therefore all the newly created critical points will be elementary critical points. If any of the resulting critical points is a critical point of higher order it can be broken up by perturbing the fields once again.

An arbitrarily small perturbation preserves an ordiary point, i.e., a point which is not a critical point remains a non critical point. Elementary critical points may shift and rotate by a small amount while the higher order critical points break up under a slight perturbation. If a higher order critical point is enclosed by a curve C in such a way that C has no critical points on itself and during a continuous perturbation, no point on it becomes a critical point. Then the Poynting vector field on C before and after the perturbation are homotopically connected. That is to say that the index of rotation on C is preserved. Therefore algebraic sum of indices of rotation of the newly created critical points is equal to the index of rotation of the original higher order critical point. This does not uniquely identify the products of break up of the higher order critical point. Instead it puts an upper limit on the algebraic sum of their indices of rotation thus limiting the possiblities. For example a critical point of order 2 with $m = 2$ and $n = 1$ may break up in two different ways. The index of rotation of this critical point according to equation

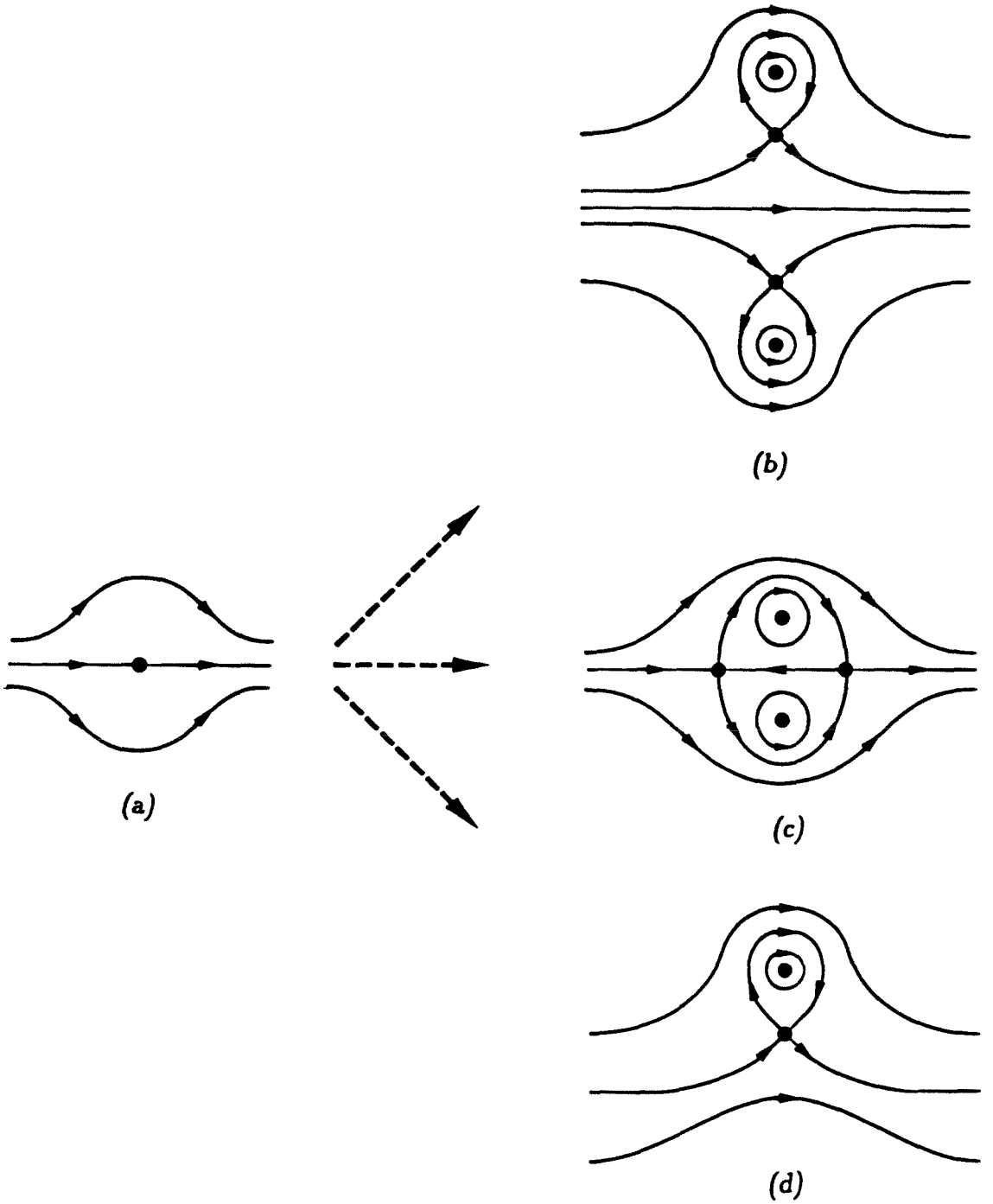

Figure 14. *Various possible outcomes of break up of a second order critical point shown in (a). (a) Critical point with $m = 2$ and $n = 1$. (b) Structurally stable break up in two saddle points and two center points.(c) Structurally unstable break up in two saddle points and two center points. (d) Break up results in only two critical points, a center point and a saddle point.*

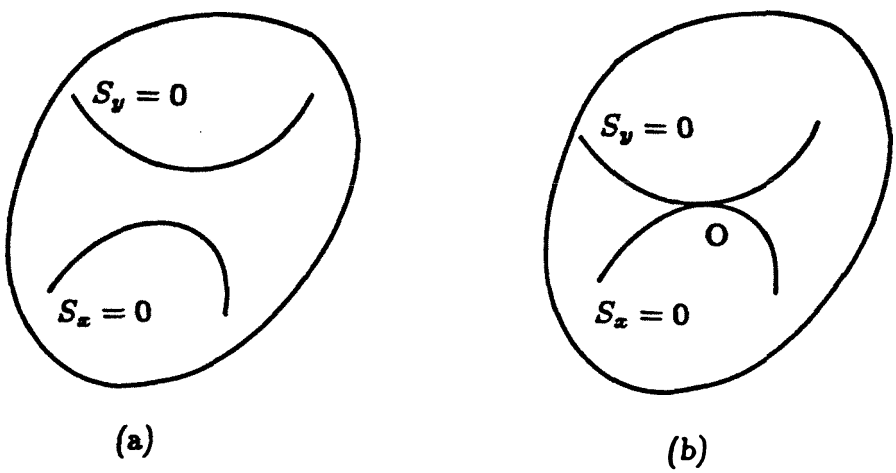

Figure 15. *(a) The two curves without contact on which the components of the Poynting vector are zero. (b) Initial contact of the curves result in a single point of contact with a common tangent.*

(40) is zero. It may break up into one elementary saddle point and one elementary center point or two critical points of each kind may be produced as a result of the break up. Since a critical point of second order can break up into a maximum of $2^2 = 4$ critical points these are the only two possible ways. Both the possiblities are graphically illustrated in figure 14. It should be noted that the exact locations of elementary critical points, which are generated in the break up process, depend on the amount and type of perturbation. There are two saddle points and two center points each in figures 14(b) and 14(c) but the local behaviour of the flow lines in each case is different. It may be observed that in figure 14(c) both the saddle points are connected together by three flow lines and hence this outcome of the break up is structurally unstable.

The higher order critical points are therefore unstable and may not be abundant. They are still important for another reason. Creation of a critical point of higher order is always the first result of a continuous perturbation in a region containing only ordinary points. Then on further perturbation higher order critical

point breaks up into a number of elementary critical points. To show the validity of the above statements, consider a region without any critical points. Suppose the cartesian components of the Poynting vector are zero on two separate curves which do not touch each other, as shown in figure 15(a). Under a continuous perturbation the curves $S_x = 0$ and $S_y = 0$ develop contact. Initially the point of contact is isolated and both the curves have a common tangent at the point of contact as shown in figure 15(b). The Taylor series for S_x and S_y at the point of contact may be written as

$$S_x = a_{11}x + a_{12}y + \text{higher order terms}, \tag{72a}$$

$$S_y = a_{21}x + a_{22}y + \text{higher order terms}, \tag{72b}$$

where the point of contact has been assumed to be the origin. The condition that the curves $S_x = 0$ and $S_y = 0$ have a common tangent is given by

$$\left(\nabla S_x \times \nabla S_y\right)\Big|_{\mathrm{O}} = (a_{11}a_{22} - a_{12}a_{21})\mathbf{e}_z = 0\,. \tag{73}$$

But the condition give by equation (73) is precisely the condition under which the linear part of the Poynting vector fails to describe the flow lines and higher order terms have to be taken into account [13]. Hence the critical point is a higher order critical point. All the statements made above remain valid if the curves $S_x = 0$ or $S_y = 0$ reduce to single points.

It is concluded that the creation of elementary critical points is characterized by an initial appearance of an higher order critical point which then breaks up into a number of elementary critical points. The reverse process of annihilation of the critical points can also be easily visualized in a similar manner. In this process many elementary critical points coalesce into a critical point of higher order which then disappears.

§16. Examples of Structural Instability

The concepts of structural stability which were studied in the last two sections will be illustrated in this section with the help of three simple examples. Consider the first example which is really an extension of the wave interference example of section 13. It was shown there that when $|\alpha| = 1$ all the critical points are of order 2. Now suppose $\alpha = 1$, $\theta = 90°$ and a linearly polarized plane wave having some small amplitude, say 0·05, travelling in a direction of $-30°$ with respect to the x-axis, is added to the system of interfering waves. Then the total electric field is given as

$$\mathbf{E} = \left\{\frac{1}{2}\exp(ikx) + \frac{1}{2}\exp(-ikx) + \exp(iky) + \cdot 05\exp(\frac{\sqrt{3}}{2}ikx - \frac{1}{2}iky)\right\}\mathbf{e}_z . \quad (74)$$

The total Poynting vector field may be calculated using equation (8). For the present purpose it is sufficient to investigate the **S** field in the vicinity of the point with coordinates $kx = 0$ and $ky = \pi$. This is the location of one of the second order critical points of the original Poynting vector field without the small amplitude wave travelling at an angle of $-30°$. The flow lines of **S** field generated by (74) are plotted for $-0{\cdot}08\pi < kx < 0{\cdot}08\pi$ and $0{\cdot}92\pi < ky < 1{\cdot}08\pi$ in figure 16. It is immediately apparent that the higher order critical point has broken up symmetrically into two elementary center points and two elementary saddle points. The combined index of rotation is zero as was the index of rotation of higher order critical points in figure 11(b).

All of the examples considered so far involved the interference of a number of plane waves. Other systems of interfering waves also produce critical points. For example a plane wave interfering with a circularly cylindrical wave also gives rise to critical points. For the sake of definiteness consider a line source of electrical current located at the origin of the coordinate system. This line source radiates

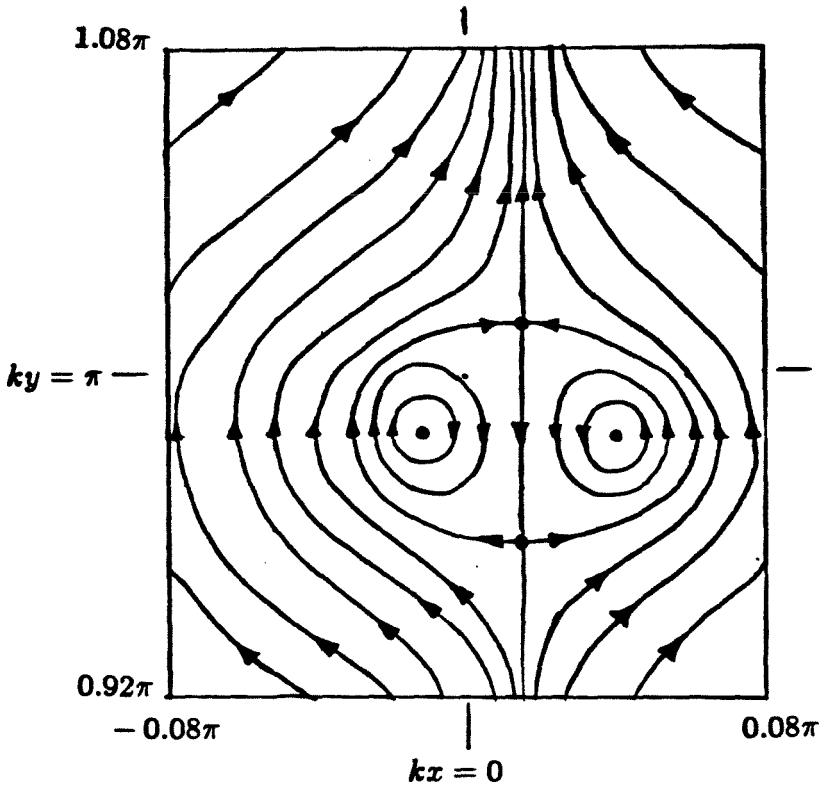

Figure 16. *The symmetrical break up of a second order critical point by a small amplitude plane wave into four critical points.*

linearly polarized circularly cylindrical waves. In addition suppose there is a linearly polarized plane wave travelling in the direction of the negative y-axis. The total electric field may be written as

$$\mathbf{E} = \left\{\exp(-iky) + bH_0^{(1)}(k\rho)\right\}\mathbf{e}_z\,, \tag{75}$$

where b is the strength of the cylindrical wave and $H_0^{(1)}$ is Hankel function of the first kind. The strength of cylindrical wave may be changed by changing the amount of current flowing in the line source. When $b = 0$ the plane wave alone does not give rise to any critical points. For an arbitrarily small but non zero b an elementary saddle point appears on the positive y-axis. As the value of b is increased the location of the saddle point moves up along the y-axis. A sketch of the flow lines of the Poynting vector field for this situation is given in figure 17(a).

The index of rotation of the source point is +1 because all the flow lines emanate radially outward from the line source. Therefore the total index of rotation in the S field remains zero. This can be verified by calculating the rotation on any closed curve which contains both the line source and the elementary saddle point. There are no other critical points of the S field. The reason for this is that the amplitude of the cylindrical wave falls with the distance as $1/\sqrt{k\rho}$ and far away from the source it is completely swamped by the field of the plane wave. The ensuing result is that all the flow lines from the source point are eventually directed towards the negative y-axis.

As the strength of the cylindrical wave is increased the location of the elementary saddle point moves up on the y-axis. Above a certain value of b two elementary center and saddle points appear as indicated in figure 17(b). The total index of rotation still remains zero. As b is increased further more pairs of critical points are created. Each of those pairs consists of an elementary center and saddle point. The creation of each of these pairs involves a higher order critical point, i.e., for a certain value of b a higher order critical point appears and as b is slightly increased from this value it breaks up into a pair of elementary critical points. This is the type of break up which was sketched in figure 14(d).

The third and the last example in this section will demonstrate how the saddle interconnections are unstable. It was pointed out in section 14 that under a rotation of the Poynting vector field the saddle interconnections are structurally unstable. The following example is an extension of the example used in section 13. Figure 11(a) displayed the flow lines in the case when $\alpha = \frac{1}{2}$ and $\theta_o = 90°$. Now the direction of the third propagating wave is changed, i.e., let $\theta_o = 80°$. Then the total electric field is given as

$$\mathbf{E} = \frac{1}{2}\Big\{\exp(ikx) + \exp(-ikx) + \exp(ikx\cos 80° + iky\sin 80°)\Big\}\mathbf{e}_z\,. \qquad (76)$$

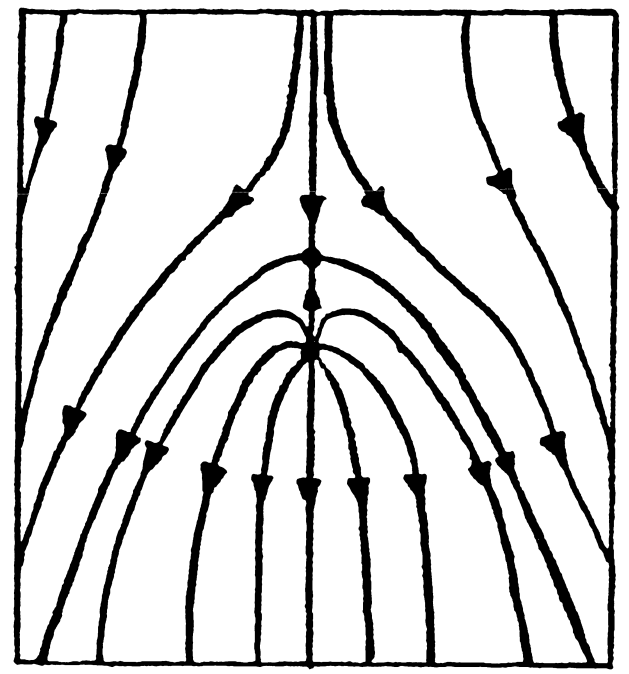

(a)

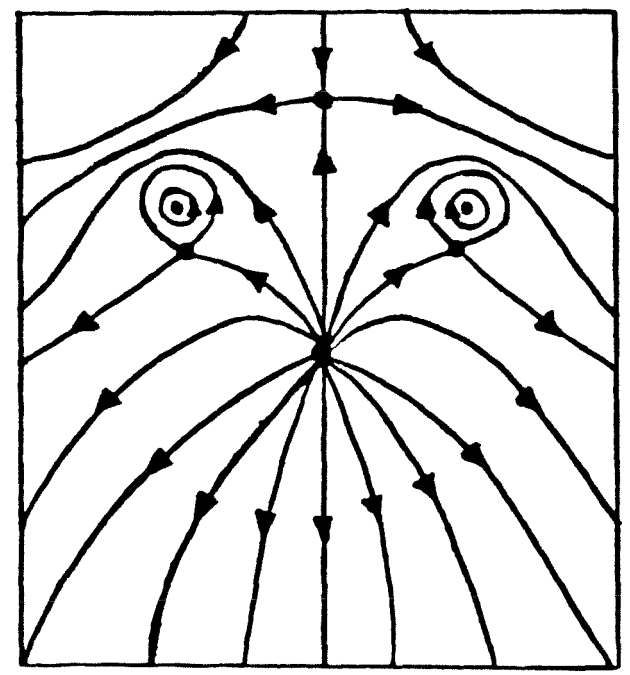

(b)

Figure 17. *Critical points resulting from the interference of a plane wave and cylindrical wave. (a) When the amplitude of cylindrical wave is small. (b) When the amplitude of the cylindrical wave is increased beyond a certain value.*

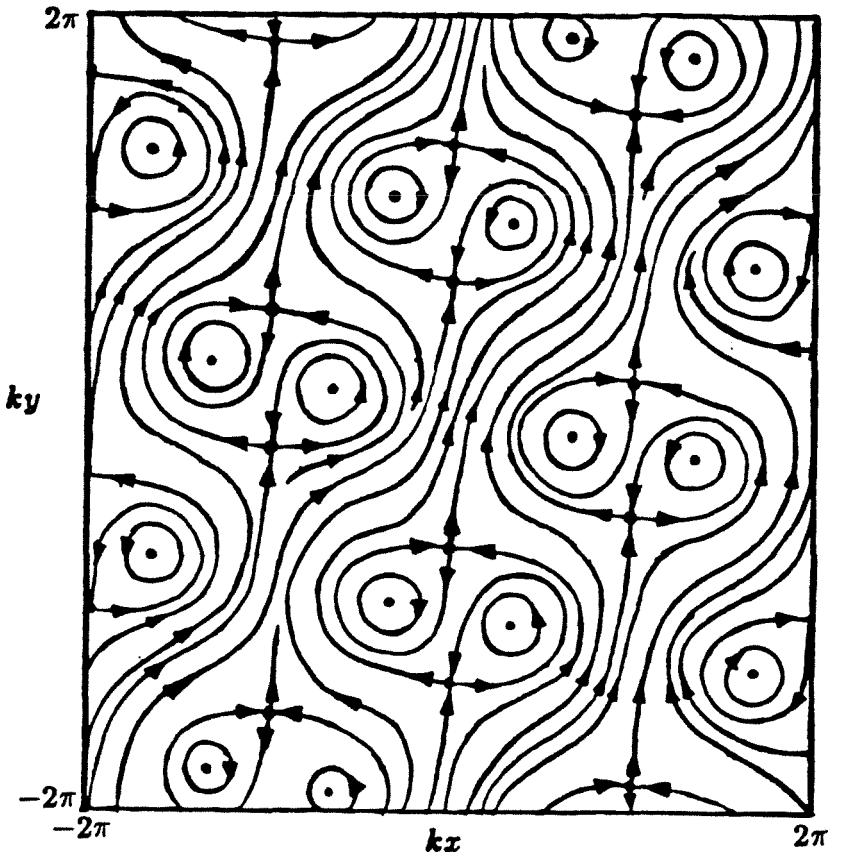

Figure 18. *The flow lines of three wave interference when* $\alpha = \frac{1}{2}$ *and* $\theta_0 = 80°$.

The Poynting vector field is once again calculated using equation (16). The flow lines of this field have been plotted in figure 18 for $-2\pi < kx < 2\pi$ and $-2\pi < ky < 2\pi$. Comparing with figure 11(a) it is observed that the elementary critical points remain elementary but they are slightly shifted from their positions. It is further observed that all the connections between two different saddle points have been broken. The self connections of the saddle points have been created. The two pictures of the flow lines in figure 11(a) and figure 18 are completely different from a qualitative point of view. All the elements in the structure of flow lines plotted in figure 18 are structurally stable. The plot of flow lines in figure 11(a) only holds true for $\theta_0 = \pi/2$. On the other hand the plot of flow lines in figure 18

is qualitatively similar to a flow line plot constructed for a value of θ_0 in the range of $(0, \pi/2)$. Thus this example serves to illustrate the fragility of the saddle point to saddle point connections.

It is true that the above examples are simple and appear to be concocted yet they are important. Some real world electromagnetic diffraction problems can be modelled as superposition of different waves. Therefore the important features of the qualitative behaviour of flow lines may be expected to crop up in real world problems as well.

Chapter IV

Applications

§17. Poynting Vector and Perfect Conductors

Up to this point the behaviour of the Poynting vector was investigated in a homogeneous medium. The next order of buisness is to investigate the behaviour of flow lines in the vicinity of a perfect conductor. The results of such an investigation will be specially valuable in the study of diffraction due to metallic objects. The cases of E-polarized and H-polarized fields will be considered separately due to different boundary conditions imposed on the perfect conductor by these fields.

The case of H-polarized field is simpler to deal with and hence will be considered first. Consider an H-polarized field whose electric and magnetic field vectors are given as

$$\mathbf{H} = A_H \exp(i\phi_H)\mathbf{e}_z\,, \tag{77a}$$

$$\mathbf{E} = \frac{i}{\omega\epsilon}\nabla\Big(A_H \exp(i\phi_H)\Big) \times \mathbf{e}_z\,, \tag{77b}$$

where A_H and ϕ_H are amplitude and phase of H_z respectively. The boundary condition on the surface of perfect conductor is

$$\mathbf{e}_n \times \mathbf{E} = 0 \qquad \text{on } \mathcal{M}\,, \tag{78}$$

where $\mathbf{e}_n$ is a unit vector normal to the surface of the perfect conductor $\mathcal{M}$. The application of the boundary condition (78) leads to the following conditions on

A_H and ϕ_H

$$\nabla A_H \cdot \mathbf{e}_n = 0 \qquad \text{on } \mathcal{M}, \tag{79a}$$

$$A_H \nabla \phi_H \cdot \mathbf{e}_n = 0 \qquad \text{on } \mathcal{M}. \tag{79b}$$

The expression for the Poynting vector in this case is given as

$$\mathbf{S} = \frac{1}{2\omega\epsilon} A_H^2 \nabla \phi_H \,. \tag{80}$$

Therefore from equations (79) and (80) it can be concluded that

$$\mathbf{S} \cdot \mathbf{e}_n = 0 \qquad \text{on } \mathcal{M}. \tag{81}$$

In the light of the above discussion the following conclusions can be drawn. The Poynting vector is completely tangential to the metallic surface $\mathcal{M}$. It may be zero on isolated points. The isolated critical points on $\mathcal{M}$ cannot be center points because in the neighbourhood of such a point the lines of flow will be normal to $\mathcal{M}$ in at least two directions as depicted in figure 19(a). Therefore the lowest order critical point possible on $\mathcal{M}$ is an elementary saddle point. Since the electromagnetic fields are zero inside the perfect conductor only half of the flow lines near the saddle point are allowed, i.e., two arms of the saddle point are tangential to $\mathcal{M}$ and one arm coincides with the outward normal. Such a critical point may be called a *half saddle point.* The flow lines of the Poynting vector field in the vicinity of an ordinary point and a half saddle point on the perfect conductor are depicted in figures 19(b) and 19(c) respectively. Higher order critical points may also exist on $\mathcal{M}$ but as discussed previously they are unstable and hence they are not worthy of consideration in real problems.

In the case of E-polarized electromagnetic field the electric and magnetic fields are given as

$$\mathbf{E} = A \exp(i\phi) \mathbf{e}_z \,, \tag{82a}$$

$$\mathbf{H} = \frac{1}{i\omega\mu} \nabla \Big(A \exp(i\phi) \Big) \times \mathbf{e}_z \,. \tag{82b}$$

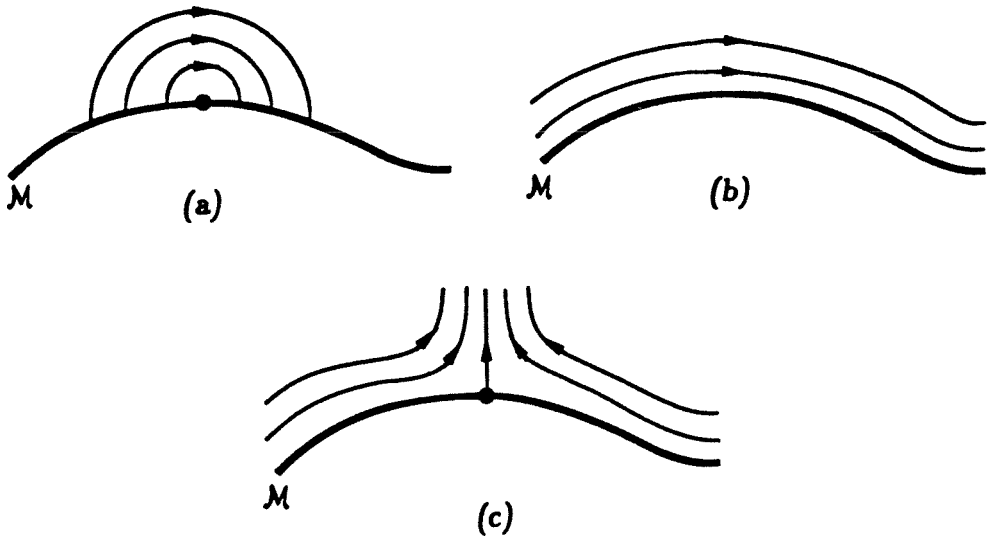

Figure 19. *Flow lines due to an H-polarized field near a perfect conductor. (a) Center point shown here is not possible since the flow lines cannot be completely tangential to the conductor in this configuration. (b) Flow lines are parallel to the conductor in absence of critical points. (c) Flow lines near a half saddle point.*

The application of the boundary condition (78) on the surface of the perfect conductor $\mathcal{M}$ yields

$$A = 0 \qquad \text{on } \mathcal{M}. \tag{83}$$

Therefore the Poynting vector vanishes identically on $\mathcal{M}$. Thus all the points on $\mathcal{M}$ are non isolated critical points of **S** field. To study the behaviour of flow lines in the vicinity of $\mathcal{M}$ the Poynting vector at each point on $\mathcal{M}$ may be expanded in Taylor series. Only the leading term should be retained as discussed previously. The system of simultaneous equations (30), reproduced below for convenience

$$\cos(m\theta + \alpha_m) = 0\,, \tag{30a}$$

$$\cos(n\theta + \beta_n) = 0\,, \tag{30b}$$

should be satisfied by at least one value of θ in the interval $[0, \pi)$ because the

critical point is not isolated. If θ_o is such a value then $\theta_o + \pi$ also satisfies the system of equations (30). These two directions are tangent to the surface $\mathcal{M}$ on which the Poynting vector is zero. It is not possible for indices m and n to be equal because this forces the two constants α_m and β_n to be equal which is not allowed as has been discussed in sections 7 and 10. Hence a non isolated point on $\mathcal{M}$ cannot be a center point. Moreover due to the condition on amplitude of E_z in equation (83) the orders of leading terms, m or n cannot be equal to zero. Therefore the leading term of S should be at least of order 2. This gives rise to two possible set of values of m and n. One possiblity is that $m = 2$ and $n = 1$. The other possiblity is that $m = 1$ and $n = 2$. Both of these cases give qualitatively similar behaviour of the flow lines so the first set of values for m and n is assumed. To further simplify the analysis, coordinate system has been rotated in such a way that $\beta_1 = 0$. Then from equation (30) it follows that $\alpha_2 = \pi/2$. The leading term of the Poynting vector is then calculated as

$$\begin{aligned} \mathbf{S}_1 &= 2C_{21}(k\rho)^2 \cos^2\theta \Big\{ \sin\theta \mathbf{e}_\rho + \cos\theta \mathbf{e}_\theta \Big\} \\ &= 2C_{21}(kx)^2 \mathbf{e}_y \,. \end{aligned} \tag{84}$$

The θ_o which satisfies equation (30) is $\pi/2$. Therefore $\theta = \pi/2$ and $\theta = 3\pi/2$ are two half rays which are tangent to $\mathcal{M}$. The Poynting vector is parallel to these half rays. If all the points in a certain interval on $\mathcal{M}$ are non isolated critical points of order 2 then the Poynting vector field in the vicinity of that interval is parallel to $\mathcal{M}$. This situation is depicted in figure 20(a) which is similar to figure 19(b) the difference being that in the later case S is not zero on $\mathcal{M}$.

At isolated points on $\mathcal{M}$ the Taylor series expansion of S may be of higher order than 2. If the order is 3 then there are again two possiblities which give qualitatively equivalent picture of the flow lines. One possiblity is that $m = 3$ and $n = 1$ and the other possible set of values is obtained by exchanging the values of

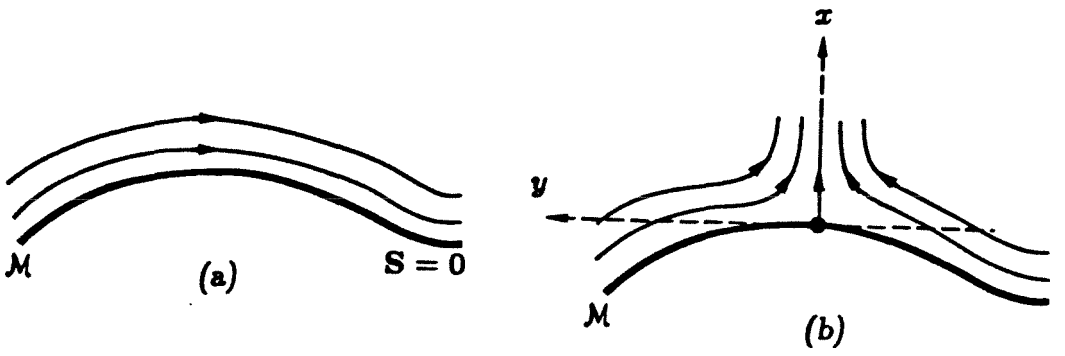

Figure 20. *The flow lines near a perfect conductor in the case of E-polarized electromagnetic fields. (a) The flow lines are parallel to the conductor and all the points on it are non isolated critical points of order 2. (b) The flow lines form a half saddle point at the critical point of order 3.*

m and n. Suppose that $m = 3$ and $n = 1$ and the coordinate system is rotated to facilitate the calculations such that $\beta_1 = 0$. Then it follows from equation (30) that $\alpha_3 = 0$ and $\theta_o = \pi/2$. The leading term in the Taylor series expansion of S can be calculated as

$$\mathbf{S}_1 = 2C_{31}(k\rho)^3 \Big\{ -\cos 3\theta \cos\theta \mathbf{e}_\rho + \cos^3\theta \sin\theta \mathbf{e}_\theta \Big\}. \tag{85}$$

The flow lines of S field have been sketched in figure 20(b) for this case. The behaviour of flow lines is immediately recognized as being similar to the behaviour of the flow lines in figure 19(c). Hence this critical point is also called half saddle point.

It is possible that the leading term in the Taylor series expansion of the Poynting vector field is of a order greater than 3. These higher order critical points are unstable and hence these points will not be considered here. It should be noted that for both cases of polarizations the lowest order term possible in the Taylor series expansion of S field gives lines of flow which are parallel to the surface of the perfect conductor. The next possible higher order term gives half

saddle point configuration for the flow lines in each case. These are the only two possiblities which are structurally stable. The behaviour of the flow lines near a perfect conductor can be easily determined by a knowledge of phase ϕ in the case of E-polarization or ϕ_H in the case of H-polarization along the conductor surface. This will be explained below.

In the case of H-polarization the flow lines are orthogonal to the family of curves ϕ_H = constant. Let the function $\phi_H(P)$ describe the phase of H_z on $\mathcal{M}$ where P is an arbitrary point on $\mathcal{M}$. The flow lines are then parallel to $\mathcal{M}$ and have the direction of increasing $\phi_H(P)$. The points at which the derivative of $\phi_H(P)$ with respect to P vanishes are the locations of half saddle points.

For the case of E-polarization the phase ϕ of the electric field is not easily determined because E_z is zero on $\mathcal{M}$. The induced surface current $\mathbf{K}$ on the perfect conductor comes to the rescue since it does not vanish identically on $\mathcal{M}$. This surface current is given as

$$\mathbf{K} = \mathbf{e}_n \times \mathbf{H} = \frac{1}{\omega\mu}\Big(\mathbf{e}_n \cdot \nabla A\Big) \exp\{i(\phi + \frac{\pi}{2})\}\mathbf{e}_z\,. \tag{86}$$

Thus the phase of the electric field can be easily determined from the phase of K_z. As in the case of H-polarization the flow lines are orthogonal to the family of equiphase lines. Therefore consider the function $\phi(P)$ where P is an arbitrary point on $\mathcal{M}$. Analogous to the case of H-polarization the flow lines are parallel to $\mathcal{M}$ and in the direction of increasing $\phi(P)$. The points where the derivative of $\phi(P)$ is zero are the locations of half saddle points.

Thus the behaviour of the flow lines in the vicinity of a perfect conductor can be very easily deduced by considering the phase of the magnetic field and the phase of the induced surface current in the cases of H-polarization and E-polarization respectively. Figure 20 illustrates this point graphically.

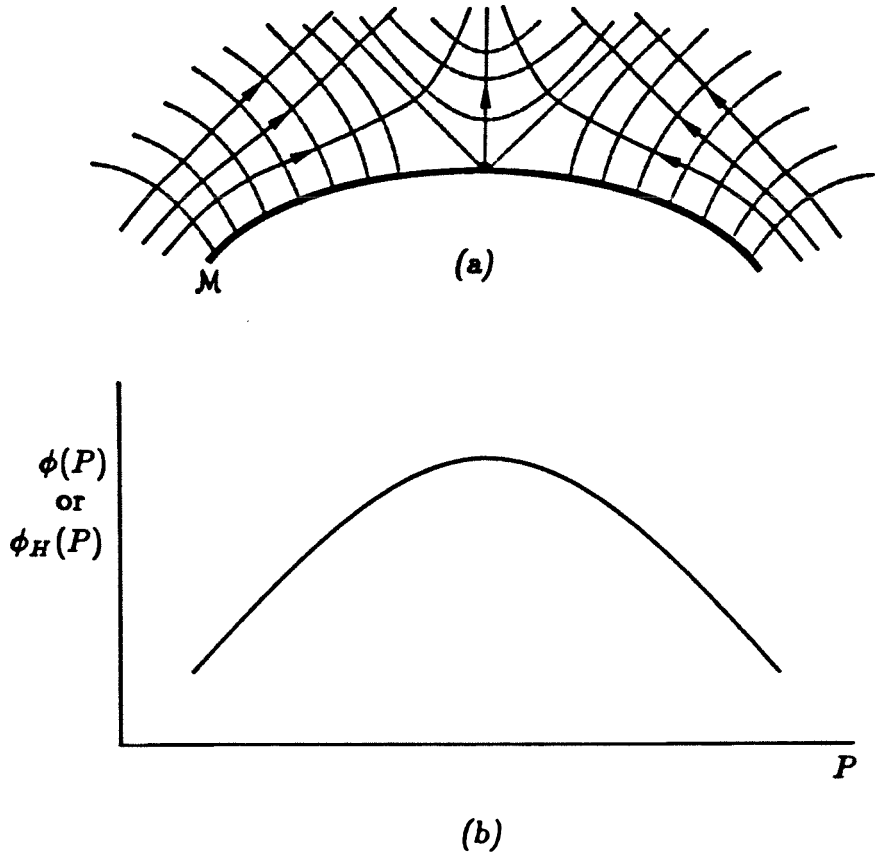

Figure 21. *(a) The lines of constant phase and the flow lines near a perfect conductor. (b) The phase function corresponding to the situation in (a). Half saddle point is located at the relative extremum of the phase.*

§18. Critical Points in Resonant Cavities

In the previous section the behaviour of the Poynting vector field near a perfectly conducting surface was determined. This knowledge can be applied to the study of flow lines in electromagnetic problems involving conductors. One class of such problems is in which electromagnetic fields are confined within a perfectly conducting surface. These problems will be called *interior problems.* The study of a two dimensional cavity resonator connected between a source and a load is a representative interior problem chosen to illustrate the use of critical points and

indices of rotation. This problem does not lend itself to an analytic solution. The methods used in the following analysis are quite general and can be utilized in the study of other interior problems as well.

First consider a completely enclosed two dimensional resonator. This resonator can be visualized as a volume generated by a closed plane curve $\mathcal{M}$ lying in the x-y plane translated in the z direction. The walls of this resonator are made of a perfectly conducting material. The modes of this resonator do not depend on the z-coordinate. Two types of modes are allowed to exist in this device, namely the modes with their electric field completely in the z direction and the modes whose magnetic field is completely z directed. It can be shown (see for example [15]) that all the mode functions and the resonant frequencies of a completely closed cavity are real. Let these E or H modes be arranged in ascending order with respect to their resonant frequencies. The qth mode function $R_q(x,y)$ with the resonant frequency ω_q satisfies the homogeneous Helmholtz's equation, i.e.,

$$\nabla^2 R_q(x,y) + k_q^2 R_q(x,y) = 0\,, \tag{87}$$

where $k_q = \omega_q\sqrt{\mu\epsilon}$. The curves in the x-y plane defined by $R_q = 0$ are called nodal lines of the mode function. It has been shown by Courant and Hilbert [16] that the nodal lines of the mode R_q divide the cavity into no more than q regions. It is then possible for some nodal lines to intersect each other. It has also been shown in [16] that such intersections of nodal lines form a system of equiangular rays. The cases of two and three intersecting nodal lines are depicted in figure 22.

Since the mode function is real the Poynting vector is identically zero inside the cavity. This agrees with the intuitive notion of energy trapped inside the resonator and having no flow. If there are two mode functions with the same resonant frequency then they may be combined with an arbitrary phase difference. In this case the Poynting vector is not zero. In absence of sources and sinks the

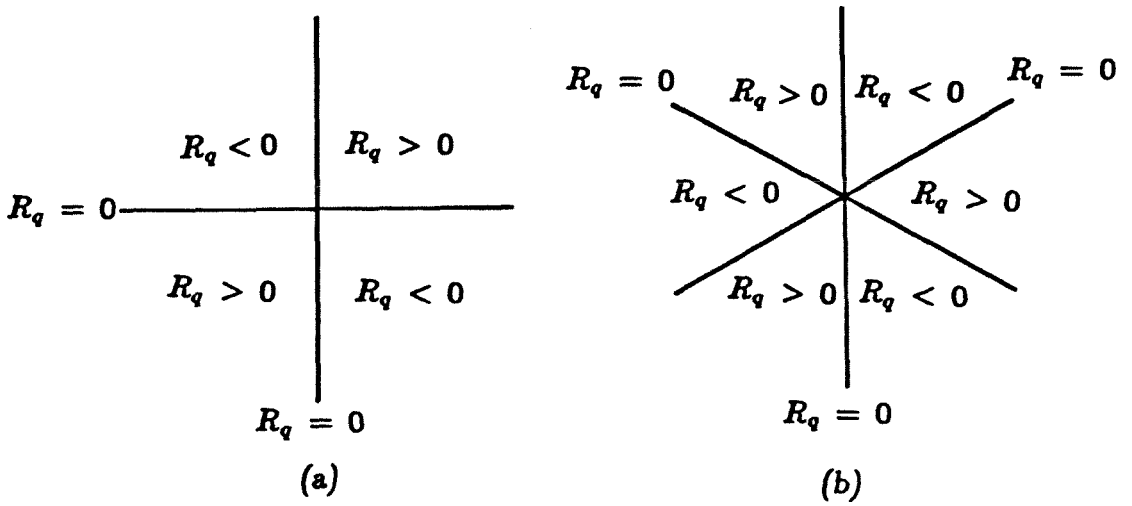

Figure 22. *(a) Intersection of two nodal lines. (b) Intersection of three nodal lines.*

flow lines of **S** will form closed loops inside the cavity. Such modes are called degenerate modes and will be excluded from further discussion.

When the cavity is resonant in a non degenerate mode with zero Poynting vector everywhere then the **S** field is structurally unstable because any region inside the cavity contains an infinite number of critical points. Let this cavity be perturbed by cutting two slits in the walls. Connect one of the slits to a generator and the other one to a load. When the cavity is configured in this manner some power flows from the source to the load and the Poynting vector field will not be zero at every point in the cavity. In what follows it will be shown that the resulting Poynting vector field may possess critical points. Figure 23 shows the cavity and how it may be connected between a source and a load.

Assuming that the slits are small it is reasonable to assume that the electric field is only slightly perturbed. That is to say that the perturbed electric field is given as

$$E_z = R + iI = (R_q + \delta R) + i(\delta I)\,, \tag{88}$$

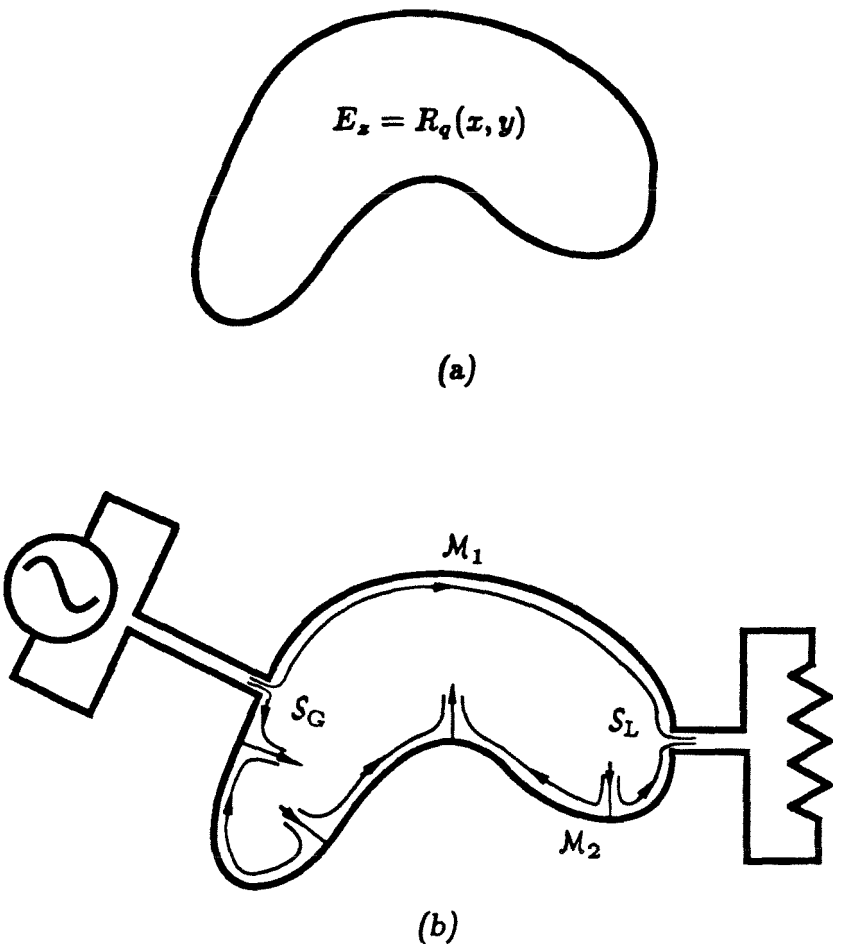

Figure 23. *(a) Completely enclosed cavity with real mode functions and no power flow. (b) Two slits S_G and S_L divide the cavity wall in two pieces M_1 and M_2. Two parallel plate guides couple the cavity to the source and the load.*

where δR and δI are functions which satisfy Helmholtz's equation and are small compared to the mode funtion R_q. It is obvious that the vector field ∇R_q has critical points at the points where nodal lines intersect. A glance at figure 22 will convince the reader of this fact. It is evident from this diagram that the critical point of ∇R_q is an elementary saddle point when two nodal lines intersect and a monkey saddle point when three nodal lines intersect. Only the elementary saddle point is stable under perturbations and hence it will be the only one considered.

Therefore the perturbed vector field ∇R will also possess an elementary saddle point near the intersection of two nodal lines. The functions R and I can be expanded in Taylor series around this critical point. These expansions up to the quadratic terms are given as

$$R = \delta A_0 + \frac{A_2}{8}(k\rho)^2 \cos(2\theta + \alpha_2)\,, \tag{89a}$$

$$I = \delta B_0 + \frac{\delta B_1}{2}(k\rho)\cos(\theta + \beta_1) + \frac{\delta B_2}{8}(k\rho)^2 \cos(2\theta + \beta_2)\,, \tag{89b}$$

where the coefficients with the prefix δ are infinitesimals because the assumed pertubation is small. The Poynting vector in the neighbourhood may be calculated up to the linear order term. The second order infinitesimal quantities should be discarded in favour of first order quantities. This calculation produces the following expression for the Poynting vector field

$$\begin{aligned}\mathbf{S} = {} & \frac{\delta A_0 \delta B_1}{4\eta}\Big\{\cos(\theta + \beta_1)\mathbf{e}_\rho - \sin(\theta + \beta_1)\mathbf{e}_\theta\Big\} \\ & + \frac{A_2 \delta B_0}{8\eta} k\rho\Big\{\sin(2\theta + \alpha_2)\mathbf{e}_\theta - \cos(2\theta + \alpha_2)\mathbf{e}_\rho\Big\}.\end{aligned} \tag{90}$$

Setting the above expression for $\mathbf{S}$ equal to zero the critical points are obtained. It is observed that a critical point exists at a distance of $k\rho = 2\delta A_0 \delta B_1 / A_2 \delta B_0$ from the origin where ∇R has a saddle point. This distance is an infinitesimal of first order and it can be easily shown that this critical point of $\mathbf{S}$ field is an elementary saddle point. Thus it has been shown that elementary saddle points in the Poynting vector field exist near the saddle points of cavity mode function R_q. It will now be shown that elementary center points may also exist under these circumstances.

Referring back to figure 23(b) it is seen that the cavity consists of two walls M_1, M_2 and two slits S_G, S_L. It is assumed that the power enters only through the slit S_G and is taken away from the cavity only through the slit S_L. It has been

shown previously that the Poynting vector is either parallel to a perfect conductor or forms half saddle points on it. It follows from the assumptions about the roles of S_G and S_L as source and sink of the Poynting vector field respectively that there can be only an even number of half saddle points on each of the walls. Let there be $2q_1$ and $2q_2$ half saddle points on the walls M_1 and M_2 respectively. The index of rotation of the Poynting vector field on a closed curve parallel to the cavity walls and across both the slits is clearly $q_1 + q_2$. If the mode function R_q has q_s saddle points in the cavity then there are q_s elementary saddle points of the Poynting vector field inside the cavity. The total index of rotation of the saddle points will be $-q_s$. The index of rotation on a curve just inside the cavity is positive. Therefore there must exist critical points of the Poynting vector field inside the cavity with positive indices of rotation. The only stable critical points with positive indices of rotation are elementary center points. Let there be q_c elementary center points inside the cavity then from theorem 1 of section 4

$$q_c = q_1 + q_2 + q_s \,. \tag{91}$$

Hence it is concluded that elementary critical points of the Poynting vector field may exist inside a tuned cavity resonator.

§19. Critical Points in Electromagnetic Scattering

Previous section was devoted to the discussion of the Poynting vector field inside a region bounded by a metallic surface. This section will be devoted to what may be termed as the *exterior problem*, i.e., the study of Poynting vector field outside a finite sized perfect conductor. For the sake of definiteness consider a linearly polarized infinite plane wave incident on a cylinder of arbitrary cross section. The cylidrical surface is perfectly conducting. The axis of the cylinder is parallel to the direction of the electric field. Let this direction coincide with the

z direction of a cartesian coordinate system. This problem is a two dimensional scattering problem. The lines of the Poynting vector field lie completely in the x-y plane.

As a first step it will be shown that the critical points of the Poynting vector field cannot exist in the far field of the scattering cylinder. This statement can be justified as follows. The total electromagnetic field is the sum of the incident field and the scattered field. The strength of the incident field components is constant at all points in space. It is a well known fact that the strength of the components of the scattered field of a finite sized scatterer decreases as $1/\sqrt{k\rho}$ in the far zone where ρ is the distance from the scatterer. At a critical point the electric field and/or the in phase component of the magnetic field vanishes. Since the scattered field strength decreases continuously in the far field it will not be enough to produce required cancellations of the incident field. Thus the critical points of the Poynting vector field, if there are any, exist only in the proximity of the scatterer.

The index of the Poynting vector field on a closed curve of a very large radius around the scatterer is zero. This is true because very far away from the scatterer the effect of the scattered field is much smaller as compared to the incident field. Therefore the total Poynting vector field is approximately equal to the incident Poynting vector field. This approximation becomes better as the distance from the scatterer increases.The flow lines far away are approximately depicted in figure 24. It is evident from a glance at figure 24 that the index of rotation of the Poynting vector field calculated on a circle of infinite radius centered on the scatterer is zero. The radius of the circle can now be made finite by bringing it in from infinity. The index of rotation will not change as long as moving boundary of the circle does not cross any critical points. Since there are no critical points in the far zone such

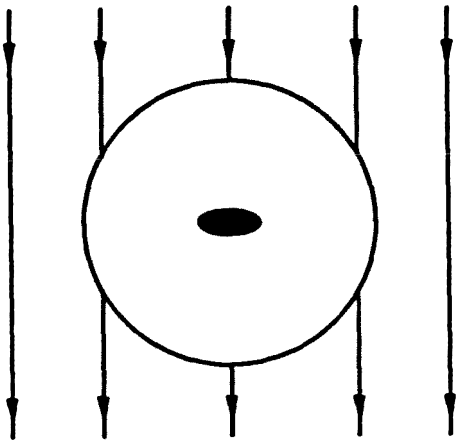

Figure 24. *The Poynting vector field at a circle of infinite radius from the scatterer. The index of rotation of the field on this circle is zero.*

a possibility will not exist. This proves the assertion that the index of rotation of the Poynting vector field in the far zone

$$\gamma_{Pz} = 0. \tag{92}$$

Next the attention is turned to the behaviour of the Poynting vector field very near the surface of the scatterer. It may be recalled from the discussion in section 17 that there are only two structurally stable configurations of the flow lines next to a perfect conductor. The flow lines may be parallel to the surface or form half saddle points. Extrema of the phase function $\phi(P)$ determine the location of the half saddle points. Let the length of the perimeter of the cross section of the cylinder be L. Then the phase function is periodic with a period L, i.e.,

$$\phi(P_o + L) = \phi(P_o), \quad (\text{mod } 2\pi), \tag{93}$$

where P_o is an arbitrary point on the perimeter. The phase function has an equal number of minima and maxima in one period. Thus there are an even number of half saddle points on the surface. Half of them are of the type in which the

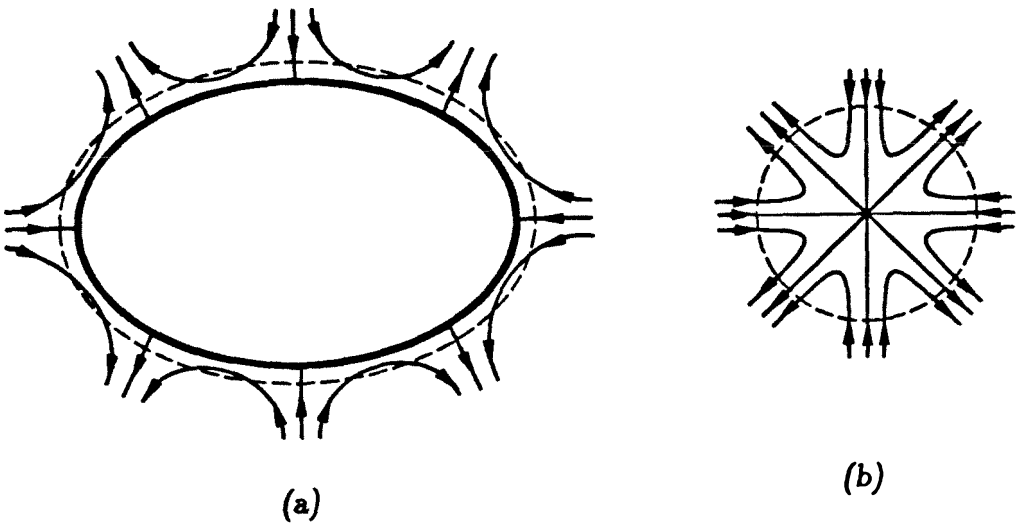

Figure 25. *The scatterer in (a) has eight half saddle points on its surface. The Poynting vector field in the vicinity of the scatterer is homotopic to a critical point with the indices $m = 4$ and $n = 0$ shown in (b). The index of rotation is calculated on the dashed curve in both cases.*

Poynting vector comes normally into the surface and the other half are of the type in which the Poynting vector emanates normally from the surface. It is assumed that the phase function will have only simple extrema as higher order stationary points of $\phi(P)$ lead to structurally unstable critical points. Let there be $2r$ extremum points of the phase function. Then the index of rotation of the Poynting vector field on a closed curve C, which encloses the scatterer but no other critical points, is given as

$$\gamma_{sc} = 1 - r\,. \tag{94}$$

The result given above in (94) follows from the fact that the Poynting vector field on the curve C is homotopic to the Poynting vector field near a critical point with the indices $m = r$ and $n = 0$. This homotopic behaviour is illustrated in figure 25.

The final conclusion of this section can now be drawn. The index of rotation

of the Poynting vector field in the far zone, γ_{FZ}, is in general different from the index of rotation of the Poynting vector field on a curve adjacent to the scatterer, γ_{SC}. This difference is compensated by the index of rotation of the critical points in the near zone of the scatterer. Let the algebraic sum of the indices of the critical points in the near zone be denoted by γ_{NZ}. Then

$$\gamma_{SC} + \gamma_{NZ} = \gamma_{FZ} = 0 . \tag{95}$$

Therefore

$$\gamma_{NZ} = -\gamma_{SC} = r - 1 . \tag{96}$$

If $r = 0$ then there is at least one elementary saddle point in the near zone. If $r > 1$ then there are at least $(r - 1)$ elementary center points in the near zone. It is assumed that there are no critical points of higher order as they are structurally unstable. This estimate of the number of critical points is only a lower bound. There can be additional critical points as long as the algebraic sum of their combined indices of rotation is zero.

§20. Examples of Critical Points in Diffraction and Scattering

This section will be utilized to present the Poynting vector field in some electromagnetic diffraction problems. In this section flow diagrams of the Poynting vector field will be shown for four different problems. These diagrams were prepared by the following method. First a map of the phase of the appropriate field E_z or H_z was made using the HALO graphics package on an IBM personal computer. In general the resolution of the phase map was $\pi/8$ radians. The resolution was increased in some cases to make more clear pictures. The orthogonality of lines of constant phase to the flow lines was then utilized to complete the diagrams. This is a tedious and time consuming method because the phase has to be calculated for every pixel. The advantage of this method is that the exact calculation of the

Poynting vector is avoided. This method can be used to produce the flow line diagrams even when an analytical expression for the electric or magnetic field is not available and instead some numerical procedure has to be applied to obtain the field values.

First the diffraction of a plane wave by a perfectly conducting circular cylinder of radius a, will be considered. The incident wave is linearly polarized with the electric field vector parallel to the axis of the cylinder which coincides with the z-axis. The direction of incidence is taken to be the x-axis. The total electric field is given as an eigenfunction expansion which satisfies the boundary condition on the perfect conductor, i.e.,

$$E_z = \exp(ik\rho\cos\theta) - \sum_{l=-\infty}^{\infty} (i)^l \frac{J_l(ka)}{H_l^{(1)}(ka)} H_l^{(1)}(k\rho)\cos l\theta\,. \tag{97}$$

The flow lines of the Poynting vector field for this case are presented in figure 26 for $-10{\cdot}0 < kx < 10{\cdot}0$ and $-10{\cdot}0 < ky < 10{\cdot}0$. The electrical radius of the cylinder is $ka = 2{\cdot}0$. There are only two half saddle points on the surface of the cylinder. One of the half saddle points is located at $\theta = \pi$ and the other half saddle point is located at $\theta = 0$. It was found out that the locations of these points are independent of the radius of the cylinder. There are no critical points in the near zone. Thus the expression (96) is verified in this case. The overall pattern of power flow is qualitatively similar to the velocity field of a highly viscous fluid past a circular cylinder.

A more interesting pattern of flow lines result when two plane waves travelling in opposite directions are incident on the circular cylinder. In absence of the cylinder these waves would have formed a standing wave. Suppose the waves are travelling in the directions $\theta = 0$ and $\theta = \pi$. Then the total electric field can be

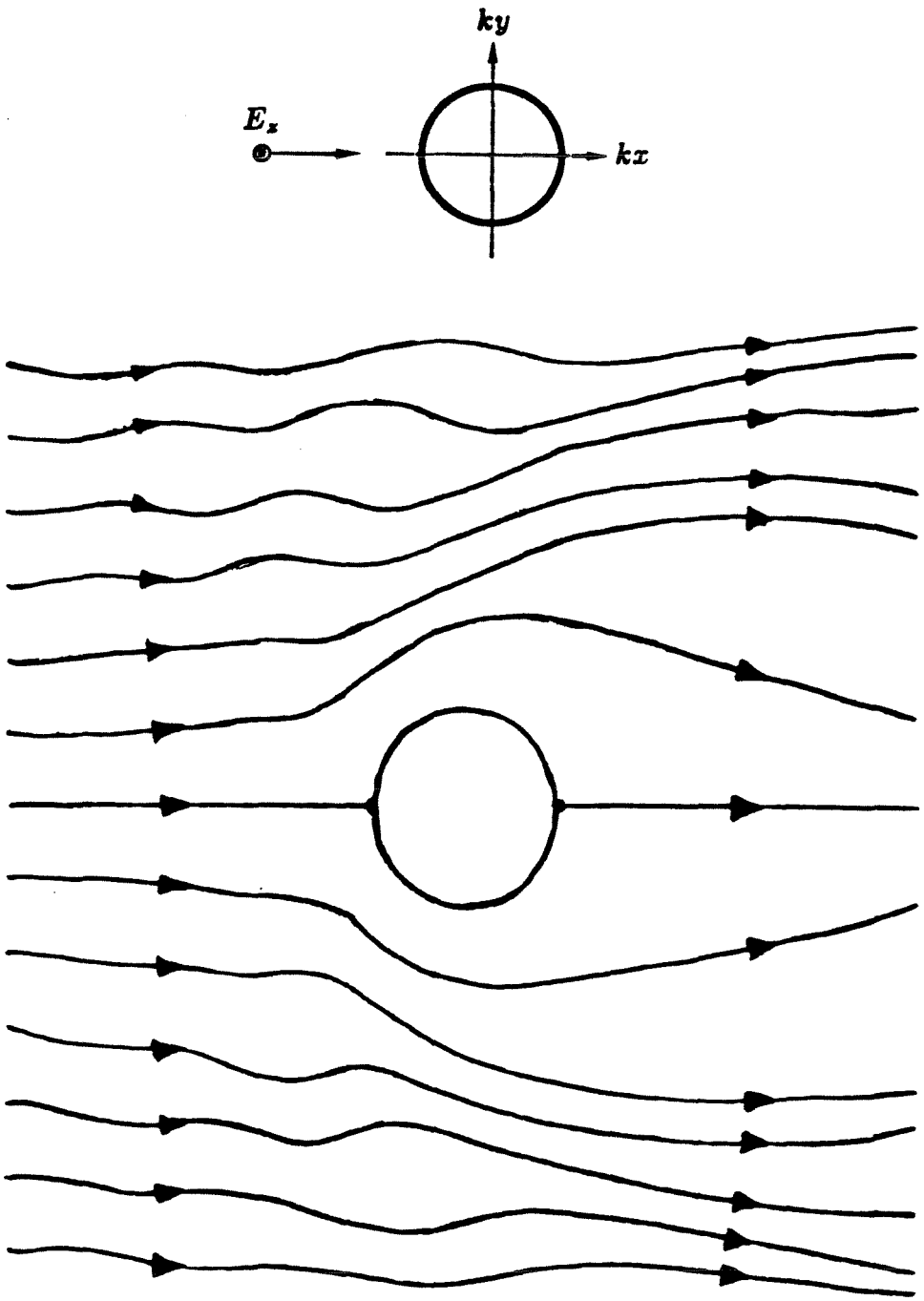

Figure 26. *Lines of flow of the Poynting vector field past a perfectly conducting circular cylinder. The radius of the cylinder is* λ/π. *The range of* kx *and* ky *is from* $-10{\cdot}0$ *to* $10{\cdot}0$.

written with the help of equation (97) and superposition. This field is given as

$$E_z = 2\cos(k\rho\cos\theta) - \sum_{l=-\infty}^{\infty} 2(-1)^l \frac{J_{2l}(ka)}{H_{2l}^{(1)}(ka)} H_{2l}^{(1)}(k\rho)\cos 2l\theta\,. \qquad (98)$$

The lines of the Poynting vector field resulting from this electric field have been plotted in figure 27 for $-10{\cdot}0 < kx < 10{\cdot}0$, $-10{\cdot}0 < ky < 10{\cdot}0$ and $ka = 2{\cdot}0$. The flow pattern is symmetric with respect to the y-axis. It is observed that the flow pattern is rich in elementary critical points. Thus the standing wave is once again demonstrated to be an unstable structure as far as flow lines are concerned. Apart from the aesthetic beauty of the pattern there are some other interesting points to be noted. Some distance away from the cylinder the scattered electric field will behave as a cylindrical wave whose wave fronts will be approximately plane over some small length. This situation resembles the example studied previously, i.e., a standing wave perturbed by a travelling plane wave. There is a strong evidence of this resemblance in the directions $\theta = \pi/2$ and $\theta = 3\pi/2$. The absence of critical points outside the cylinder in the directions $\theta = 0$ and $\theta = \pi$ is also in accordance with the aforementioned example. The resemblance becomes more and more striking as one gets farther away from the cylinder.

One of the classical problems in the diffraction theory has been the diffraction by a perfectly conducting half plane. This problem was solved by Sommerfeld for an arbitrary angle of incidence θ_i. The solution can be found in Born and Wolf's classical text on optics [17] for both cases of polarization. Consider a half plane which extends in the direction of positive x-axis with its edge coinciding with the z-axis. For the case when incident wave is a linearly polarized plane wave whose the magnetic field is completely in the z-direction the total magnetic field is given as

$$H_z = \frac{\exp(ik\rho - i\pi/4)}{\sqrt{\pi}} \left\{ G\Big(-\sqrt{2k\rho}\cos(\frac{\theta-\theta_i}{2})\Big) + G\Big(-\sqrt{2k\rho}\cos(\frac{\theta+\theta_i}{2})\Big) \right\}, \qquad (99)$$

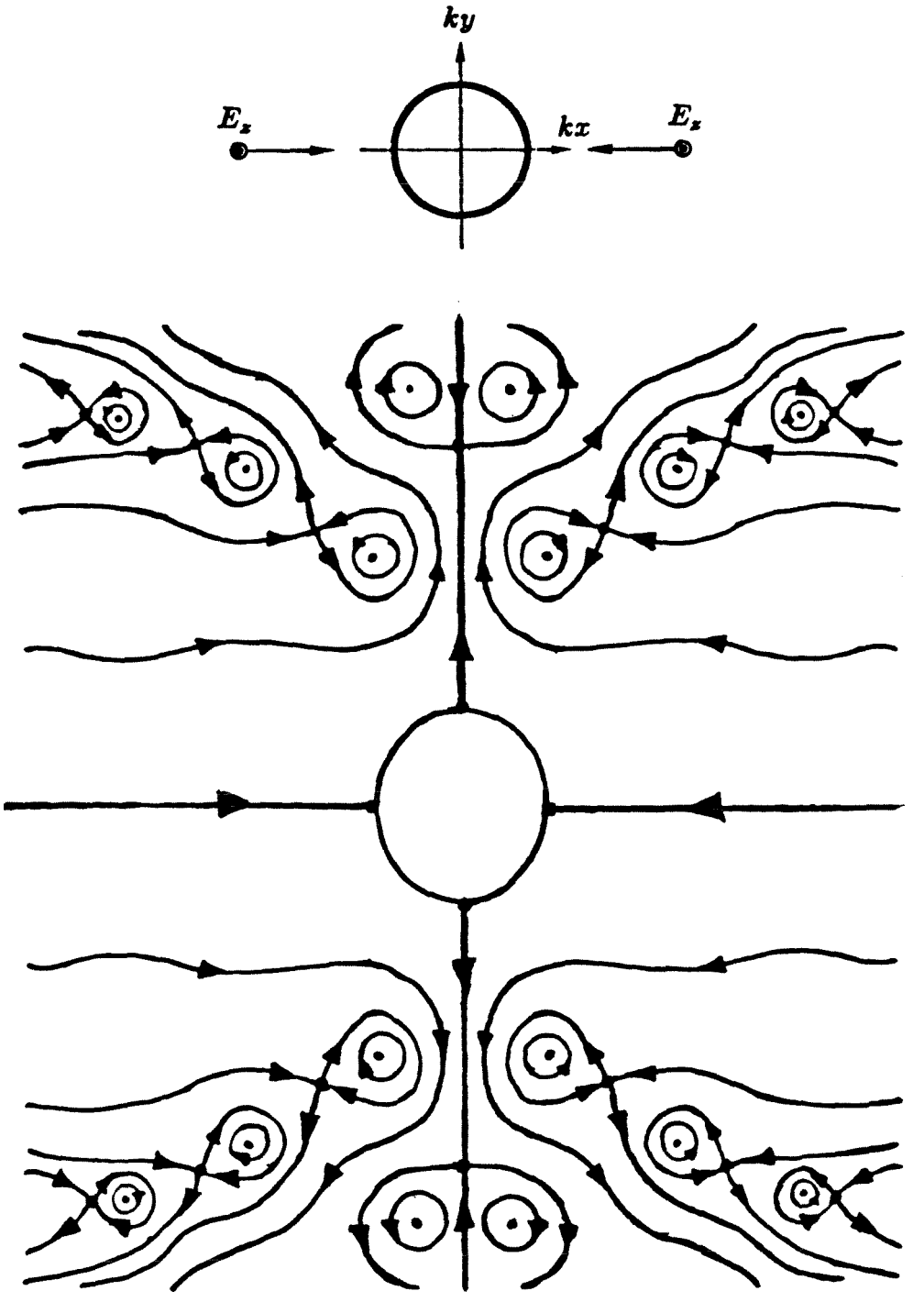

Figure 27. *The flow lines of the Poynting vector field for a perfectly conducting cylinder of radius* $a = \lambda/\pi$ *immersed in a standing wave. The range of* kx *and* ky *is from* $-10{\cdot}0$ *to* $10{\cdot}0$.

where the function G is a form of complex Fresnal integral given by

$$G(\alpha) = \exp(-i\alpha^2) \int_{\alpha}^{\infty} \exp(i\beta^2)\, d\beta\,. \tag{100}$$

The plots of the flow lines were constructed for different angles of incidence using the methods described above. Three plots for angles of incidence $\theta_i = 0{\cdot}3\pi$, $\theta_i = 0{\cdot}5\pi$ and $\theta_i = 0{\cdot}7\pi$ are presented in figures 28(a), (b) and (c) respectively. The Poynting vector plot for the incidence angle $\theta_i = 0{\cdot}5\pi$ was previously worked out by Braunbek and Laukien [18] and it agrees with figure 28(b). It is observed that the critical points are present only in the region in front of the half plane in which a directly reflected wave exists. The existence of the critical points in such regions can be explained as follows. First consider the sum of magnetic field of the incident and the reflected waves. This field is zero on some evenly spaced lines parallel to the x-axis and it is small in the neighbourhood of these lines. The in phase component of the electric field is also zero on the same lines and similarly weak in the vicinity of these lines. There is a cylindrical wave being emitted from the origin due to the edge diffraction. This wave adds up with the total field and causes isolated zeroes, of the magnetic field or the in phase component of the electric field, at locations where they are already weak. The locations of isolated zeroes of the magnetic field coincide with the center points and locations of the isolated zeroes of the in phase part of the electric field coincide with the saddle points.

Another point which may be noted is that there are half saddle points on the front face of the half plane only in the case of normal incidence, i.e., when $\theta_i = 0{\cdot}5\pi$. The power flow parallel to the conducting surface is towards the edge for the angle of incidence $\theta_i = 0{\cdot}3\pi$ and away from the edge for the angle of incidence $\theta_i = 0{\cdot}7\pi$. This can be understood with the help of phase of H_z along the surface as it varies with the angle of incidence. It may be recalled that half

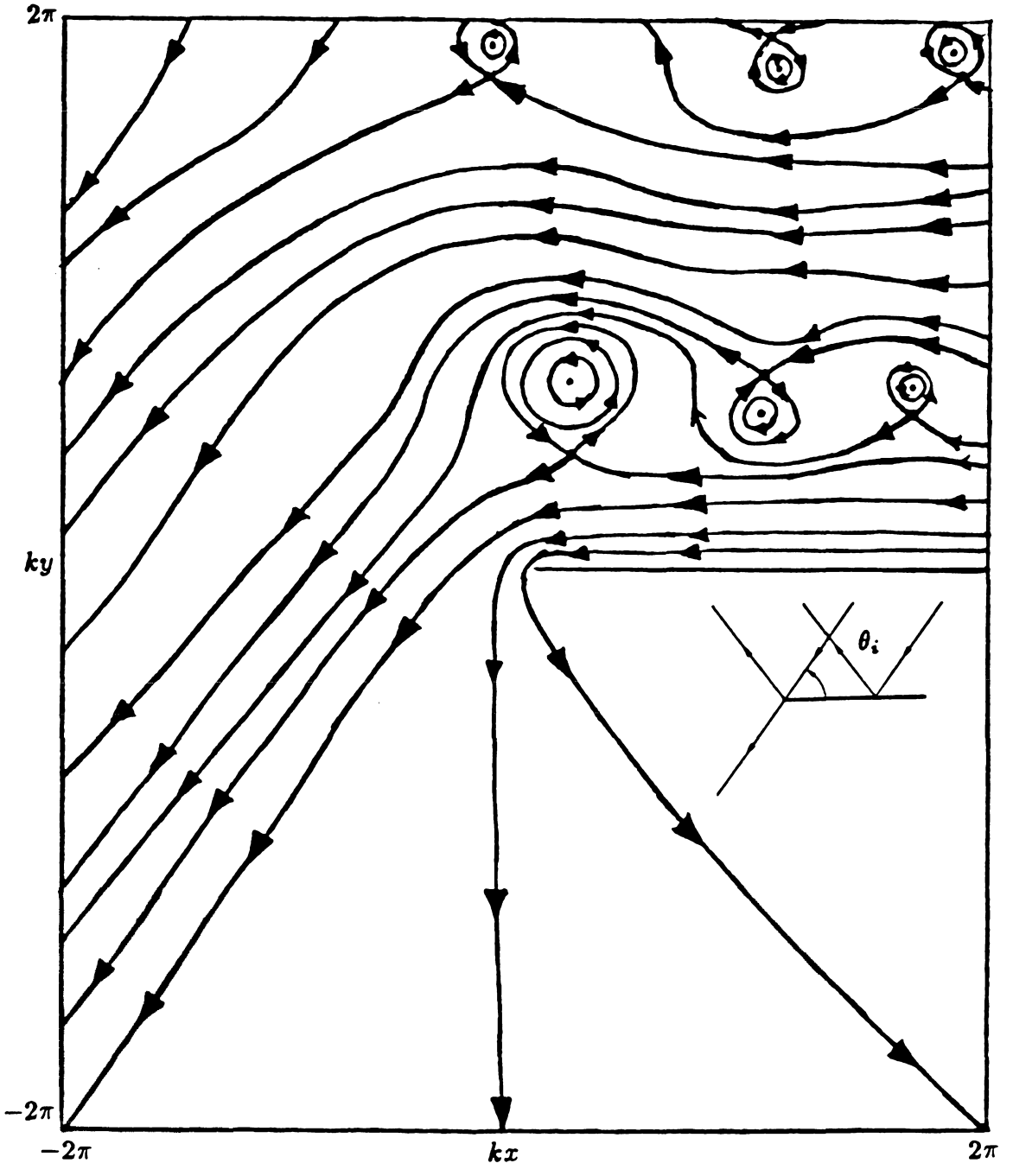

Figure 28. *(a) The lines of flow of the Poynting vector field near the edge of a diffracting half plane. The angle of incidence is* $\theta_i = 0{\cdot}3\pi$.

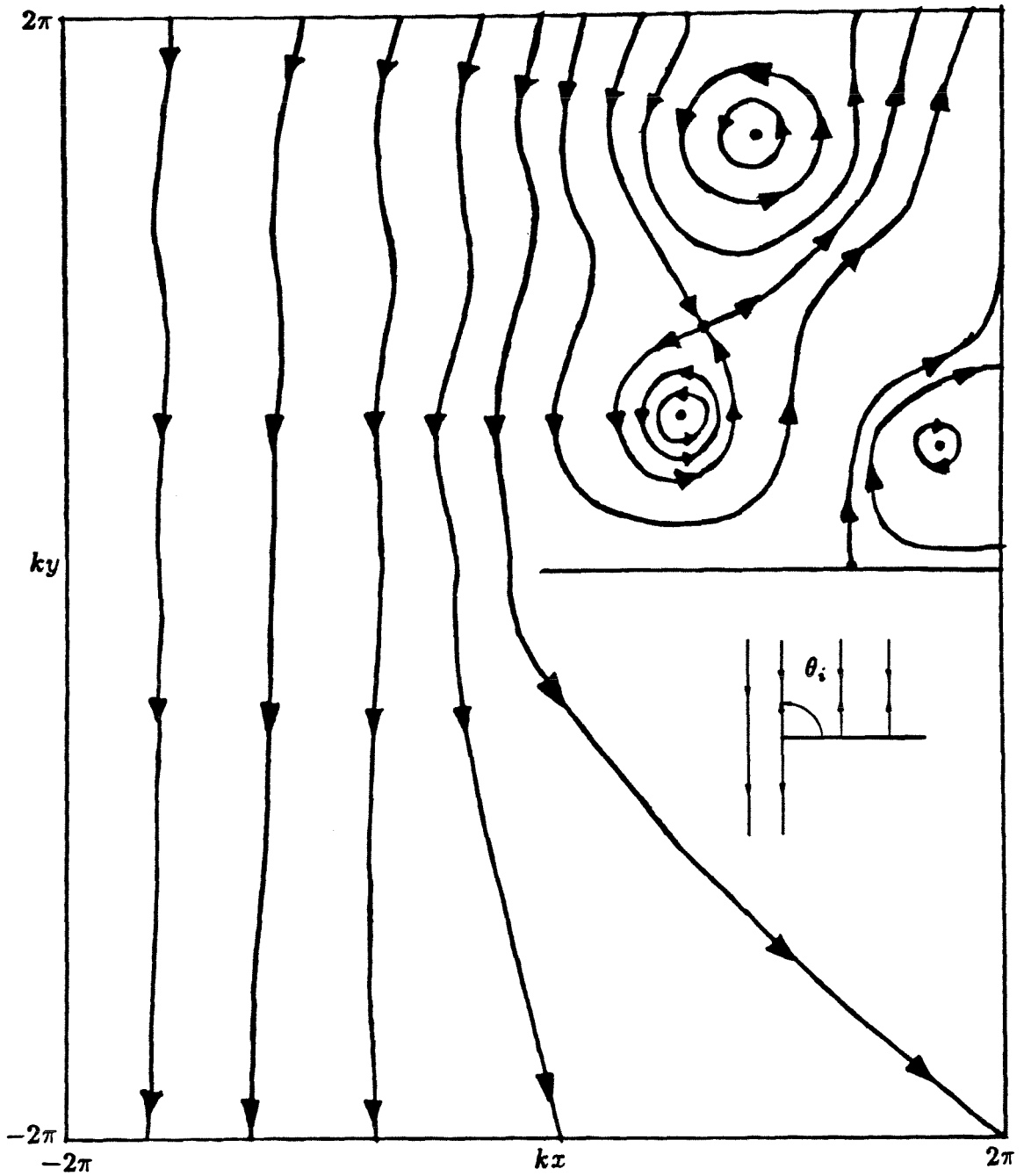

Figure 28. *(b) The lines of flow of the Poynting vector field near the edge of a diffracting half plane. The angle of incidence is* $\theta_i = 0{\cdot}5\pi$.

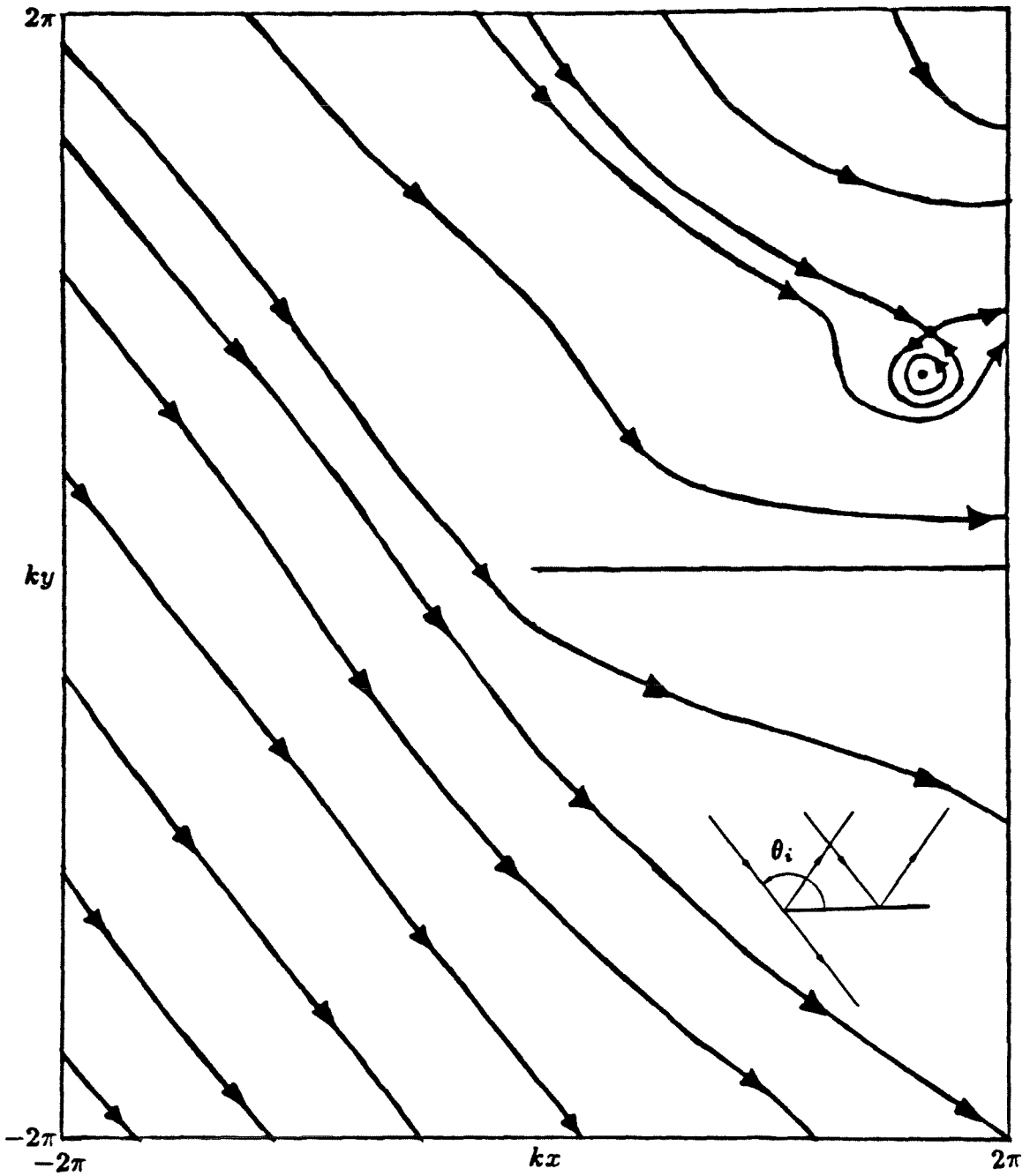

Figure 28. *(c) The lines of flow of the Poynting vector field near the edge of a diffracting half plane. The angle of incidence is* $\theta_i = 0{\cdot}7\pi$.

saddle points on a conducting surface can be identified with the extrema of the phase of H_z. This phase has been plotted versus increasing distance from the edge for the angles of incidence $\theta_i = 87°$, $\theta_i = 90°$ and $\theta_i = 92°$ in figures 29(a), (b) and (c) respectively. The phase function for $\theta_i = 90°$ is approximately a damped periodic function with zero mean. The average value of the phase decreases with the distance from the edge in the case $\theta_i = 87°$ and it increases in the case $\theta_i = 92°$. On further increasing or decreasing the angle of incidence, maxima and minima of the figure 29(b) come together and annihilate each other. The phase of H_z becomes a monotonic function of the distance from the edge. This explains the absence of the half saddle points on the half plane when the incidence is much different from normal.

The last problem to be discussed in this section is the diffraction of a plane wave by two identical perfectly conducting circular cylinders. This problem was solved by Olaofe [19] for two dielectric cylinders with arbitrary refrective index. His solution is adapted to the present case by taking the refrective index to be infinity. The geometry of the problem and the coordinate systems involved are given in figure 30. The incident wave is travelling in the direction $\theta = 0$ and it is linearly polarized with its electric field in the direction of z-axis. Olaofe's solution for the total electric field is given as a sum of incident wave and two eigenfunction expansions around the cylinders as

$$E_z = \exp\left(ikx_1 - i\frac{\pi}{2}\right) + \sum_{l=-\infty}^{\infty} b_{1l} H_l^{(1)}(k\rho_1) \exp\left(i\pi\frac{l+1}{2} - il\theta_1\right)$$
$$+ \sum_{l=-\infty}^{\infty} b_{2l} H_l^{(1)}(k\rho_2) \exp\left(i\pi\frac{l+1}{2} - il\theta_2\right). \qquad (101)$$

The coefficients of the eigenfunction expansion b_{1l} and b_{2l} are unknown. The translation theorem of the Bessel functions is utilized to transform the coordinates of the eigenfunction expansion so that the boundary conditions could be applied.

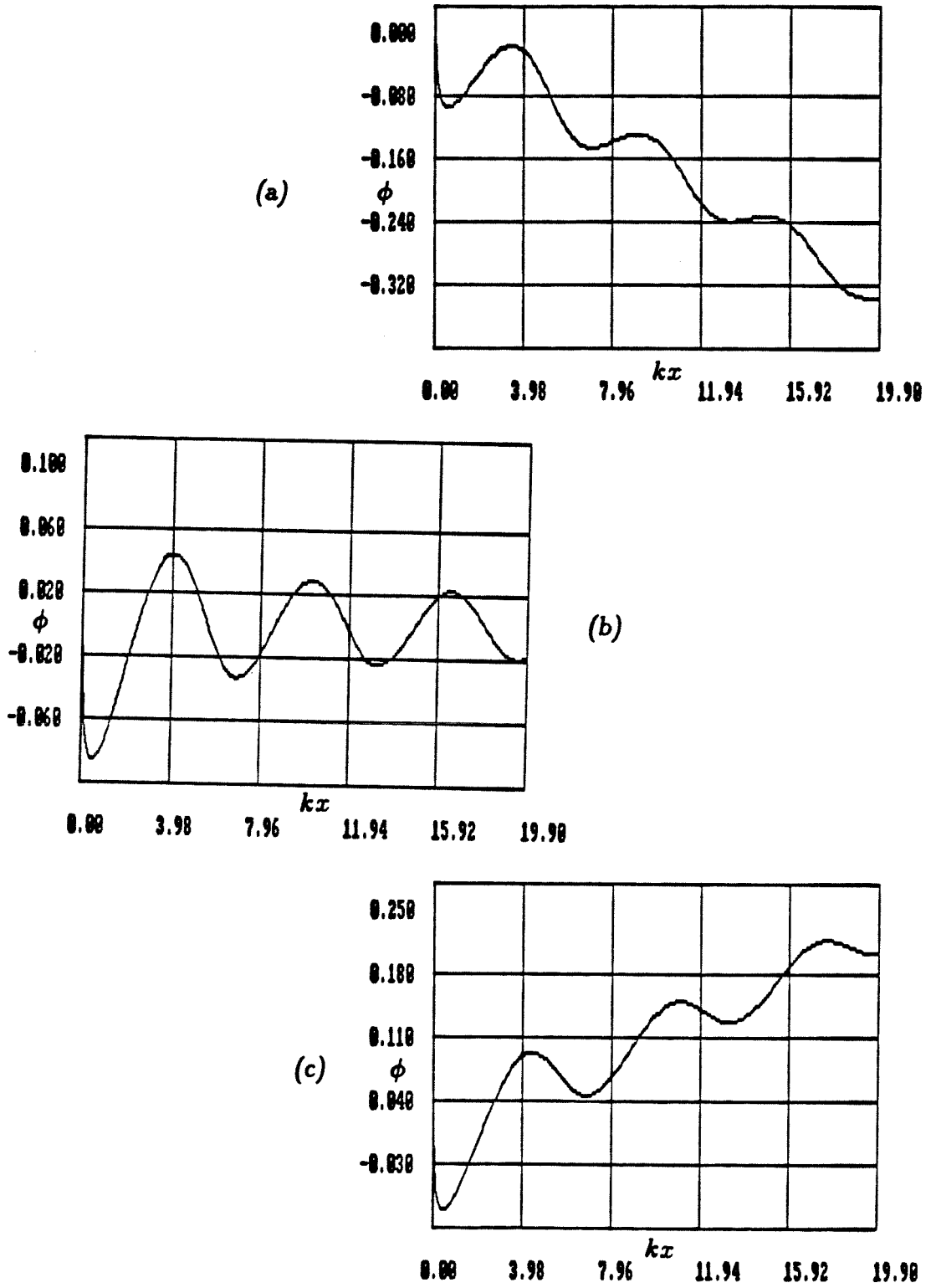

Figure 29. *The phase of H_z on the front face of the half plane for three angles of incidence (a) $\theta_i = 87°$, (b) $\theta_i = 90°$ and (c) $\theta_i = 92°$.*

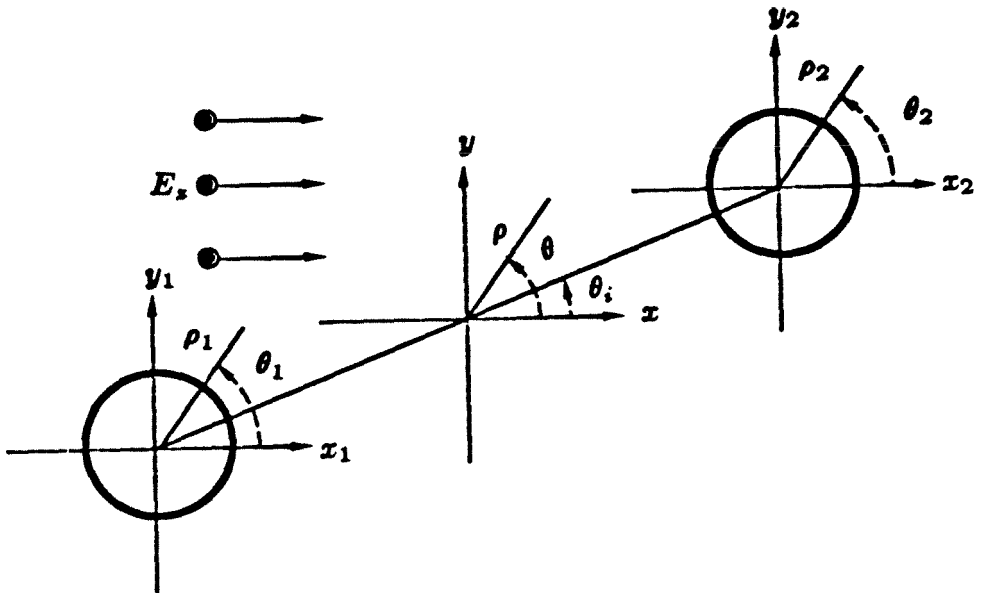

Figure 30. *A plane wave is incident in the direction of the x-axis on the two perfectly conducting cylinders.*

This procedure results in a linear system of equations for unknown coefficients b_{1l} and b_{2l}. The infinite expansions are then truncated and the resulting system of linear equations is solved by iteration. To keep matters simple only broadside incidence is considered, i.e., θ_i is taken to be $\pi/2$. Using the expression (101) and the methods described above the diagrams for the flow lines of the Poynting vector field are drawn. The electrical separation between the cylinders is kept constant at $kd = 9{\cdot}0$ while the radius of the cylinders is varied. Three plots of the flow lines for $ka = 2{\cdot}0$, $ka = 3{\cdot}0$ and $ka = 4{\cdot}0$ are presented in the figures 31(a), (b) and (c) respectively. These plots are symmetric with respect to the x-axis and therefore only portions of them above the x-axis are presented for the cases $ka = 3{\cdot}0$ and $ka = 4{\cdot}0$.

It is observed that when the radius of the cylinders is small compared to their

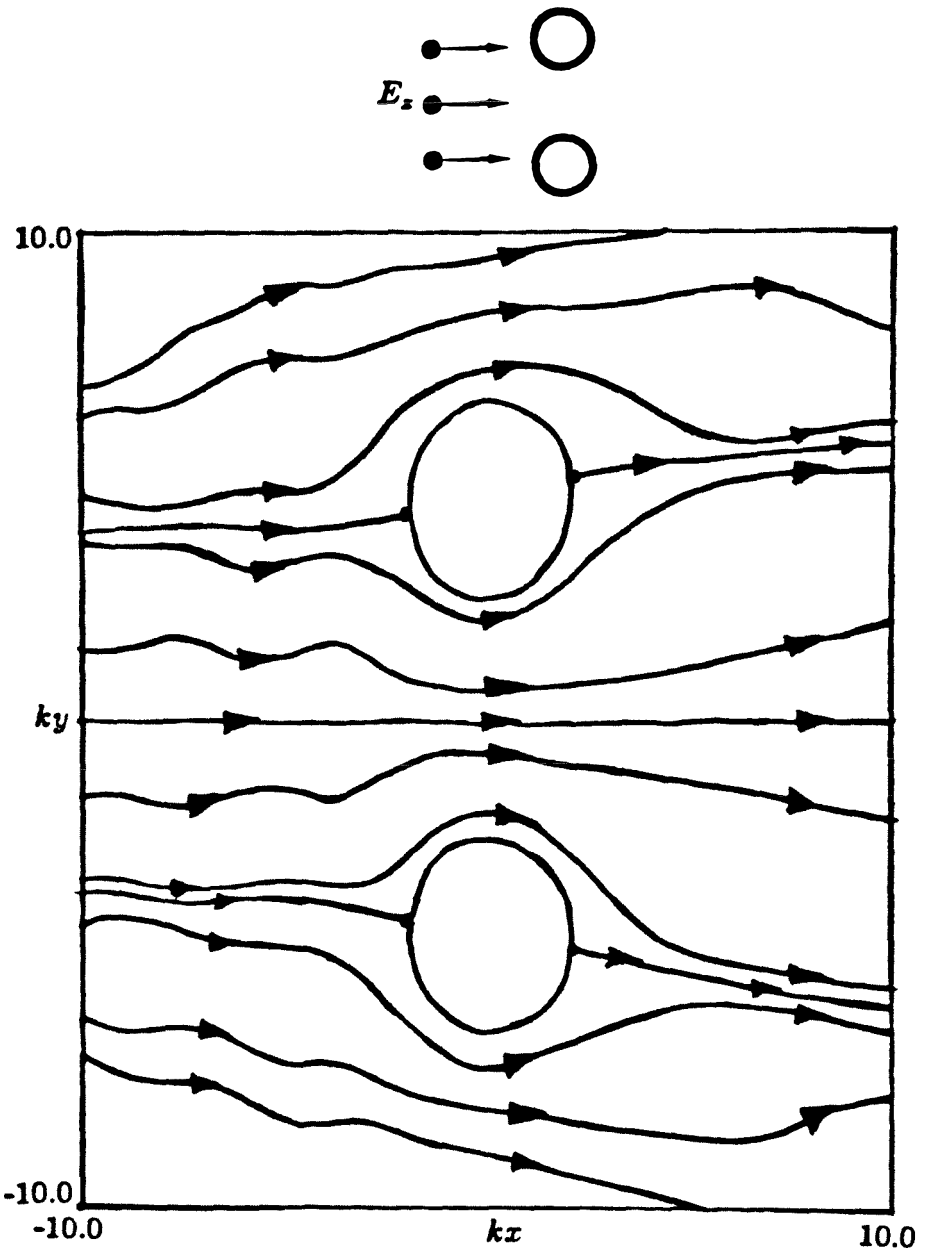

Figure 31. *(a) Flow lines of the Poynting vector field when a plane wave is scattered by two perfectly conducting cylinders. Separation* kd *is* 9·0 *and the radius* ka *is* 2·0 *for each cylinder.*

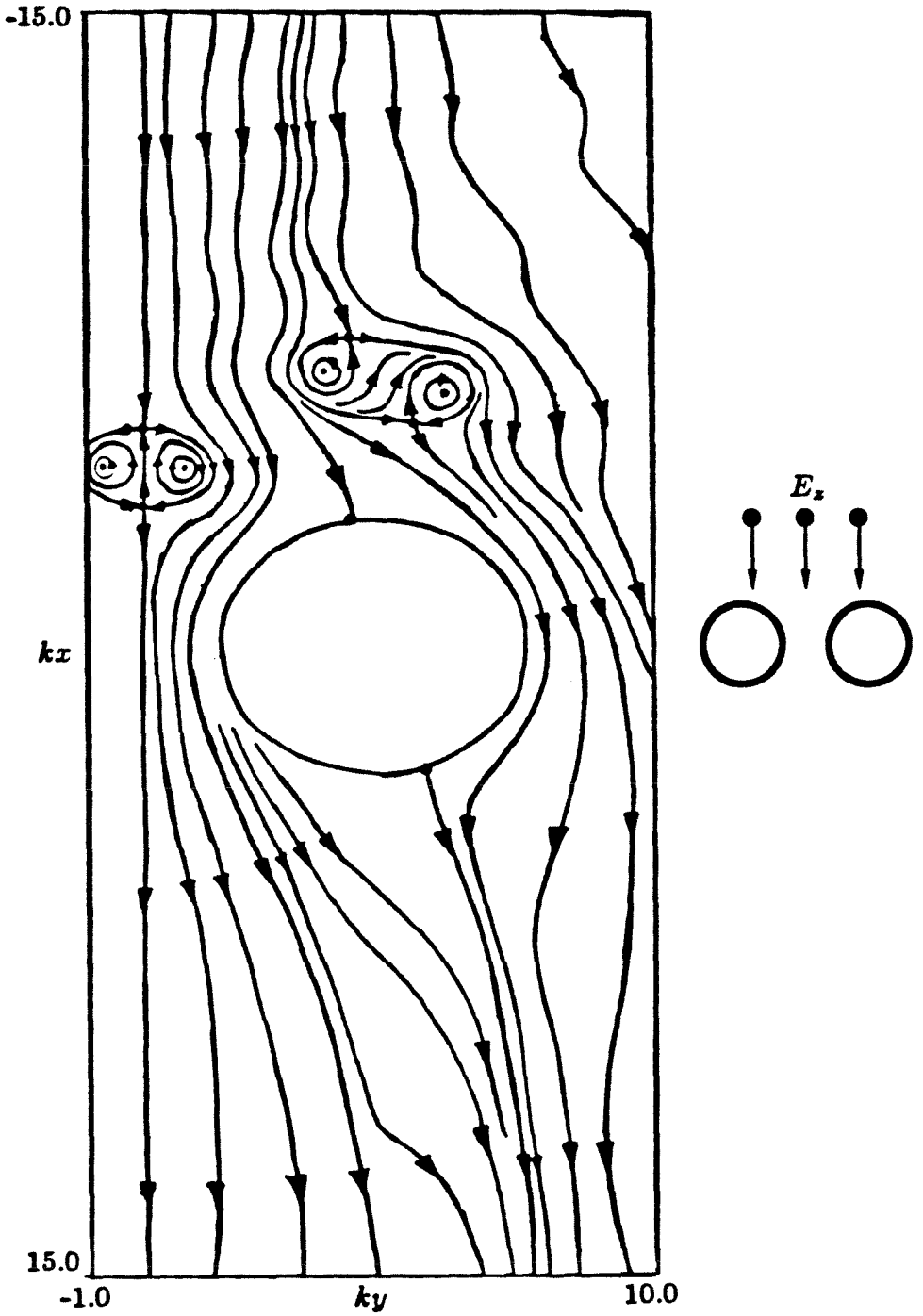

Figure 31. *(b) Flow lines of the Poynting vector field when a plane wave is scattered by two perfectly conducting cylinders. Separation kd is* 9·0 *and the radius ka is* 3·0 *for each cylinder.*

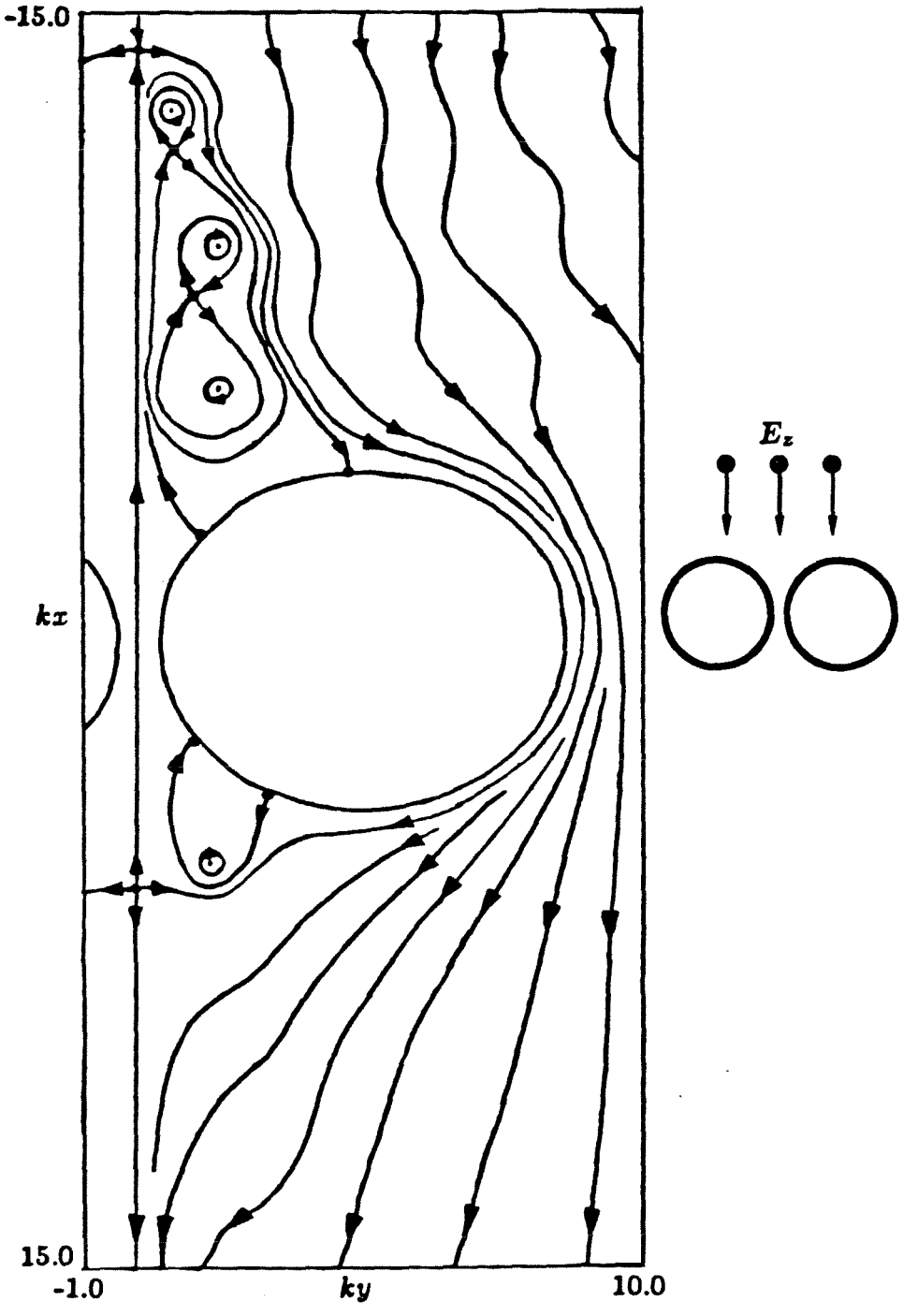

Figure 31. *(c) Flow lines of the Poynting vector field when a plane wave is scattered by two perfectly conducting cylinders. Separation* ***kd*** *is* 9·0 *and the radius* ***ka*** *is* 4·0 *for each cylinder.*

mutual separation the lines of flow behave as if there is no interaction between the cylinders. Flow lines in figure 31(a) are qualitatively similar to the the flow lines near a single cylinder which are given in figure 26. The situation changes as the radius of the cylinders is increased because the reflecting surfaces come closer and their scattered fields start to interact. In figure 31(b) there are six elementary center points and six elementary saddle points. There are two half saddle points on each cylindrical surface. The index of rotation of the Poynting vector field on the two part scattering surface is

$$\gamma_{SC} = \gamma_{SC1} + \gamma_{SC2} = 2\left(1 - \frac{2}{2}\right) = 0. \tag{102}$$

Therefore expression (96) is verified because the sum of the indices of rotation of elementary critical points in the near zone, γ_{NZ}, is also zero. The pattern of the flow lines in front of the cylinders resembles the pattern of a standing wave being perturbed by another wave. Now consider figure 31(c). Reflection from the structure is so intense that the lines of flow between the cylinders are in opposite direction to the incident power flow. The lines of flow also indicate a very strong coupling between the two cylinders. There are four half saddle points on each cylinder. There are a total of eight elementary center points and six elementary saddle points in the near zone. The total index of rotation on the scatterer is

$$\gamma_{SC} = \gamma_{SC1} + \gamma_{SC2} = 2\left(1 - \frac{4}{2}\right) = -2. \tag{103}$$

The sum of the indices of rotation of elementary critical points is

$$\gamma_{NZ} = +8 - 6 = 2 = -\gamma_{SC}. \tag{104}$$

Thus the expression (96) is once again verified.

The phase of the induced current on the cylinders has been studied to understand the creation of half saddle points. Current on one cylinder can be computed

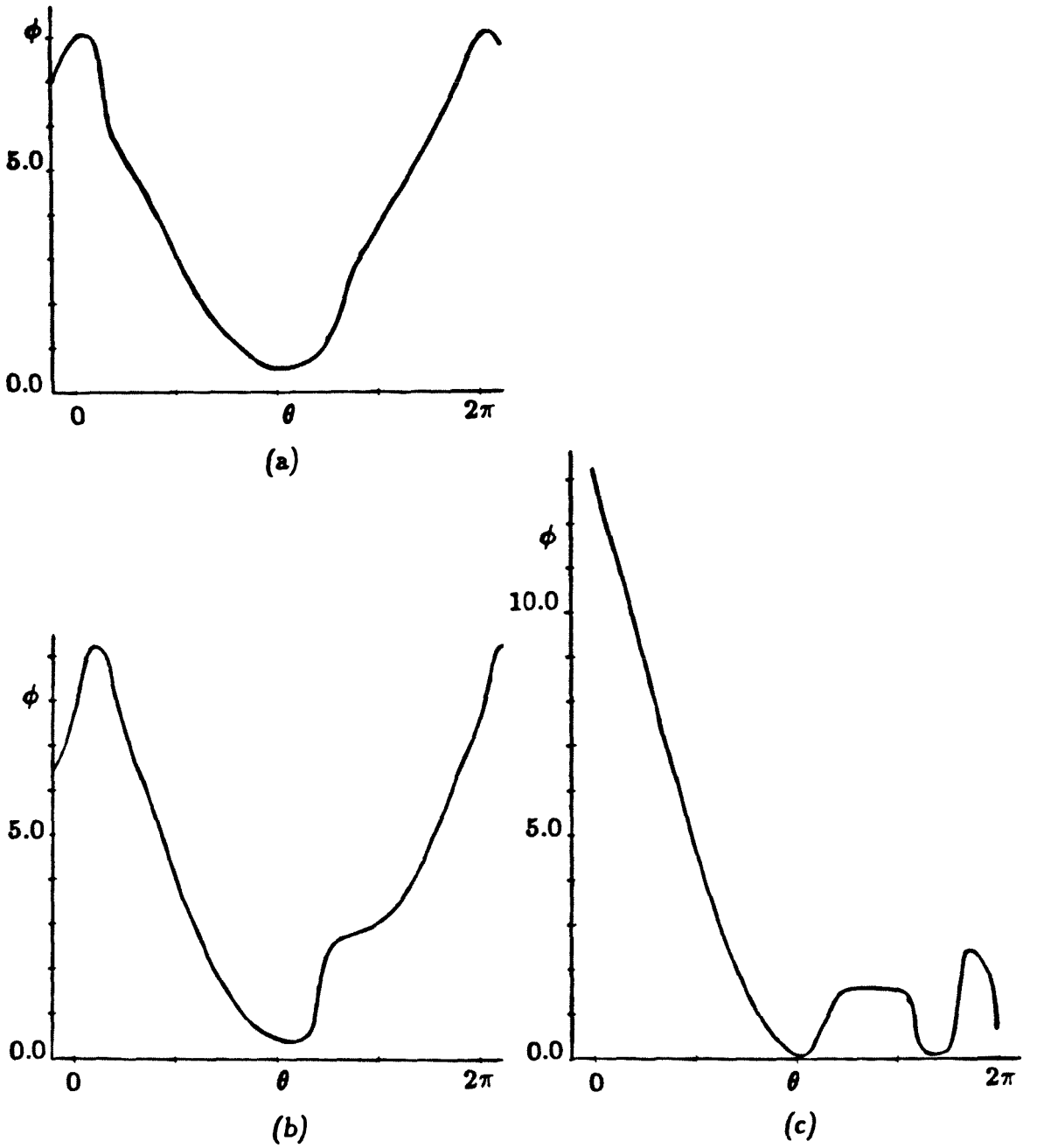

Figure 32. *The phase of the induced surface current on one cylinder in the problem of diffraction by two cylinders for the three cases (a) $ka = 2{\cdot}0$, (b) $ka = 3{\cdot}0$ and (c) $ka = 4{\cdot}0$.*

from the knowledge of the electric field as follows,

$$\mathbf{K}_2 = \mathbf{e}_z \frac{i}{\omega\mu} \left(\mathbf{e}_{\rho_2} \cdot \nabla E_z \right|_{\rho_2 = a} . \tag{105}$$

The phase of $\mathbf{K}_2$ is presented in figure 32(a), (b) and (c) for the cylinder radii $ka = 2{\cdot}0$, $ka = 3{\cdot}0$ and $ka = 4{\cdot}0$ respectively. For the radius $ka = 2{\cdot}0$ the phase has only two extrema. An increase in radius to $ka = 3{\cdot}0$ does not change the number of extrema. It is observed that the phase funtion is quite flat near $\theta = 3\pi/2$ just like an inflection point. This inflection point then breaks up into a maximum and a minimum and thus two new half saddle points are created as ka is increased to 4·0. This is evident in figure 32(c). It may be noted that figure 32(c) has two more points where the phase function is very flat. Therefore it may be expected that more half saddle points will be created and the flow line pattern will become more complex as the radius is increased.

§21. Other Examples of Critical Points

There are not many examples of the critical points of the Poynting vector field in the published literature. The reason for this may be that in many problems it is sufficient to find the electric or the magnetic field. Poynting vector is seldom calculated. Even in the cases where it is calculated the flow lines are almost never illustrated. There are some solutions to the electromagnetic problems found in literature where the authors have consdidered the Poynting vector important enough to illustrate its behaviour with field plots. Some of these problems will be cited below to point out the relevence of critical points of the Poynting vector field in electromagnetic problems.

It appears that for the first time the existence of the critical points in Poynting vector fields was demonstrated by Wolter [20]. He was investigating the phenomenon of total internal reflection and the penetration of energy into the less

dense medium. This phenomenon, also known as the Goos-Haenchen effect, is a spatial displacement of a totally reflected beam with respect to a ray reflected by the geometrical interface. Wolter modelled the incident beam as a sum of two plane waves propagating in the directions $\theta_o + \delta\theta$ and $\theta_o - \delta\theta$. The surfaces of constant phase of the resulting wave are planes which are orthogonal to the direction θ_o. The amplitude of this wave varies in the transverse direction as a sinusoid and this variation becomes slower as $\delta\theta$ is decreased. The field between two consecutive nulls of the sinusoid was considered to be a beam by Wolter. It is supposed that the incident wave strikes the less dense medium from the denser medium and it is further assumed that $\theta_o + \delta\theta$ and $\theta_o - \delta\theta$ are both greater than the critical angle. This problem is easily solved using superposition and Fresnel's coefficients for reflection and transmission. The resulting plots of the Poynting vector field in [20] show that the power enters the less dense medium in the vicinity of the point at which the null in the amplitude of the incident wave strikes the interface. These plots also show a series of saddle points and center points in the same region and in the region directly above it, i.e., in the dense medium. These critical points are all located in the dense medium except for one saddle point in the less dense medium. The existence of these critical points is easily explained when one considers that they are the result of a superposition of two plane waves whose amplitudes vary in the transverse direction.

Most recently Gesche and Lõchel [21] have solved the problem of diffraction by a lossy dielectric cylinder in a rectangular waveguide. They considered only TE_{m0} modes. This problem is classified as an interior problem in the terminology of this thesis. This structure was shown to behave as a notch filter when the cylinder was asymmetrically placed in the waveguide. Two plots of the Poynting vector field were presented: one for a frequency above the resonant frequency and

the other for a frequency below the resonant frequency. In each case a center point can be observed near the cylinder. In the first plot there are two half saddle points on one wall and in the second plot there are two half saddle points on the other wall of the guide. Since the authors have provided only two plots, it is difficult to say how the half saddle points migrated to the other wall as frequency was varied. It may be worthwhile to plot a few more flow diagrams of the Poynting vector field for different values of frequency. The behaviour of the flow lines can then be studied with frequency being the perturbing parameter. A more clear understanding of the phenomenon can be obtained from this endeavor. Gesche and Lõchel have proposed to use of many dielelectric cylinders in order to make a filter whose frequency response can be tailored to suit a given specification.

Another problem in which the critical points make an appearance is the problem of scattering by an iris in a rectangular waveguide. A solution to this problem accompanied by quite a few number of plots of the Poynting vector field has been given by Ziolkowski and Grant [22]. They considered only longitudnal sectional modes [15] for primary excitation. These electromagnetic fields are not truly two dimensional though all the field components can be derived from H_x or E_x. Suppose the primary excitation is given as the mode with $E_x = 0$ and

$$H_x = H_0 \sin(\frac{l\pi x}{a}) \cos(\frac{p\pi y}{b}) \exp(-i\gamma_{lp} z)\,, \tag{106}$$

where l and p are integers, γ_{lp} is the propagation constant in the guide, a is the width of the guide and b is the height of the guide. The iris is taken to be uniform in the direction of x-axis. Therefore the total magnetic field in the direction of the x-axis is given as

$$H_x = \sin(\frac{l\pi x}{a}) A(y,z) \exp\big(i\phi(y,z)\big)\,, \tag{107}$$

where A and ϕ are some real valued unknown functions. Then it can be easily

shown that the Poynting vector is given as

$$\mathbf{S} = \frac{\omega\mu}{2\left[k^2 - (l\pi/a)^2\right]} \sin^2\left(\frac{l\pi x}{a}\right) A^2 \nabla\phi . \tag{108}$$

From the above expression it is evident that the flow lines of the Poynting vector field are curves in the y-z plane. This field is two dimensional except that its amplitude varies in the transverse direction. The flow lines can be drawn for any constant x such that $\sin(l\pi x/a) \neq 0$. It has been shown in [22] that when the frequency is low there are no critical points in the flow diagrams. As the frequency increases critical points begin to appear. When the frequency is lower than the cut off frequency of the next higher order mode, the locations of the critical points are limited to the vicinity of the iris. At this point the interfering higher order modes are still evanescent and their effect cannot be felt far away from the iris. The authors note that as soon as the next higher order mode starts propagating there appears a whole series of critical points located periodically inside the guide. This fact is quite comprehensible in the light of the previous discussions on generation of critical points by interfering waves.

Chapter V

Generalization

§22. Critical Points of Three Dimensional Poynting Vector Fields

Plane Poynting vector fields have been discussed exclusively in the previous sections. It seems only logical to try to extend the classification scheme of the critical points of plane Poynting vector field to the case of general three dimensional Poynting vector fields. Alas, this is no easy task. Reasons for this pessimistic statement will be explained below. Although a general classification of the critical points cannot be easily made, a list of structurally stable critical points will however be given.

A Taylor series expansion of the Poynting vector field is necessary to study the behaviour of its critical points. Since this field is divergence free it should be completely described by two scalar functions. But it is not known what kind of equations these functions satisfy. Hence it becomes necessary to resort to the electric field and the magnetic field because it is known that they satisfy Helmholtz's equation. It was shown by Whittaker [23] that only two functions of space and time are needed to describe any solution to the homogeneous Helmholtz's equation. If the time dependence is included as $\exp(-i\omega t)$ then these functions become two complex functions of space alone. It may be recalled that in the case of plane

Poynting vector fields it is the phase of only one complex function that controls the direction of the Poynting vector. It appears that in general this is not possible. Many authors have persevered to find a representation of the Poynting vector field in such a way that the flow lines should be orthogonal to the surfaces of constant phase. The efforts of Green and Wolf [24], Wolf [25] and Roman [26] are especially noteworthy in this regard. The two complex functions which turn out to be very convenient are the radial components of the electric and magnetic fields, i.e., E_r and H_r. The total electromagnetic field can be expressed as a sum of two fields, one derived from E_r and the other derived from H_r. E_r and H_r can be expanded in an eigenfunction expansion around the origin. This expansion is in terms of spherical Bessel functions $j_n(kr)$ and surface spherical harmonics $Y_n^m(\theta, \varphi)$. The spherical Bessel functions can be approximated near the origin as

$$j_n(kr) = \frac{(kr)^n}{(2n+1)!!} + O(kr)^{n+1}. \tag{109}$$

For every term of degree n there are $2n + 1$ terms involving surface harmonics. Even for a small n the number of constants in the leading term of the eigenfunction expansion becomes very large. This approach becomes very cumbersome and is abandoned at this point.

From the experience of plane Poynting vector fields it is known that higher order critical points are not structurally stable. Therefore it is reasonable to look for only the structurally stable critical points in the three dimensional Poynting vector field. Suppose a critical point exists at the origin. If this point is structurally stable then the Taylor series expansions of S_x, S_y and S_z should start with the linear terms. If the linear terms are all zero then the point of contact of the surfaces $S_x = 0$, $S_y = 0$ and $S_z = 0$ is of order greater than unity. Such a point of contact is structurally unstable. Neglecting higher order terms the Poynting

vector can be written as

$$\mathbf{S} = \mathcal{A}\mathbf{r}, \tag{110}$$

where $\mathbf{r}$ is the position vector and $\mathcal{A}$ is a 3×3 matrix whose elements are given as

$$a_{ij} = \left.\frac{\partial S_{x_i}}{\partial x_j}\right|_O \qquad (x_1 = x, x_2 = y, x_3 = z). \tag{111}$$

The differential equation for the flow lines given by expression (6) can be conveniently written in terms of a parameter t as follows

$$\frac{d\mathbf{r}(t)}{dt} = \mathcal{A}\mathbf{r}(t). \tag{112}$$

Equation (112) given above is linear and can be readily integrated to yield an expression for the flow lines. If a flow line passes through a point $\mathbf{r}_o$ then the equation for that flow line is given as

$$\mathbf{r}(t) = \exp(\mathcal{A}t)\mathbf{r}_o\,. \tag{113}$$

The behaviour of the flow lines depends on the roots of the characteristic equation of $\mathcal{A}$ which is given by

$$\lambda^3 + (\text{sum of principal minors of } \mathcal{A})\lambda - (\text{determinant of } \mathcal{A}) = 0\,. \tag{114}$$

The coefficient of λ^2 in the characteristic equation is zero because the divergence of $\mathbf{S}$ is zero. This implies that the sum of roots of the characteristic equation is also zero. Only the distinct and non zero roots of (114) should be considered because multiple roots and zero roots are coincidental. Hence the structures they represent are unstable. There are only two possible cases which will be considered below.

Suppose λ_1, λ_2 and λ_3 are real and distinct roots of the characteristic equation. Then there exists a real, non singular linear transformation $\mathcal{T}$ (see, e.g. Shilov [27]) such that

$$\tilde{\mathbf{r}} = \mathcal{T}\mathbf{r} \tag{115}$$

and

$$\frac{d\tilde{\mathbf{r}}(t)}{dt} = \mathcal{T}\mathcal{A}\mathcal{T}^{-1}\tilde{\mathbf{r}}(t) = \begin{pmatrix} \lambda_1 & 0 & 0 \\ 0 & \lambda_2 & 0 \\ 0 & 0 & \lambda_3 \end{pmatrix} \tilde{\mathbf{r}}(t). \tag{116}$$

The effect of this transformation is to change the length of position vectors and to change the angles between two vectors. The solution of the above differential equation is trivial and is given by

$$\begin{aligned} \tilde{x} &= \tilde{x}_o \exp(\lambda_1 t) \\ \tilde{y} &= \tilde{y}_o \exp(\lambda_2 t) \\ \tilde{z} &= \tilde{z}_o \exp(\lambda_3 t). \end{aligned} \tag{117}$$

If two roots, for example, λ_1 and λ_2 have the same sign then the third root λ_3 will have the opposite sign. The flow lines described by the parametric equations (117) are sketched in figure 33(a). The flow lines in the x-z and y-z planes behave as if the critical point is a saddle point and in the x-y plane they behave as if it is a nodal point. Such a critical point has been termed as a saddle point by Myškis [28]. This is unfortunate. To avoid confusion with the saddle point of plane vector fields and to emphasize the three dimensional nature of this critical point it will be called *Saddle-S point*. The flow lines in the original coordinate system can be found by the application of inverse linear transformation $\mathcal{T}^{-1}$, to the equation (117).

The second case occurs when there is only one real root and the other two roots are complex conjugates of each other. Let these roots be given as $-2\lambda_r$, $\lambda_r \pm i\lambda_i$. As in the previous case a linear transformation $\mathcal{T}$ of the coordinate system can be found such that

$$\frac{d\tilde{\mathbf{r}}(t)}{dt} = \mathcal{T}\mathcal{A}\mathcal{T}^{-1}\tilde{\mathbf{r}}(t) = \begin{pmatrix} \lambda_r & -\lambda_i & 0 \\ \lambda_i & \lambda_r & 0 \\ 0 & 0 & -2\lambda_r \end{pmatrix} \tilde{\mathbf{r}}(t). \tag{118}$$

The details of this transformation can be found in Shilov [27]. The parametric equations for the flow lines in the transformed coordinate system can be written

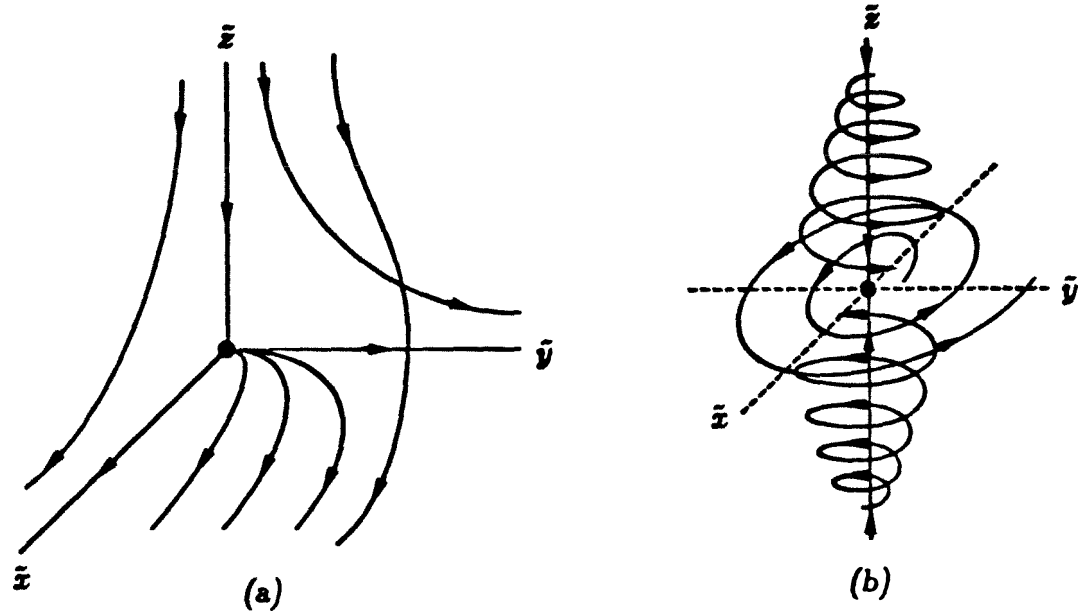

Figure 33. *Behaviour of flow lines in the neighbourhood of two types of structurally stable critical points of three dimensional Poynting vector fields. (a) The saddle-3 point and (b) the saddle-focal point.*

as

$$\begin{aligned} \tilde{x} &= (\tilde{x}_o \cos \lambda_i t - \tilde{y}_o \sin \lambda_i t) \exp(\lambda_r t) \\ \tilde{y} &= (\tilde{y}_o \cos \lambda_i t + \tilde{x}_o \sin \lambda_i t) \exp(\lambda_r t) \\ \tilde{z} &= \tilde{z}_o \exp(-2\lambda_r t). \end{aligned} \tag{119}$$

The flow lines are helical in the neighbourhood of this type of critical point except in the x-y plane. Flow lines in the x-y plane behave as if the critical point is a spiral point. The envelope of the helical flow lines is a hyperbola in any plane which is perpendicular to the x-y plane. Such a point is called a *Saddle-focal point* [28]. A sketch of the behaviour of flow lines near this type of critical point is given in figure 33(b). As in the previous case parametric equation (119) can be transformed back to the original coordinate system but such a transformation does not change the qualitative behaviour of the flow lines.

§23. Example of Critical Points in Three Dimensional Fields

Structurally stable critical points of the Poynting vector field were categorized in the previous section. It is appropriate at this point to give an example which demonstrates their existence. The simplest example which can be concocted in this regard is the example of a field due to the interference of three parallel dipoles. To be more specific consider three identical dipoles oriented in the direction of z-axis, located on the corners of an equilateral triangle. The triangle lies in the x-y plane. Let the dipole moment of each dipole be given as p_z. The electric and magnetic fields of a radiating dipole are given in any good text on electromagnetic theory. See for example Papas [1]. Using superposition the total electric and magnetic field of the three radiating dipoles can be found. To keep the matters simple consider electromagnetic fields only in the x-y plane. There are only three components of the field in the x-y plane. They are given as

$$E_z = \frac{k^3 p_z}{4\pi\epsilon} \sum_{n=1}^{3} \left\{ 1 + \frac{i}{k\rho_n} - \frac{1}{(k\rho_n)^2} \right\} \frac{\exp(ik\rho_n)}{k\rho_n}, \tag{120}$$

$$H_x = \frac{\omega k^2 p_z}{4\pi} \sum_{n=1}^{3} (ky - ky_n) \left\{ 1 + \frac{i}{k\rho_n} \right\} \frac{\exp(ik\rho_n)}{(k\rho_n)^2}, \tag{121}$$

$$H_y = \frac{\omega k^2 p_z}{4\pi} \sum_{n=1}^{3} (kx_n - kx) \left\{ 1 + \frac{i}{k\rho_n} \right\} \frac{\exp(ik\rho_n)}{(k\rho_n)^2}, \tag{122}$$

where

$$k\rho_n = \sqrt{(kx - kx_n)^2 + (ky - ky_n)^2}, \tag{123}$$

and the coordinates

$$(kx_1 = 2{\cdot}0, ky_1 = 0{\cdot}0), (kx_2 = -1{\cdot}0, ky_2 = \sqrt{3}), (kx_3 = -1{\cdot}0, ky_3 = -\sqrt{3}),$$

are the locations of the dipoles. The Poynting vector can be calculated with the help of expression (3) as

$$\mathbf{S} = \frac{1}{2} \Re \left[E_z H_x^* \mathbf{e}_y - E_z H_y^* \mathbf{e}_x \right]. \tag{124}$$

It is evident from expression (103) that the Poynting vector field in the x-y plane is completely two dimensional. A plot of the flow lines of this field is given in figure 34.

A study of figure 34 brings out the following points. There are three source points at the locations of the dipoles. This is hardly surprising. There is one spiral point located at the origin of the coordinates which is also the centroid of the equilateral triangle. The flow lines in the neighbourhood of this critical point are qualitatively similar to the flow lines in the $\tilde{x}$-$\tilde{y}$ plane of figure 33(b). These lines are also in a form which will satisfy expression (119) with $\tilde{z}_o = 0$. Thus this critical point is a saddle-focal point. There are three more critical points in the figure. In the vicinity of these critical points the flow lines behave like the flow lines near a saddle point. These lines are of the form which will satisfy expression (117) with $\tilde{z}_o = 0$. These lines are also qualitatively similar to the flow lines in the $\tilde{y}$-$\tilde{z}$ plane of figure 33(a). Therefore this critical point is a saddle-3 point. Thus in one simple example the existence of both the structurally stable critical points has been demonstrated.

It is appropriate at this juncture to point to a paper by Boiven et al. [29] in which critical points of three dimensional Poynting vector field have been shown to exist. These authors considered the energy flow in the neighbourhood of the focus of a coherent beam. The energy in the beam is flowing in the direction of z axis which is called the optical axis. The flow lines are planar, i.e., they are confined to the plane φ = constant. The energy flow is rotationally symmetric with respect to the optical axis. The Poynting vector is zero on concentric circles in the focal plane which is orthogonal to the optical axis. In a plane φ = constant the Poynting vector appears to be zero on isolated points which behave as center points and saddle points of a two dimensional field. Since the Poynting vector is

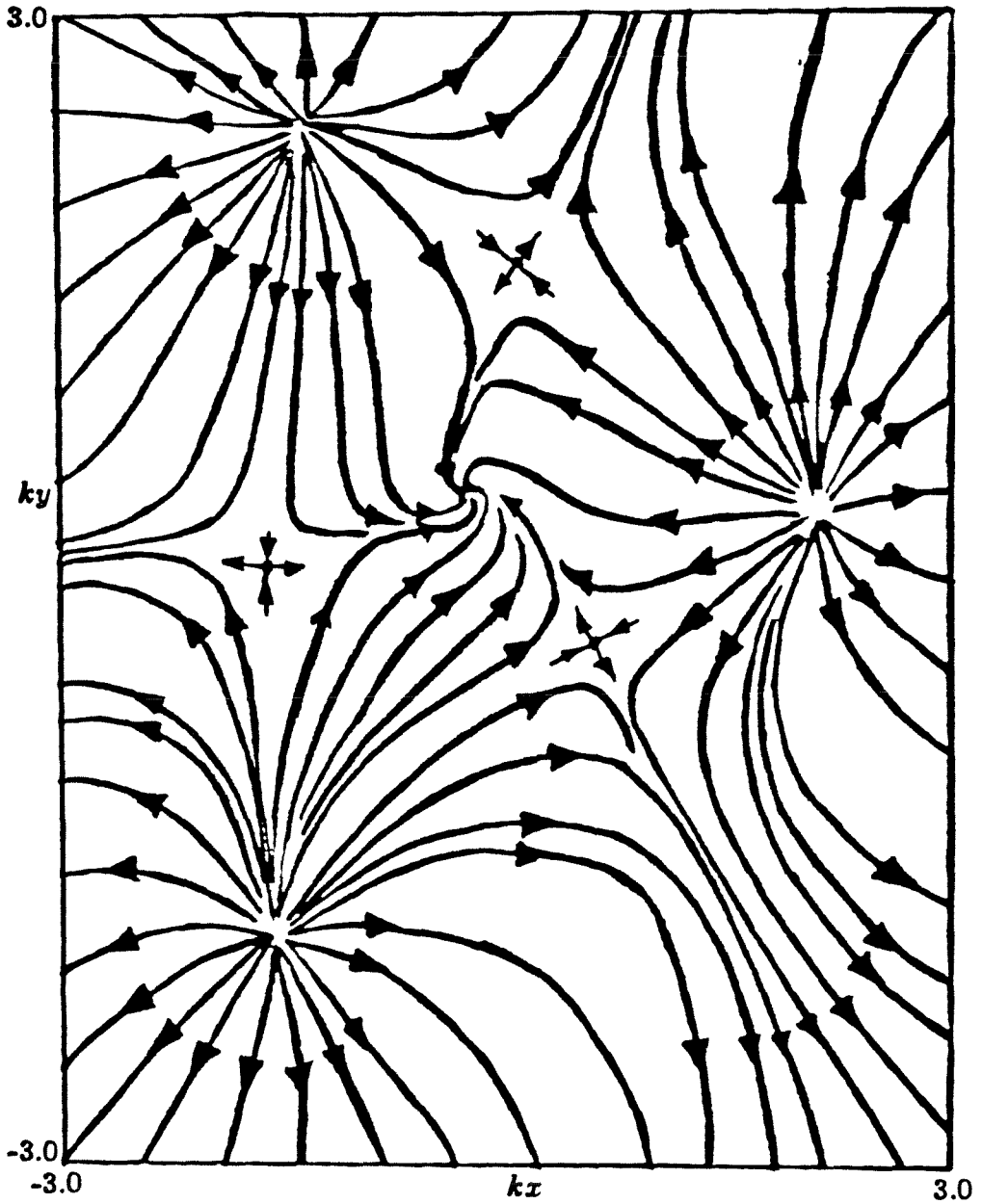

Figure 34. *The flow lines of the Poynting vector field due to three dipoles located at the corners of an equilateral triangle. Their dipole moments are identical and they are directed towards the z-axis.*

zero on a continuous curve therefore the critical points are not isolated. These type of critical points result when the characteristic equation of A has one real root which is zero. Hence these critical points are structurally unstable.

Chapter VI

Conclusion

§24. Summary and Reflections

As all things eventually come to an end, this thesis will now be closed. This is the time to present a summary of the work done and to reflect on some possiblities which might exist for the future.

A major objective of this thesis is to classify the critical points of plane Poynting vector fields according to the behaviour of the flow lines in the neighbourhood of these points. The index of rotation of the vector field around the critical point is not sufficient for such a classification because it is not unique. The objective of classification has been realized. The procedure for analysis of a critical point is summarized below. The real and imaginary parts of the electric field E_z, or the magnetic field H_z, are expanded in a series of eigenfunctions, appropriate to the Helmholtz's equation. If the first terms in the two series are proportional, then these series are converted to the canonical form using relations (54) and (55), otherwise the series are in the canonical form. The first terms in these series are checked for angular degeneracy according to the criteria given in section 6. If the leading term is non degenerate then the critical point is sufficiently characterized by the order of the Bessel functions in the leading terms of the eigenfunction ex-

pansion. If the order of both the terms is equal, then the critical point is a center point. Otherwise the flow lines are homeomorphic to a saddle point with $2|m-n|$ arms where m and n are the orders of the leading terms. If the leading term is degenerate then the critical point cannot be classified in terms of m and n alone. In this case higher order terms are taken into account. Thus except for the case of degeneracy a critical point of any order can be classified.

Although critical points of an infinite variety are possible, only elementary critical points, i.e., the critical points of the lowest order, occur most frequently. This observation is explained by the fact that only these critical points are structurally stable. The interconnection of saddle points by the flow lines is structurally unstable. This fact can be utilized in the construction of qualitative plots of the flow lines. The concept of structural stability also explains the creation and annihilation of elementary critical points. Under a continuous perturbation, an initial number of elementary critical points, say n_i, may come together and form a higher order critical point. This critical point being structurally unstable immediately splits up into a number of elementary critical points n_f which may be different from n_i. The overall structure of the flow lines can change under this perturbation but the total index of rotation is preserved.

The behaviour of the flow lines on a perfectly conducting surface and its neighbourhood has been studied for both types of polarizations. It is found that the flow lines are parallel to the surface. The most elementary critical point on the conducting surface is found to be the half saddle point. The locations of half saddle points is found to coincide with the extrema of the phase of K_z in one polarization and the phase of H_z in the other polarization. When the electromagnetic power flows inside a region bounded bounded by a perfectly conducting surface half saddle points appear on the inner surface of the bounding conductor.

Half saddle points appear on the outside surface of a perfect conductor in electromagnetic scattering problems. The number of these points on the conducting surface determines the index of rotation of the Poynting vector field on a curve near the surface. The presence of other critical points in the neighbourhood can then be predicted with the help of index of rotation. It is shown with the help of these methods that when a plane wave is incident on a scatterer of finite size, the critical points, can exist only in the near zone of the scatterer.

Finally a classification of critical points of a general three dimensional Poynting vector field has been attempted. This attempt is only partially sucessful. Only the structurally stable critical points are identified. They come in two varieties. One of them is labelled as a saddle-3 point and the other one is referred to as a saddle-focal point.

Some problems may be solved qualitatively in so far as the structure of the flow lines is concerned using the concepts developed in this thesis. For example it was shown by Moullin and Phillips [30] that the surface current induced on a sufficiently wide strip, when a plane wave is incident on it, is essentially the same as the current induced on a half plane. If the incidence is normal, considerations of symmetry will imply existence of two half saddle points, one on the front face and one on the back. The number of extrema in the phase function can be counted from figure 29(b). A lower bound on the number of center points in the near zone can therefore be given. It is also evident from symmetry considerations that center points will not exist on the line normal to the strip which is also the axis of symmetry. Saddle points can exist symmetrically on this axis. Admittedly this is insufficient amount of information to construct a complete plot of flow lines but an adventurous reader may hazard a guess.

REFERENCES

[1] C. H. Papas, *Theory of Electromagnetic Wave Propagation,* McGraw-Hill, New York (1965)

[2] J. A. Stratton, *Electromagnetic Theory,* McGraw-Hill, New York (1941)

[3] J. Slepian, "Energy and Energy Flow in the Electromagnetic Field", *Journal of Applied Physics,* **13**, 512–518 (1942)

[4] H. M. Macdonald, *Electric Waves,* Cambridge University Press, (1902)

[5] P. Lorrain, "Alternative Choice For The Energy Flow Vector Of The Electromagnetic Field", *American Journal of Physics,* **50**, 492 (1982)

[6] K. Birkeland, "Ueber Die Strahlung Electromagnetischer Energie im Raume", *Annalen der Physik und Chemie,* **52**, 357–380 (1894)

[7] G. Latmiral, "Curl of Poynting vector and differential radiation pressure", *Alta Frequenza,* **13**, 287–289 (1984)

[8] M. A. Krasnoselskiy, A. I. Perov, A. I. Povolotskiy and P. P. Zabreiko, *Plane Vector Fields,* Academic Press, New York (1966)

[9] H. Forster, "Über das Verhalten der Integralkurven einer gewöhnlichen Differentialgleichung erster Ordung in der Umgebung eines singulären Punktes", *Mathematische Zietschrift,* **43**, 271–320 (1937)

[10] V. V. Nemytskii and V. V. Stepanov, *Qualitative Theory of Differential Equations,* Princeton University Press, (1960)

[11] P. Hartman, *Ordinary Differential Equations,* John Wiley & Sons, New York (1964)

[12] V. W. Braunbek, "Zur Darstellung von Wellenfeldern", *Zeitschrift Naturforschung,* **6a**, 12–15 (1951)

[13] Solomon Lefschetz, *Differential Equations: Geometric Theory,* Dover, New York (1977)

[14] G. Sansone and R. Conti, *Non Linear Differential Equations,* Macmillan, New York (1964)

[15] F. E. Borgnis and C. H. Papas, *Electromagnetic Waveguides and Resonators,* in Vol. XVI of *Handbuch Der Physik,* ed. S. Flugge, Springer–Verlag, Berlin (1958)

[16] R. Courant and D. Hilbert, *Methods of Mathematical Physics,* Vol I, John Wiley & Sons, New York (1953)

[17] M. Born, E. Wolf, *Principles of Optics,* Pergamon Press, New York (1980)

[18] V. W. Braunbek and G. Laukien, "Einzelheiten zur Halbebenen-Beugung", *Optik,* **9**, 174–179 (1952)

[19] G. O. Olaofe, "Scattering by two cylinders", *Radio Science,* **5**, 1351–1360 (1970)

[20] V. H. Wolter, "Zur Frage des Lichtweges bei Totalreflexion", *Zeitschrift Naturforschung,* **5a**, 276–283 (1950)

[21] R. Gesche and N. Lōchel, "Scattering by a Lossy Dielectric Cylinder in a Rectangular Waveguide", *IEEE Transactions on Microwave Theory and Techniques,* **MTT–36**, 137–144 (1988)

[22] R. W. Ziolkowski and J. B.Grant, "Vortex Formation Near an Iris in a Rectangular Waveguide", *IEEE Transactions on Microwave Theory and Techniques,* **MTT–34**, 1164–1182 (1986)

[23] E. T. Whittaker, "On an Expression of the Electromagnetic Field due to Electrons by Means Of Two Scalar Potential Functions", *Proceedings of London Mathematical Society,* **1**, 367–372 (1904)

[24] H. S. Green and E. Wolf, "A Scalar Representation of Electromagnetic Fields", *Proceedings of Physical Society, London,* **A 66**, 1129–1137 (1953)

[25] E. Wolf, "A Scalar Representation of Electromagnetic Fields: II", *Proceedings of Physical Society, London,* **74**, 269–280 (1959)

[26] P. Roman, "A Scalar Representation of Electromagnetic Fields: III", *Proceedings of Physical Society, London,* **74**, 281–289 (1959)

[27] G. E. Shilov, *Linear Algebra,* Dover, New York (1977)

[28] A. D. Myškis, *Advanced Mathematics for Engineers,* Mir Publishers, Moscow (1975)

[29] A. Boiven, J. Dow and E. Wolf, "Energy Flow in the Neighborhood of the Focus of a Coherent Beam", *Journal of Optical Society of America,* **57**, 1171–1175 (1967)

[30] E. B. Moullin and F. M. Phillips, "On the current induced in a conducting ribbon by the incidence of a plane electromagnetic wave", *The Proceedings of the Institution of Electrical Engineers,* 99, Part IV 137–150 (1952)